1957

Quasi-optimization of two phase induction motor relay servos.

Egan, Henry W.

Monterey, California: Naval Postgraduate School, 1957.

http://hdl.handle.net/10945/14539

QUASI-OPTIMIZATION OF TWO PHASE INDUCTION MOTOR RELAY SERVOS

Henry W. Egan

34

QUASI-OPTIMIZATION OF TWO PHASE INDUCTION MOTOR RELAY SERVOS

* * * * *

Henry W. Egan

QUASI-OPTIMIZATION OF TWO PHASE INDUCTION MOTOR RELAY SERVOS

by

Henry W. Egan

Lieutenant, United States Navy

Submitted in partial fulfillment of
the requirements for the degree of

MASTER OF SCIENCE
IN
ELECTRICAL ENGINEERING

United States Naval Postgraduate School
Monterey, California

1 9 5 7

QUASI-OPTIMIZATION OF TWO PHASE INDUCTION MOTOR RELAY SERVOS

by

Henry W. Egan

This work is accepted as fulfilling

the thesis requirements for the degree of

MASTER OF SCIENCE
IN
ELECTRICAL ENGINEERING

from the

United States Naval Postgraduate School

ABSTRACT

It is the aim of this paper to investigate the use of dynamic braking in the dead zone of a relay servo to improve its performance as a positioning device. The torque element of the servo is a two phase induction servomotor.

The investigation was conducted at the U. S. Naval Postgraduate School at Monterey, California, during the period September, 1956, to May, 1957.

The investigation was suggested and supervised by Professor George J. Thaler of the U. S. Naval Postgraduate School. His assistance and encouragement were greatly appreciated by the author.

TABLE OF CONTENTS

LIST OF ILLUSTRATIONS

TABLE OF SYMBOLS

A	Magnitude of step input
a.c.	Alternating current
B	Magnetic field strength
C	Coulomb friction
d.c.	Direct current
E	Applied voltage
E	Error position angle
$\dot{E} = dE/dt$	Error rate or error angular velocity
$\ddot{E} = d\dot{E}/dt = d^2E/dt^2$	Error angular acceleration
e_d	Error change during relay drop-out delay
e_i	Error change during inductive delay
f	Viscous friction coefficient
I, i	Current
J	Moment of inertia
K	Conversion factor or amplification factor
K_b	Braking torque constant
K_e	Proportionality constant relating torque and control voltage
K_n	Proportionality constant relating torque and motor speed
K_t	Tachometer constant
l	Length of rotor conductor
m_r	Slope of motor load trajectory in dead zone
m_{sl}	Slope of switching locus
mmf	Magnetomotive force
m.a.	Milliamperes
n	Isocline slope constant

R	Resistance
r	Potentiometer setting
RPM	Revolutions per minute
S	Slip
s	Switch
T	Motoring torque
T_b	Braking torque
V_c	Control phase voltage
V_d	Relay drop-out voltage
V_p	Relay pull-in voltage
Z	Impedance
θ	Angular position
$\dot{\theta} = d\theta/dt$	Angular velocity
$\ddot{\theta} = d\dot{\theta}/dt = d^2\theta/dt^2$	Angular acceleration
θ_o	Output position angle
$\ddot{\theta}_o = d\dot{\theta}_o/dt = d^2\theta_o/dt^2$	Output angular acceleration
θ_i	Input angular position
$\dot{\theta}_i = d\theta_i/dt$	Input angular velocity
$\ddot{\theta}_i = d\dot{\theta}_i/dt = d^2\theta_i/dt^2$	Input angular acceleration
ϕ	Motor phase
w	Angular velocity of ramp input
I, II, III	Zones of relay operation
$\| \|$	Absolute value
∞	Infinity
$\sim$	Cycle or alternating current source

d/dt	First time derivative
d^2/dt^2	Second time derivative
δ/δ	Partial derivative

CHAPTER I

INTRODUCTION

The use of the two phase induction motor is widespread in applications where the continuous positioning type of servo is used. The relay servo, however, has been limited in its use because of the problems associated with stability, speed of response, and steady state accuracy. Consequently investigations into relay servos using different type motors controlled by various methods have not been extensively carried out.

Work has been done by Thaler (1), Harris (2), and McDonald (3) in demonstrating the use of dynamic braking in the dead zone of relay servos. It was shown effectively that an armature shunt resistor may be used on a d.c. shunt motor to provide an energy sink for the application of dynamic braking. Stability, speed of response, and steady state accuracy were shown to be greatly improved.

The objective of this paper is to analyze the use of dynamic braking in the dead zone of a relay servo in which the motor used is a two phase induction servomotor. It is proposed that direct current be applied to the control phase of the servomotor in the dead zone to affect the dynamic braking or in this instance eddy current braking. While direct current braking is the main topic of this paper, dynamic braking obtained by supplying an energy sink in the form of a shorted control phase is also discussed. Both methods will be shown to be feasible and to reduce the problems mentioned above that are normally inherent in relay servos.

Chapter II presents a historical review of the two phases of the paper. First a review of the method of phase plane analysis is given. This is then applied to a relay servo which has viscous friction and in

which error rate feedback is used. Secondly, a review of induction motor theory is presented so that the operating characteristics of the two phase induction motor under various braking conditions may be explained. Several methods of induction motor braking are discussed.

Chapter III includes a phase plane analysis of the proposed relay servo demonstrating the dynamic braking principles involved. The practical effects of relay hysteresis, delay time, circuit induction, and coulomb friction are shown.

Chapter IV presents the experimental verification of the dynamic braking of the relay servo as proposed above. Torque speed tests on various motors, retardation tests, and test runs on a relay servo system are presented.

The results of this investigation show that the relay servo problems mentioned in the first paragraph of this chapter are greatly reduced when proper dynamic braking is used. Coulomb friction is shown to have negligible effect under certain direct current braking conditions. Relay delay time is shown to have adverse time lag effects for high speed two phase induction servomotor systems. The response of the system is shown to be practically identical to that predicted by the theory.

CHAPTER II

HISTORICAL REVIEW

1. Relay Servo Theory

a. Basic Concepts: Relay Characteristics

The relay servo is an all-on, all-off system of control. This differentiates such a servo from an continuous servo in which any change in input is reflected by a change in output. In a relay servo the relay is made to actuate causing a pair of contacts to close by the presence of a certain voltage input. In most applications it is desired for the response to be positive or negative as the input to the relay is positive or negative. Consequently, a relay for such an operation has at least two output contacts--one for positive and one for negative control. When the input signal magnitude is sufficient, the closing of the output contacts provides a completed circuit to the control field of a servo motor. The direction of rotation of the motor is determined by whether the relay was actuated by a positive or negative signal.

When the relay closes in either direction, the magnitude of the control voltage applied to the motor is not a function of the relay input signal. The control voltage is always the maximum desired by the design of the system. This feature is one of the advantages of the relay servo in that both maximum torque and velocity of the motor are available. Thus when the relay actuates, the motor-load combination tends to velocity saturate and will do so providing the time before relay drop-out occurs is sufficiently long.

While a relay must have a pull-in potential in either direction, $+V_p$ and $-V_p$, it must also have a corresponding drop-out potential,

$+V_d$ and $-V_d$. In an ideal relay, one with no dead zone, the relay would pull in and drop out at the same potential; i.e., $+V_p = +V_d$ and $-V_p = -V_d$. And $+V_d + (-V_d)$ would be infinitesimally small so that any input would actuate the relay in the proper direction. However, practically, a relay requires a certain voltage to pull in and a different one to drop out. The two pull in potentials are usually of different magnitudes. This is also true of the drop out potentials. Figure 1 shows graphically these relay characteristics. The dead zone is here defined as the difference in relay input between the drop-out voltage in one direction and the pull-in voltage in the other direction.

These relay characteristics have important effects. Since the servo is usually designed so that the relay is actuated by an amplified signal, the gain of the amplifying components effects the pull-in and drop-out points. For a given amplifier input signal, a gain increase effectively narrows the dead zone. A gain decrease widens it. Consider also that any motor-load combination has some inherent or designed-in damping present as either viscous or coulomb friction - friction proportional to or independent of velocity. This damping is present and acting whether the relay is operating in a controlling state or in the dead zone. If the dead zone is wide enough, the friction may act long enough to brake the motor-load to stand still without the relay closing in the opposite direction. A more narrow dead zone will allow the motor-load to drift through the dead zone and overshoot causing the relay to pull-in in the opposite direction and an oscillation will occur. This oscillation may damp out and the system "dead beat," or stop with a steady state error, which is limited in magnitude by the dead zone width. However,

the oscillation may reach a limit cycle and continue to oscillate if the damping is small or the gain high. Thus the stability of the system and the steady state error can both be acutely altered by changes in gain.

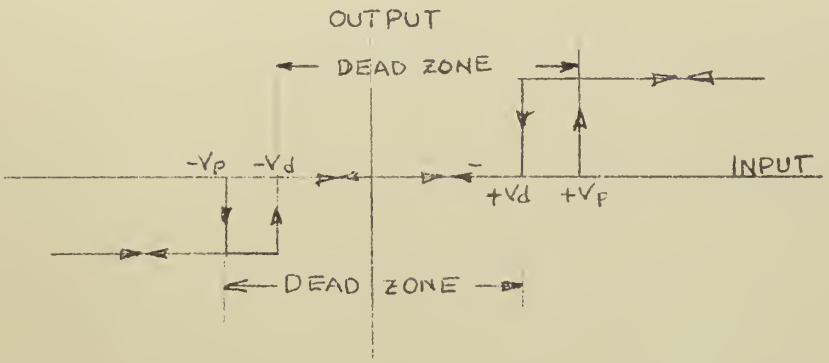

FIGURE 1 - RELAY CHARACTERISTICS

That the relay does have a dead zone requires having three differential equations to describe the action of the motor-load combination --when the relay is actuated in the positive sense, the negative sense, and when it is in the dead zone. However, since most motor-load combinations can be adequately described by second order differential equations, this is not a critical condition. The treatment of the three governing equations using the phase plane method of analysis will be demonstrated later.

The time delay due to the physical movement of relay parts when it pulls in or drops out also has an effect on the response of the system. If the system contains a motor that has a low order saturation velocity of a few hundred RPM, the effect may be negligible. But if the motor has a saturation velocity of several thousand RPM, the rate of signal correction may be large enough to cause the effect of relay drop out delay to be quite significant.

Another effect that is akin to drop out delay time is contact arcing. If the relay is controlling d.c. current, the relay contact opening has to be wide enough to allow breaking of the arc. The arcing itself adds to delay time. The faster acting a relay is, the less the effect will be noticed. An attempt to decrease the arcing by decreasing the controlled voltage will slow the response. This in turn will also decrease the effect of relay time lag.

When the relay is controlling an a.c. potential, the arcing problem is not so severe, since the potential drops to zero every half cycle. In a 400 cycle system this is a small delay. Even so, with a high saturation velocity it can represent a considerable portion of dead zone travel and should be recognized as a source of system instability.

b. The Phase Plane Method of Analysis.

The phase plane method is usually used as a routine for solving the differential equations of systems of the second order. This is done by plotting the first time derivative of the dependent variable against the dependent variable. This effectively eliminates the independent variable time from the solution of the problem. Included in the routine are methods for graphically arriving at the solution in terms of time and the dependent variable. So this method may be thought of as an extension of the more classical transient forms of analyses.

There are several sub-methods available for carrying out the phase plane analysis.(4) But in general the simplest to apply and one which also gives results with good accuracy is the isocline method. As with any analytical method that must be handled graphically, this too is often a tedious routine. But once the isocline equation is developed and the isocline plotted, the system response may be readily studied. The great convenience lies in that various initial conditions may be

dealt with without much additional difficulty.

As stated above, the various methods of phase plane analyses involve the graphical relation of the time derivative of the dependent variable with the dependent variable. Consider a servo system in which the position and the rate of change of position or velocity are time dependent. Then the phase plane analysis would show a graphical presentation of position and velocity. Any trajectory on the plot would have as its slope a value related to the coordinate value of position and velocity. In symbolic form the slope could be written:

$$\frac{d\dot{\theta}}{d\theta} = f(\theta, \dot{\theta}) \qquad (1)$$

If the slope so defined is given a constant value, n, then (1) becomes an explicit expression of a curve on the phase plane. One property of this curve is that if a phase plane trajectory drawn as a solution of the servo system under investigation crosses the curve, then the trajectory must have the slope, n, at the point of intersection. When sufficient constant values are supplied for n and the isoclines thus defined plotted, the development of the phase portrait follows quite readily. The phase portrait is the graphical solution of the differential equation with sufficient variation in initial conditions to develop a complete picture of the response characteristics of the system. This, of course, may consist of many trajectories on the phase plane plot.

As an example consider the equation,

$$J\ddot{\theta} + f\dot{\theta} + C = T \qquad (2)$$

which in general represents the differential equation governing a motor-

load combination of a system which is being driven by a torque T developed by a servomotor.

This may be rearranged to,

$$\ddot{\theta} = -\frac{f}{J}\dot{\theta} - \frac{(C-T)}{J} . \tag{3}$$

Dividing through by $\dot{\theta}$, (3) becomes,

$$\frac{\ddot{\theta}}{\dot{\theta}} = -\frac{f}{J} - \frac{(C-T)}{J\dot{\theta}} \tag{4}$$

Defining $\dot{\theta}$ as,

$$\dot{\theta} = d\theta/dt, \tag{5}$$

then

$$\frac{\ddot{\theta}}{\dot{\theta}} = \frac{d\dot{\theta}}{dt} \Big/ \frac{d\theta}{dt} = \frac{d\dot{\theta}}{d\theta} . \tag{6}$$

And (4) may be written as,

$$d\dot{\theta}/d\theta = -\frac{f}{J} - \frac{(C-T)}{J\dot{\theta}} . \tag{7}$$

Equation (7) is thus the general isocline equation in the form of (1) and may be numercially dealt with to provide the graphical solution of the differential equation (2) on the phase plane. A constant being substituted for $d\dot{\theta}/d\theta$ in (7) allows the determination of the value of $\dot{\theta}$, regardless of θ, at which the slope of $d\dot{\theta}/d\theta$ is equal to the constant. Therefore in this case the isoclines, or lines of constant slope, are parallel to the position axis. Figure 2 shows a typical solution

when the initial conditions specifying point A are given.

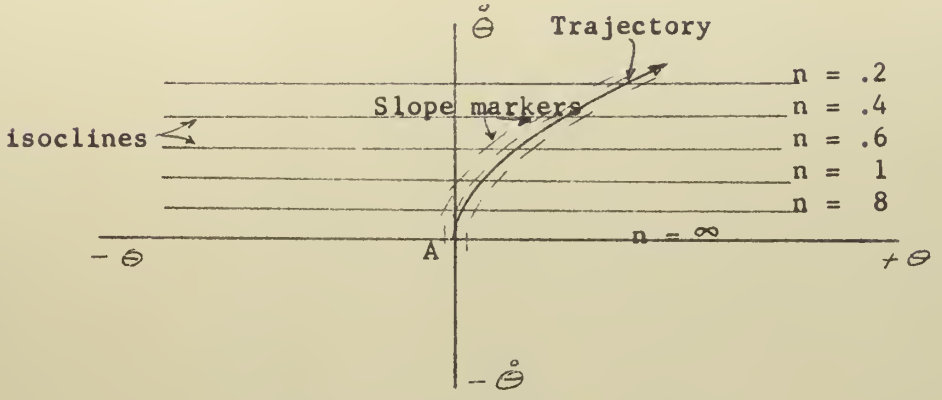

FIGURE 2 - PHASE PLANE PLOT

From such a phase plane solution the transient response of the system may be developed recalling from equation (5) that $\dot{\theta} = d\theta/dt$. Hence the graphical integration proposed by,

$$t = \int \frac{d\theta}{\dot{\theta}} \tag{8}$$

would give the time response desired.

c. The Analysis of a Relay Servo

In the previous section one method of graphically solving the differential equations that govern a second order system was shown. Here a relay servo system using error rate feedback as shown in Figure 3 will be analyzed.

(1) Step Input : $\theta_i = A$

If a step input is assumed, θ_i is constant and $\dot{\theta}_o = -\dot{E}$. Also, any change in θ_o causes an equal change in E. Thus the governing equations in θ_o and $\dot{\theta}_o$ may be replaced by equations in E and $\dot{E}$.

The use of tachometer feedback will be such as to cause the relay input voltage to be less at any time. This will cause a counterclockwise rotation of the switching locus as shown in Figure 4 and will cause the relay to actuate before it would without feedback; i.e., anticipate.

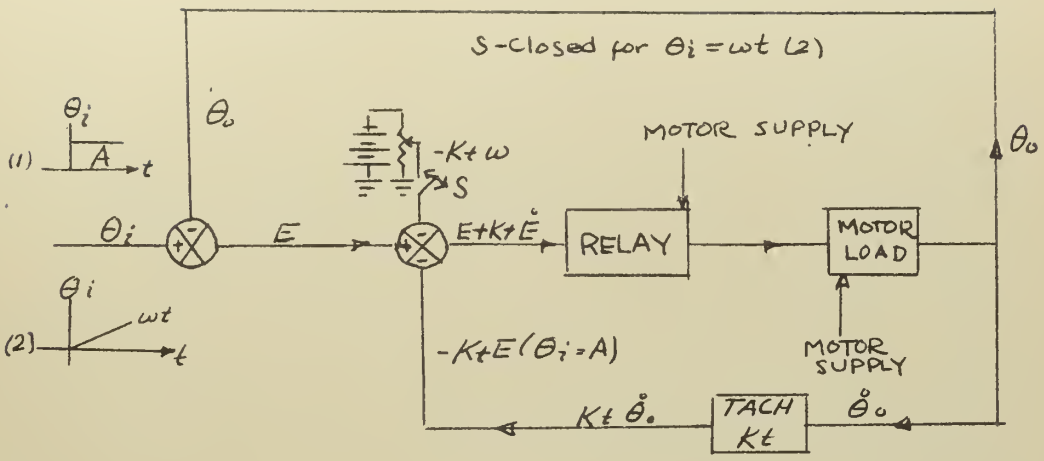

FIGURE 3 - RELAY SERVO WITH TACHOMETER FEEDBACK

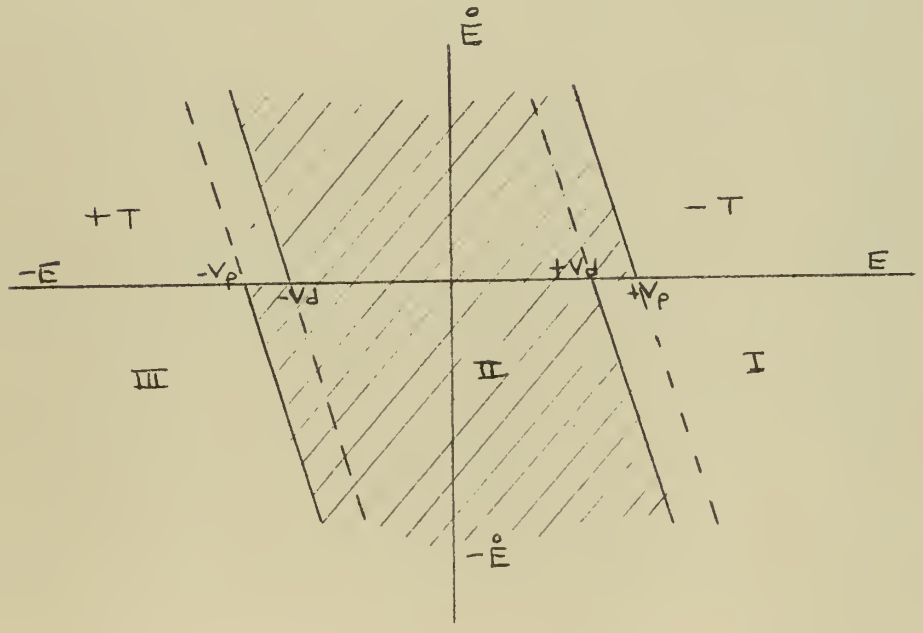

FIGURE 4 - PHASE PLANE PLOT OF RELAY CHARACTERISTICS

Also shown in Figure 4 are the three zones of relay action. In Zone I a positive error of sufficient magnitude will cause the relay to close and a negative torque to be developed at the motor shaft which will drive the error toward zero.

The equation which governs the action of the motor-load combination in this zone is,

$$J\ddot{\theta}_o + f\dot{\theta}_o = T \tag{9}$$

or

$$-J\ddot{E} - f\dot{E} = T \tag{10}$$

or

$$J\ddot{E} + f\dot{E} = -T \tag{11}$$

assuming that no coulomb friction is present.

In Zone II, the relay dead zone, no torque is being developed by the motor and the equation analogous to (11) is,

$$J\ddot{E} + f\dot{E} = 0 \tag{12}$$

In Zone III the relay actuates to decrease a negative error with a positive torque and the defining equation is,

$$J\ddot{E} + f\dot{E} = T \tag{13}$$

Collecting equations (11), (12), and (13) and noting the relay switching loci characteristics we have,

Switching Criterion	System Equations
$E + KtE \geqslant V_p \mid \dot{E}+$	
$E + KtE \geqslant V_d \mid \dot{E}-$	$J\ddot{E} + f\dot{E} = -T$ Zone I (14)
$-V_p \mid \dot{E}- \quad E + KtE \leqslant V_p \mid \dot{E}+$	
$-V_d \mid \dot{E}+ \quad E + KtE \leqslant V_d \mid \dot{E}-$	$J\ddot{E} + f\dot{E} = 0$ Zone II (15)
$E + KtE \leqslant V_p \mid \dot{E}-$	
$E + KtE \leqslant V_d \mid \dot{E}+$	$J\ddot{E} + f\dot{E} = +T$ Zone III (16)

These are the equations for negative feedback as shown in Figure 4. Note must be taken of the relay characteristics applying to equations (14) and (16). With a positive error greater than that required for a voltage of $+V_p$ to be applied to the relay, the relay will close. But it will not open unless the voltage is reduced to $+V_d$. The trajectory on the phase plane will be clockwise, crossing the upper switching loci from left to right and the lower switching loci from right to left. This leads to the shift in the dead zone about the E axis and shows the effect of relay hysteresis upon system operation.

Equation (14) may be manipulated for plotting on the phase plane by the following steps,

$$\ddot{E} = \frac{-f\dot{E} - T}{J} \qquad (17)$$

Defining $\dot{E}$ as dE/dt then

$$\ddot{E}/\dot{E} = d\dot{E}/dE = -\frac{f}{J} - \frac{T}{\dot{E}J} \qquad \text{Zone I} \qquad (18)$$

Equation (15) becomes,

$$\ddot{E}/\dot{E} = d\dot{E}/dE = -\frac{f}{J} \qquad \text{Zone II} \qquad (19)$$

and equation (16) becomes,

$$\ddot{E}/\dot{E} = d\dot{E}/dE = -\frac{f}{J} + \frac{T}{\dot{E}J} \qquad \text{Zone III} \qquad (20)$$

Figure 5 may represent the typical trajectory defined by equations (18), (19), and (20) when an initial step input $\theta_i = E_o = A$ is given. In Zones I and III the plotting of isoclines and slope markers is necessary to complete any trajectory part in either zone. In Zone II the slope is always -f/J and is easily drawn. It should be noted that without derivative feedback and little viscous damping, an inherent characteristic of servomotors in general, the oscillation might not stop and the system come to rest. Instead, a limit cycle about the origin might develop, and, if the system is unstable, the limit cycle would be bounded by the saturation velocity limits as shown in Figure 6. Thus the stabilizing effect of derivative or tachometer feedback and viscous damping is shown. Of course it must be remembered that the width of the dead zone and the relay hysteresis zone as governed by the gain of the amplifying components can offset the influence of both feedback and damping.

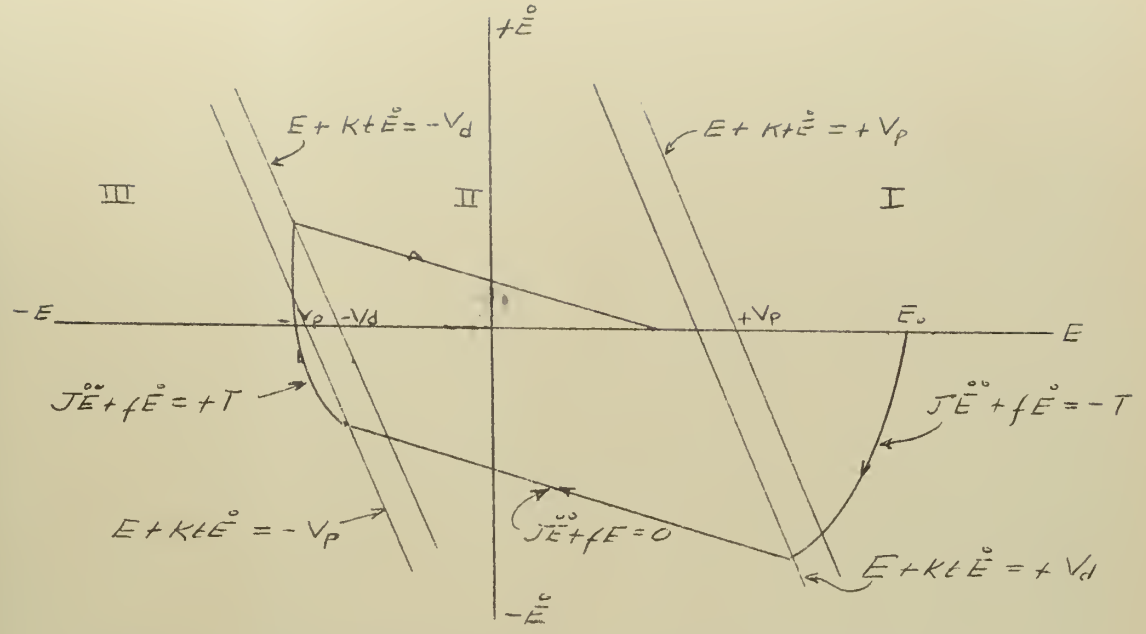

FIGURE 5 - PHASE PLANE PLOT OF RELAY SERVO WITH VISCOUS DAMPING AND TACHOMETER FEEDBACK

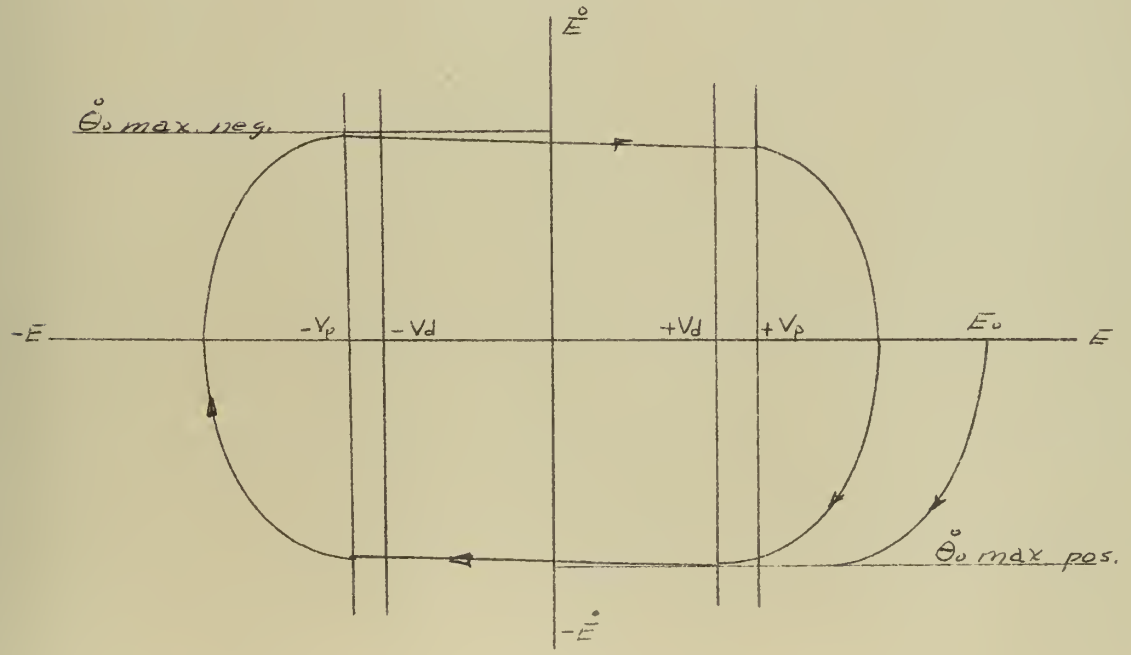

FIGURE 6 - PHASE PLANE PLOT OF RELAY SERVO WITH MAXIMUM LIMIT CYCLE

To improve the stability of the relay servo viscous damping may be added. If added during both the accelerating and decelerating stages of the operation, the response of the system will be retarded. Therefore it is advantageous to add such damping discontinuously and only during the decelerating stage, i.e., during the dead zone travel of the motor-load combination.

A direct friction brake can be employed for low power and low speed applications where the braking is applied on relay drop out. Ideally, assuming no slippage, braking would be instantaneous and the velocity of the system reduced to zero immediately on relay drop out. However, the predictability of direct friction braking is quite poor and other methods of damping allow analysis and give good braking effects.

Dynamic braking may be employed where discontinuous viscous damping is desired. Section 3 of this chapter explores several methods of accomplishing this with particular regard to braking of the induction motor.

(2) Ramp Input: $\theta_i = wt$

In the previous section the general error-error rate relay servo was analyzed with the input being a step function. This section deals with the analysis of the same system when the input is a ramp function. It will be shown that not only are the phase plane equations of the system more complex, but also that the response of the system is totally different. The trajectory of the system within the dead zone is no longer a straight line and depending upon the magnitude relation between $\underline{w}$ and $\dot{\theta}_o$ the system will develop a limit cycle or a continuously increasing error.

Figure 4 showing the relay characteristics applies as in the previous section, since the switching loci equations are independent of the system

equations. They are related in that the boundary conditions for the system equations are set by the switching loci.

In Zone I the following equation governs,

$$J\ddot{\theta}_o + f\dot{\theta}_o = T \tag{21}$$

Since,

$$\theta_o = wt - E \quad , \text{ and} \tag{22}$$

$$\dot{\theta}_o = w - \dot{E} \quad , \text{ and} \tag{23}$$

$$\ddot{\theta}_o = -\ddot{E} \tag{24}$$

then equation (21) may be written

$$-J\ddot{E} + fw - f\dot{E} = T \quad , \text{ or} \tag{25}$$

$$J\ddot{E} + f(\dot{E} - w) = -T \quad \text{for Zone I} \tag{26}$$

For Zone II the defining equation is,

$$J\ddot{E} + f(\dot{E} - w) = 0 \tag{27}$$

and for Zone III,

$$J\ddot{E} + f(\dot{E} - w) = +T \tag{28}$$

Equations (26), (27), and (28) are analogous to equations (14), (15), and (16) for the step input and may be manipulated in a similar manner to obtain the isocline equations for the phase plane plot. Equation (26) may be written,

$$\ddot{E} = -\frac{T}{J} - \frac{f(\dot{E} - w)}{J} \tag{29}$$

and again noting that $dE/dt = \dot{E}$, it becomes,

$$\ddot{E}/\dot{E} = d\dot{E}/dE = -\frac{T}{J\dot{E}} - \frac{f}{J}\left(\frac{\dot{E} - w}{\dot{E}}\right) \qquad \text{Zone I} \qquad (30)$$

Equation (27) becomes,

$$\ddot{E}/\dot{E} = d\dot{E}/dE = -\frac{f}{J}\left(\dot{E} - w/\dot{E}\right) \qquad \text{Zone II} \qquad (31)$$

and equation (28) becomes,

$$\ddot{E}/\dot{E} = d\dot{E}/dE = \frac{T}{J\dot{E}} - \frac{f}{J}\left(\dot{E} - w/\dot{E}\right) \qquad \text{Zone III} \qquad (32)$$

Equations (30), (31), and (32) are analogous to equations (18), (19), and (20) for the step input. In (19) it was shown that the slope of the trajectory in the phase plane in the dead zone was a constant, - f/J. Equation (31) shows that this does not hold for the ramp input. Examination of equation (31) shows that the slope of the trajectory in the dead zone will be zero at the error velocity where $\dot{E} = w$. $d\dot{E}/dE = 0$ can also be obtained by setting either equation (30) or (32) equal to zero, as

$$d\dot{E}/dE = -\frac{T}{J\dot{E}} - \frac{f}{J}\left(\frac{\dot{E} - w}{\dot{E}}\right) = 0 \qquad (33)$$

then

$$T = f(\dot{E} - w) \qquad (34)$$

and

$$w - T/f = \dot{E} \qquad (35)$$

Substituting $w - \dot{\theta}_o$ for E in (35) then

$$+ T/f = \dot{\theta}_o \text{ , and} \qquad (36)$$

$$\dot{E} = w - \dot{\theta}_o \qquad (37)$$

The same result may be obtained by a similar manipulation of equation (32) for Zone III. Thus it is shown that whatever the trajectory in the phase plane may be, it must have the slope of zero twice: once when $\dot{E} = w$ and at $\dot{E} = w - \dot{\theta}_o$, which can only occur if the relay closes so that a $\dot{\theta}_o$ exists. A third slope of zero is obtained if the relay dead zone is overshot and the relay pulls in in the opposite direction. Again $\dot{E} = w - \dot{\theta}_o$, but here in Zone III $\dot{\theta}_o$ is negative rather than positive as on the initial closure of the relay.

From equations (30), (31), and (32) it can be seen that $d\dot{E}/dE = \infty$ when $\dot{E} = 0$. Therefore, the trajectory must be vertical when crossing the E axis at any point. The above discussion leads to a qualitative picture of the phase plane plot of the trajectory as shown in Figure 7, which is a plot of a system wherein there is little viscous damping and no feedback. In such a case the motor-load combination would accelerate to a velocity, which may be saturation velocity if motor response is fast enough, to produce a certain error rate. If the motor-load velocity saturates, the trajectory will have a zero slope in Zone I. If it does not, the trajectory will go through zero slope at the drop out point--on the boundary of Zone I. The trajectory proceeds across the dead zone with almost zero slope (see equation (31) with $\underline{f}$ very small) and the relay pulls in in the reverse direction. As $\dot{\theta}_o$ decreases from its dead zone exit value to zero and then increases in the negative direction, $\dot{E}$ increases from $w - |\dot{\theta}_o|$ to $w + |\dot{\theta}_o|$. Again the slope goes through zero at $-V_d$ or in Zone III. With a negligible inherent viscous damping the oscillations, which may commence with less than output velocity saturation, will quickly build up to that shown in Figure 7.

The addition of negative feedback does not alter the fact that a limit cycle will be reached, since it does not enter directly into the

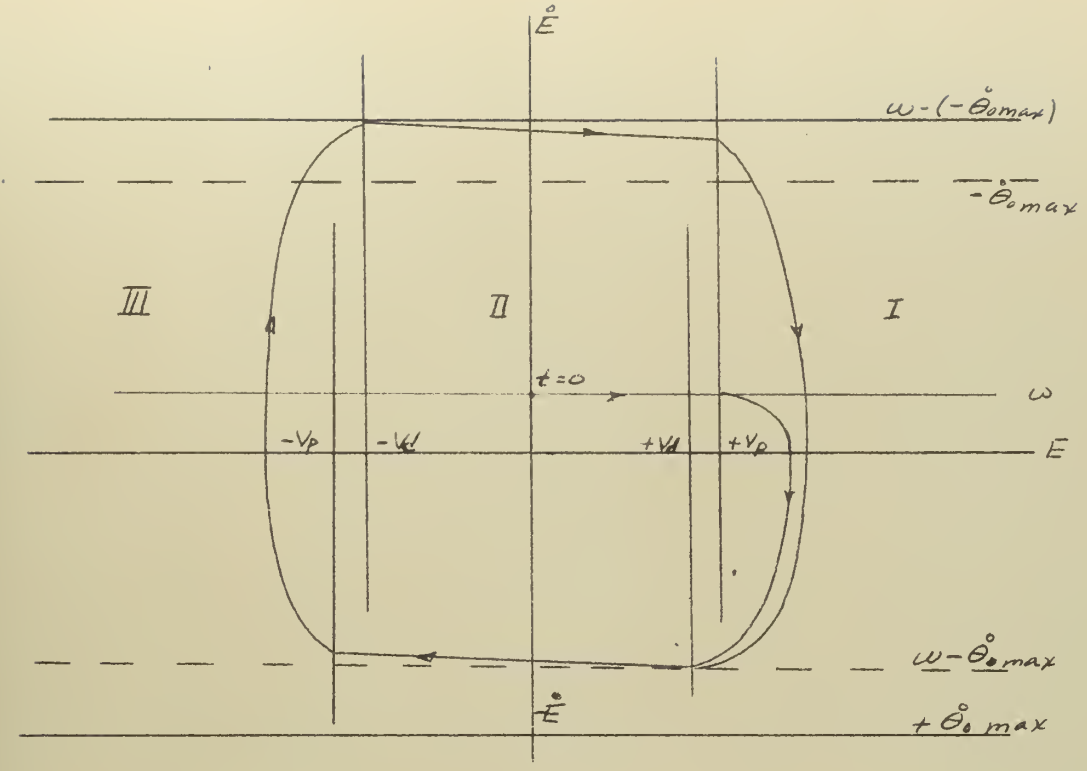

FIGURE 7 - PHASE PLANE PLOT OF RELAY SERVO WITH RAMP INPUT

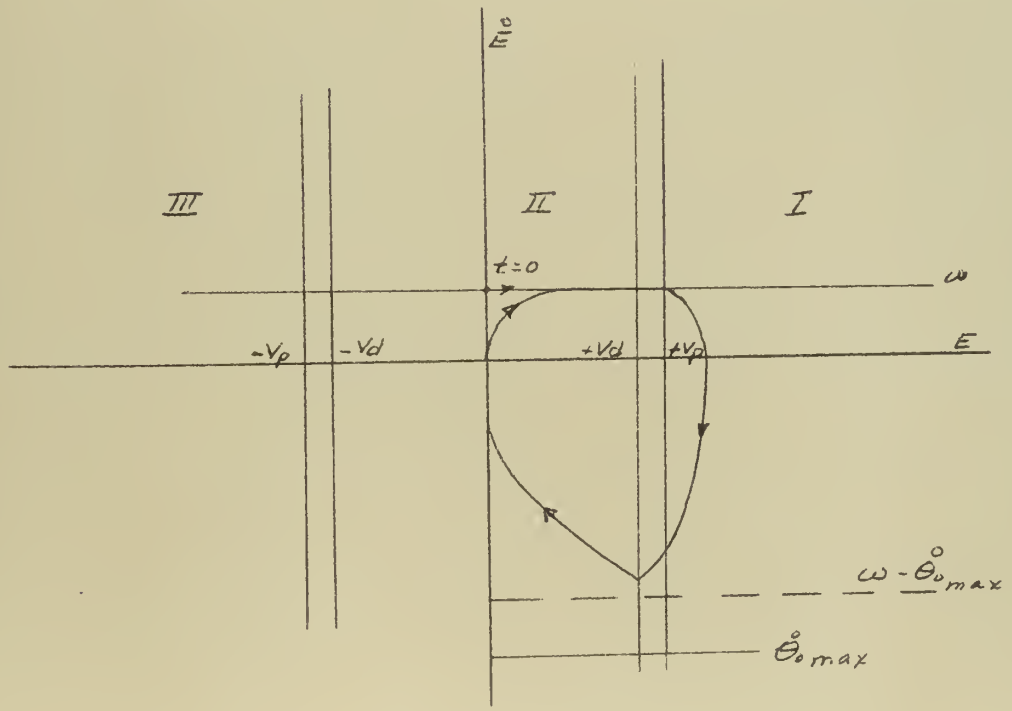

FIGURE 8 - PHASE PLANE PLOT OF RELAY SERVO WITH RAMP INPUT AND DISCONTINUOUS VISCOUS DAMPING

system equations. However, since boundary conditions are set by the switching loci, the shape of the limit cycle, its maximum limits in error and error-rate, and the frequency of the cyclic oscillations will be altered by feedback. With negative feedback the maximum error deviation and the maximum error-rate deviation will be decreased and the frequency of oscillation will be increased.

If viscous damping or dynamic braking is employed, the slope in the dead zone may be altered to the degree that the system does not pull-in in the reverse direction. In such a case the limit cycle will be limited to Zones I and II. Again the zero slopes will be in Zone I where $\dot{E}$ equals the maximum attained value of $w - \dot{\theta}_o$ and in Zone II where $\dot{E}$ equals $\underline{w}$, which is the positive limit of the error rate, since at this point $\dot{\theta}_o$ is equal to zero. Figure 8 shows this effect of dynamic braking.

The effect of dynamic braking may be optimized by the use of error-rate feedback. Again, the reduction in error deviation and error-rate deviation is gained along with an increase in frequency of oscillation. This is shown in Figure 9.

Another method of stabilizing the system which may be used to dead beat the response at an error slightly greater than $\pm V_d$ is by the use of an magnetic eddy current brake operating on $\dot{\theta}_o$. Having determined the input rate, the output rate is limited to that value so that $\dot{\theta}_o = w$. Therefore the error rate would be zero and the system would hang at the error where this equality is reached. Figure 10 shows the trajectory of such a system. Figure 10 is ideal in the sense that the error-rate cutoff is sharp. Practically, the output velocity would reach the limiting value with nearly zero slope causing an increase in error from the ideal. Or the limit velocity of the output could be made slightly

greater than that necessary for dead beat operation which would lead to a very small limit cycle. Then some method of self-adjusting control could be used to decrease the braking until the relay "chatter" stops. Ideally, such a method could lead to the development of a system which would continuously follow a ramp input with a constant error which could be made to approach zero as the dead zone is narrowed.

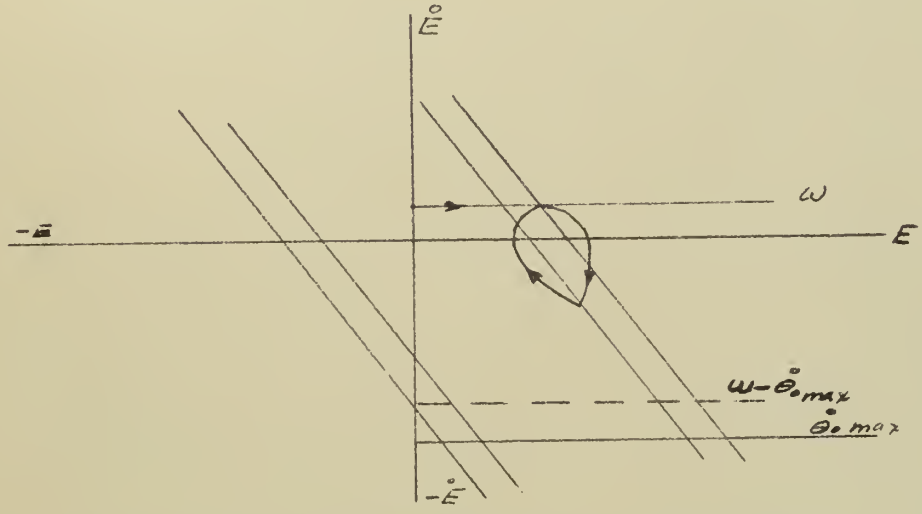

FIGURE 9 - RELAY SERVO WITH RAMP INPUT, VISCOUS DAMPING AND TACH FEEDBACK

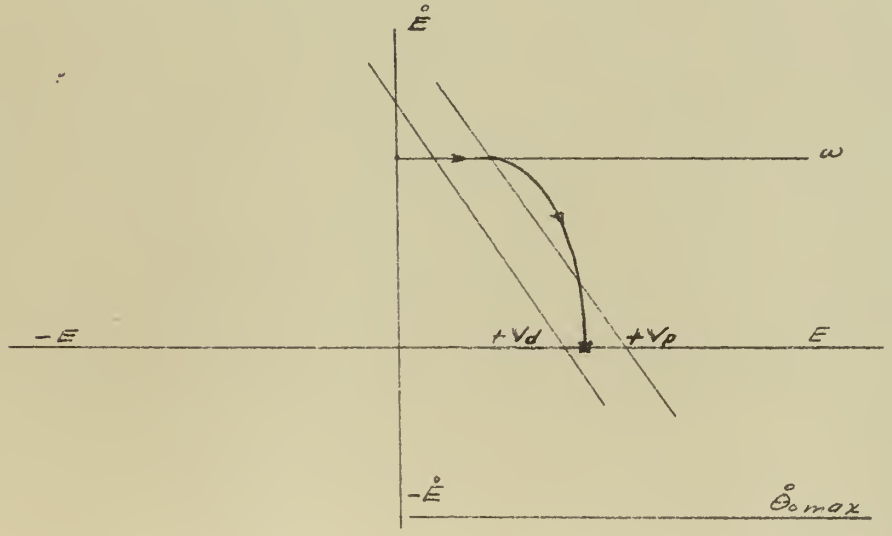

FIGURE 10 - RELAY SERVO WITH RAMP INPUT, TACH FEEDBACK AND OUTPUT VELOCITY LIMITER

2. The Two Phase Induction Servomotor

Whether an induction motor is to be used for large power applications or to deliver a few ounce-inches of torque, whether it is a three, two or single phase motor, as far as the basic theory is concerned, there is really no difference. The application directs the design alterations that permit variation in the characteristics of the particular induction motor. In this section it is planned to outline some of the variable physical features of the polyphase induction motor. In the following sections the methods with which these variables are dealt to produce the two phase induction motor will be examined. And, finally, the operating characteristics of the two phase induction servomotor will be explained for normal excitation, single phase excitation and semi-single phase excitation.

a. Theory of the Induction Motor (5)

The premise upon which all motor theory is based is that a conductor capable of carrying current is in motion in a magnetic field. In the induction motor both the field and the rotor with its conductors rotate. The field rotates due to the excitation of the phase windings in the stator in a particular manner. For instance, in a three phase induction motor the windings of the stator are such that within 180 electrical degrees (for a full pitch winding) three phase belts occur. Each phase belt includes one side of the coils for one phase winding. Thus the second phase windings are placed 60 electrical degrees out of phase with the first and the third phase 120 electrical degrees out of phase with the first. The phases are then excited in turn by sinusoidally varying potentials which are 120 electrical degrees out of phase. The variation in magnitude of the applied voltage to any one phase produces an mmf

which varies in amplitude in time phase with the current amplitude in the winding. The mmf, in the full pitch winding, contains all of the space harmonics of a square wave, that is, a fundamental and the odd harmonics. These all fluctuate sinusoidally in amplitude at line frequency, the frequency of the applied voltage. The magnitude of the fundamental is $4/\pi$ times as large as the magnitude of the square wave. The third harmonic is $4/3\pi$ times as large as the square wave; the fifth $4/5\pi$ as large, etc. Each harmonic is a standing wave varying sinusoidally in amplitude. Such a wave type can be substituted for by two waves fixed in amplitude that move in opposite directions at the proper velocity. To produce the standing wave the gliding waves must be equal to half of maximum of the standing wave in amplitude and move at synchronous velocity. The synchronous velocity is a function of the frequency of the standing wave and the number of poles it encompasses. Thus it is possible to replace the harmonics which are stationary in space and sinusoidally varying in amplitude by waves constant in amplitude and each rotating at its synchronous velocity--half in one direction and half in the opposite direction.

The winding position and the excitation sequence of the three windings result in a specific summation or cancellation of the gliding waves. For the full pitch, three phase winding, the fundamental waves gliding in one direction add while those in the other direction completely cancel out each other. This results in one wave which has an amplitude three times as large as the individual gliding waves and which is traveling around the rotor at the synchronous velocity of the machine. The third harmonic is completely cancelled out in both directions and the fifth space harmonic becomes a wave revolving opposite to the fundamental at one

fifth the velocity of the fundamental. Frequently it is desired to suppress various harmonics and this is accomplished by selecting the proper coil pitch and the number of slots per pole per phase.

The revolving mmf for a two phase induction motor may be deduced in the same manner by an investigation of the gliding waves set up by two phase windings wound 90 electrical degrees apart and excited out of phase by 90 electrical degrees. These also produce a fundamental mmf revolving at synchronous velocity plus harmonics which revolve with and against the main mmf with slower velocities and lesser magnitudes. In most analytical studies concern is taken only with the fundamental, it being assumed that the other space harmonics can be eliminated by design or at least made negligible in their effect.

From the development of the revolving field it is a simple step to the motor action involved in the induction motor. Considering the rotor to be at standstill, the mmf of the stator sets up a revolving flux field in phase with its mmf. The flux passing over the rotor conductors induces in them voltages which in turn cause current to flow. The induced current in the conductors is in such a direction as to cause a force to be developed on the conductors in the direction of the rotating field. The flow of current in the rotor conductors produces a secondary mmf which moves with a velocity relative to the rotor which is the difference between the actual rotor velocity and the synchronous velocity. This is usually termed slip velocity. Since this secondary mmf is set up by rotor currents, it is carried along by the rotor so that its velocity with respect to the stator is synchronous velocity. Thus, it is stationary with respect to the primary mmf and adds to it. It is this combined mmf that sets up the actual revolving flux field.

This addition of mmfs is the basis for the analysis of the induction motor with a transformer type circuit diagram.

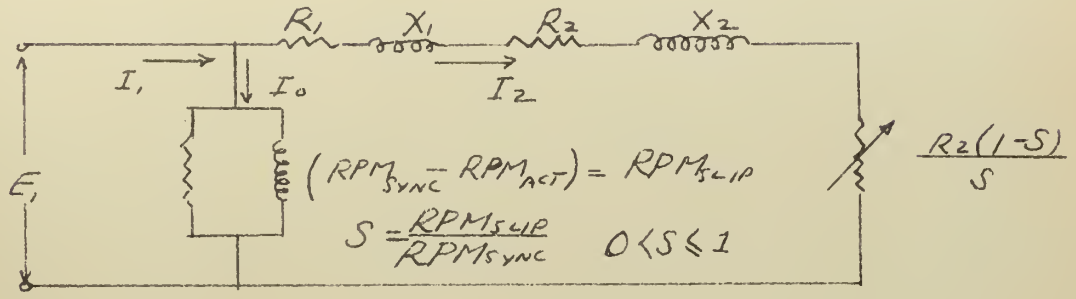

FIGURE 11 - EQUIVALENT CIRCUIT DIAGRAM - INDUCTION MOTOR

From such an equivalent circuit as shown in Figure 11, the torque developed in synchronous watts is given by

$$T = K I_2^2 \frac{R_2}{S}, \tag{38}$$

where $K = \frac{33{,}000}{2\pi\,(746)\,RPM_{sync.}}$

It should be noted that

$$\frac{R_2}{S} = R_2 + \frac{R_2\,(1 - S)}{S}, \tag{39}$$

I_2^2 may be replaced by its equivalent

$$I_2^2 = \frac{E_1^2}{(R_1 + \frac{R_2}{S})^2 + (X_1 + X_2)^2}, \tag{40}$$

so that (38) becomes

$$T = \frac{K\,E_1^2\,R_2\,S}{(SR_1 + R_2)^2 + S^2(X_1 + X_2)^2} \tag{41}$$

If for a given motor design, where all of the quantities in (41) are constant with the exception of S, torque is plotted as a function of S, a curve such as in Figure 12 will be formed. By differentiating equation (41) and setting the result equal to zero, the relation between S and the motor constants can be found. This manipulation gives

$$S = \frac{R_2}{\sqrt{R_1^2 + (X_1 + X_2)^2}} \quad \text{for maximum torque} \qquad (42)$$

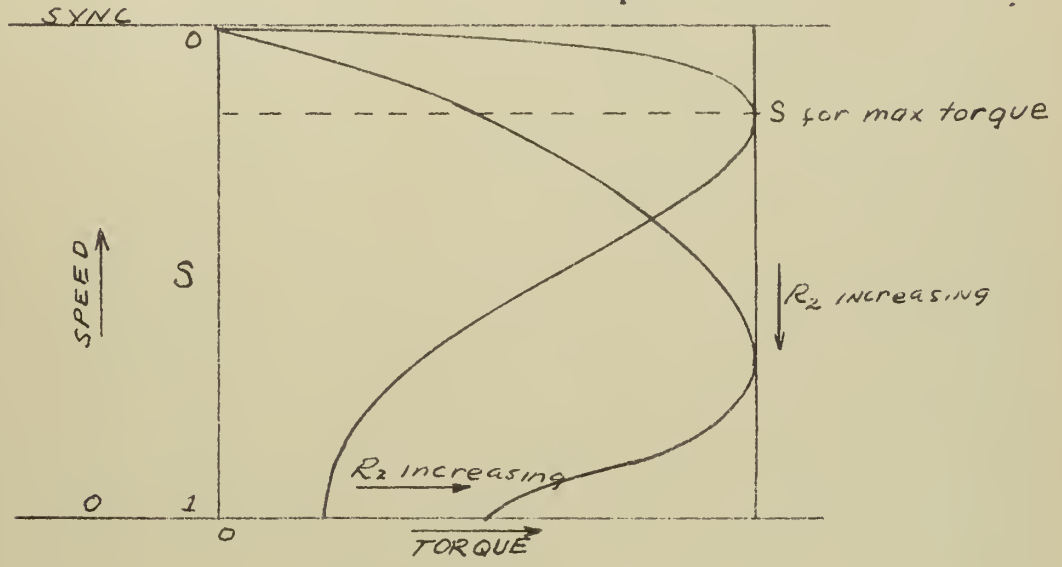

FIGURE 12 - TORQUE vs VELOCITY CURVES

Since X_1, X_2, and R_1 cannot be varied with any good effect, it becomes obvious that S for maximum torque is directly proportional to R_2. To determine the relation between maximum torque and R_2 substitution of equation (42) in (41) for S will give,

$$T = \frac{KE_1^2 \sqrt{(\quad)}}{(R_1 \sqrt{(\quad)} + 1) + \frac{(X_1 + X_2)^2}{\left[\sqrt{(\quad)}\right]^2}} \qquad (43)$$

where

$$\sqrt{(\quad)} = \sqrt{R_1^2 + (X_1 + X_2)^2}$$

Equation (43) shows no dependence on R_2 for maximum torque. Thus, looking at Figure 12, the point of maximum torque may be moved up or down the maximum torque line by merely varying R_2. For a given design, as R_2 is increased the point of maximum torque moves down. In power applications where wound rotor induction motors are normally used, additional resistance is added to the rotor circuit at starting but removed as the machine comes up to speed. This is done to prevent a lowering of efficiency which would result for sustained running with the added high rotor resistance. However, this dependence on R_2 of S for maximum torque is the important design variable in the two phase induction servomotor.

b. Operating Characteristics of the Two Phase Induction Servomotor

(1) Normal Operation

As mentioned in the preceding section, the slip velocity at which maximum torque occurs is dependent upon the magnitude of the rotor resistance. Although the efficiency of the induction servomotor is decreased, the rotor resistance is maintained at a permanent high value. This is done to provide for one of the two basic characteristics of the induction servomotor. This is, that the motor develop maximum usable torque at standstill. This characteristic allows for rapid response of the system. Carrying the increase in rotor resistance further than in Figure 12, it can be seen in Figure 13 that the point of maximum torque can be moved down into the region where S is greater than unity. If R_2 is increased beyond that value which produces maximum possible torque at starting, the maximum possible torque would be obtained only if the rotor were moving backward with respect to the field. This is

an unlikely situation, to be sure, and although the maximum usable torque still occurs at standstill, it may be considerably less than the maximum

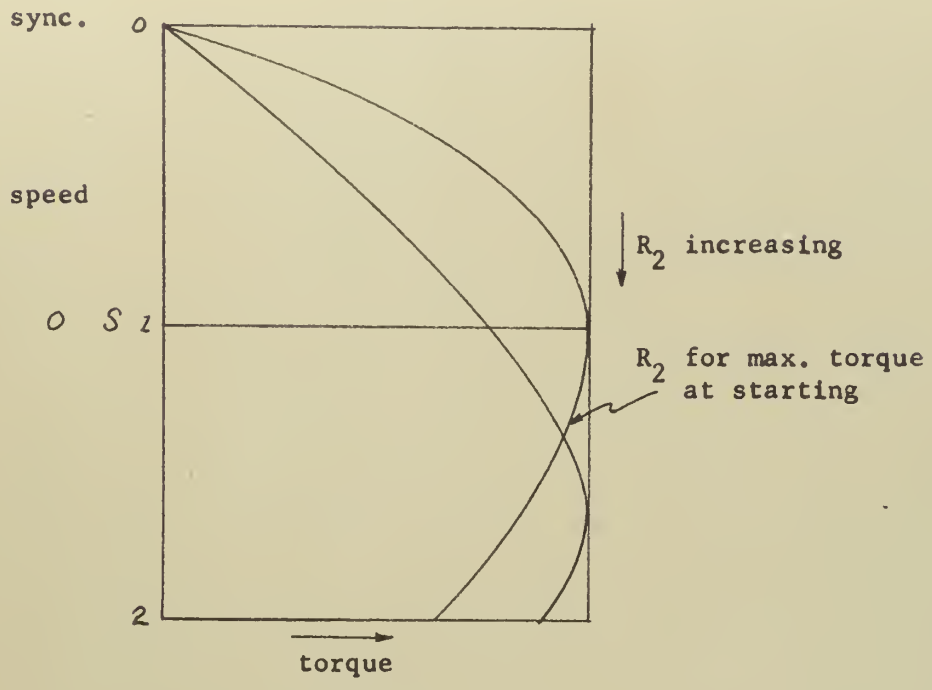

FIGURE 13 - TORQUE vs VELOCITY CURVES

possible torque obtainable from the machine with less rotor resistance. However, from Figure 13 another desirable characteristic of an induction servomotor may be seen. With R_2 increasing the torque-speed curve becomes more linear in the operating range. Although this feature may be desired, it is by no means a required characteristic. Consequently, while all two phase induction servomotors are designed with a rotor resistance sufficiently large to insure that the torque-speed curve has a negative slope at zero speed, the resistance is not large enough in most to insure a near linear torque-speed curve. One point should be emphasized with respect to this negative slope at zero speed. Unless a motor has this characteristic, its use in closed loop control systems will make the

system unstable unless sufficient load friction or derivative feedback is provided. (6)

In the following chapter where the phase plane analysis of the proposed system is undertaken, the assumption is made that the torque-speed curve is linear when the motor is operating normally. Also the internal damping factor, which is a component of the coefficient of the velocity term in the differential equation that governs the motor-load combination, is assumed constant. In applications where the motor is operated with a varying control voltage, it is generally assumed, also, that the variation of torque with control voltage is normally linear. It has been shown that in general these three assumptions are not valid. (6) However, choosing a motor of the proper design will make the first two assumptions valid. Using a relay control so that the control voltage is all-on or all-off eliminates the need for the third assumption.

(2) Single Phase Operation

In a servo application where the possibility of the control phase being equal to zero is considered, it must be assumed that the motor is in a single phase condition. Here the reference phase remains excited normally and the control phase is open. In a true single phase condition the impedance as seen by the control winding at its open terminal is infinite, and consequently no current may flow through it. It has been explained that when the stator impedance is high or the impedance of the exciting circuit is low in comparison to rotor impedance, the motor will not develop a single phasing torque. (6) This is the second basic characteristic required of two phase induction servomotors. It is desired that a single phasing torque not be developed at any speed at which the motor may be caused to rotate. A somewhat more exacting

analysis has been made by Chang. (7) He has shown that with the control phase voltage at zero, a motor will develop negative torque (braking) single phase at all speeds only if $R_2 > |Z|$ where Z is a parallel combination of the exciting impedance with stator impedance in series with external control impedance and this combination in series with rotor reactance. If R_2 is $< |Z|$ then single phasing will develop in the range where

$$0 < s < \sqrt{1 - R_2^2 / |Z|^2} \qquad (44)$$

In (44) S is defined as the ratio of actual rotor speed to synchronous speed.

In the proposed application where the control voltage circuit is to be opened or closed by relay action, the control winding will see at its terminals an infinite impedance when the relay drops out. The velocity of the motor at that time will depend upon the size of the step input and the rate of motor response. Since the velocity can be near zero or near saturation depending upon the conditions stated, the motor may tend to single phase during the short interval of time between relay drop-out and the onset of the dynamic braking.

(3) Semi-Single Phase Operation

Semi-single phase operation concerns the condition where the control phase voltage is removed but in which the control phase is looking into a finite impedance at its terminals. This condition would occur where the control phase is shorted directly or through an impedance. Koopman has shown mathematically by the method of symmetrical components that such an operation always results in a negative (braking) torque,

when imposed on a two phase induction servomotor. A necessary motor characteristic for such braking is that the motor have a torque-speed curve of negative slope at the zero speed position. The degree of linearity of the resulting torque-speed curve will depend upon the overall shape of the motoring torque-speed curve for the range of S from S = 0 to S = 2. For negative torque, or braking, at all speeds, it is necessary that the value of the torque from S = 1 to S = 2 be always greater than the torque from S = 0 to S = 1. For a motor having the characteristics shown previously as being desirable, this latter torque relation will be inherent.

Some care must be taken when considering semi-single phase operation. If the control phase is shorted through a resistance of sufficient magnitude that the induced control winding current becomes negligible, the action of the motor will be as though it were operating single phase. This phenomenon is of some concern in this investigation, since with direct current braking the magnitude of the direct current is limited by a variable resistance in series with the control winding. Thus for small braking currents, it is quite feasible that inadvertently a large enough value of resistance will have been added to the control circuit to make a motor that will normally not single phase do so. What has effectively occurred in this case is that the magnitude of $|Z|$ as noted preceding equation (44) has been increased to a value greater than R_2. Hence single phasing occurs.

3. Induction Motor Braking

Aside from the direct friction method mentioned earlier, there are many possible methods of stopping an induction motor. The obvious method is to disconnect it from the supply and, in many power applications,

where the polyphase induction motor is the prime mover, this is the method used. Another equally simple method, but one which has frequently become quite complicated in application, is the practice known as blocking the motor. This is merely the reversal of two of the phase leads. This amounts to the reversal of one phase of a two phase motor so that the driving torque is in the direction opposite the rotation. Where the starting torque of the machine is low, this method may be readily used. However, for the induction servomotor which has a high starting torque the problem with blocking arises in the removal of the reversed phase excitation at the exact instant that will let the motor stop without a velocity reversal. With low inertia rotors, blocking to standstill and reversal to full reverse velocity can occur in a fraction of a second.

The use of an eddy current magnetic brake has in recent years come into fairly wide use in speed control of many types of motors and is excellent for maintaining precise speeds which are required in some manufacturing processes. However, the application is generally to remove the braking force as the normal load increases allowing the motor to carry the increased load without a change in speed. Then when the load is decreased, the braking load is reapplied so that effectively the load on the motor is constant. It was shown earlier in this chapter that such a braking scheme might be feasible for operating a relay servo with a known ramp input.

Another method of braking an induction motor is the application of a d.c. potential to one phase when the a.c. potential to that phase has been removed. It was concluded by Specht that for most power applications this method was not as practical as blocking the motor. (8) This conclusion was based primarily on the fact that since the rotor voltage is proportional

to the slip, that with d.c. braking the induced voltages in the rotor at near synchronous speed would be nearly twice that at standstill. In a wound rotor motor the danger of insulation breakdown seemed to overshadow the reduced energy requirements of the d.c. braking. For in d.c. braking only the I^2R loss of the control winding is necessarily assumed, while with a.c. braking the act requires full torque power.

Kirkpatrick in a paper published in 1923 noted that when direct current is applied to one phase of a wound rotor induction motor with a high resistance added to the rotor circuit, the torque-speed curve obtained is practically linear. (9) He also noted that the torque-speed curve for d.c. braking with no added rotor resistance was an inverted mirror image of the driving torque-speed curve. This effect is shown in Figure 14.

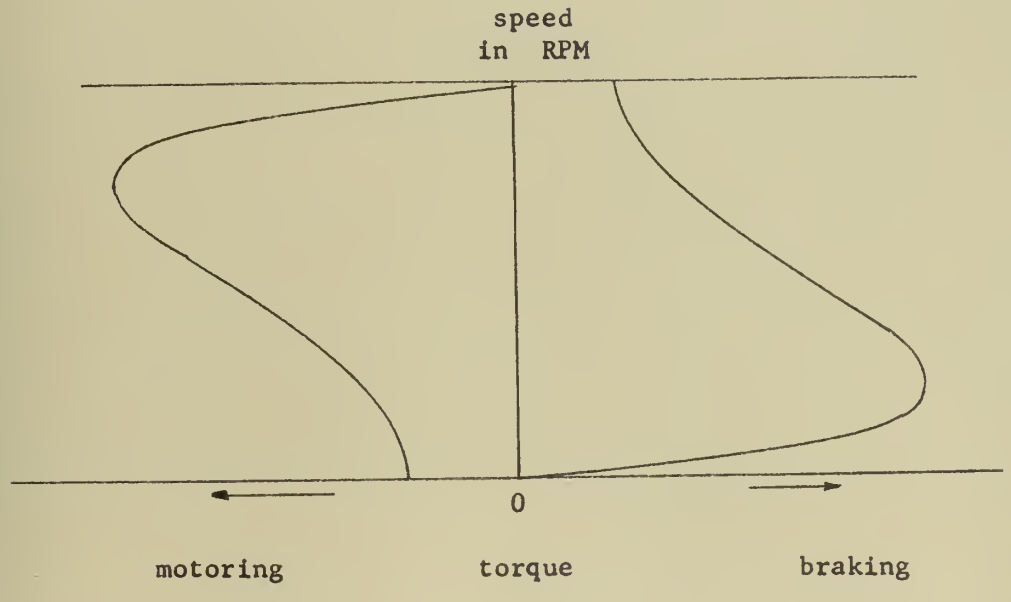

FIGURE 14 - MOTORING AND BRAKING TORQUE-SPEED CURVES

Hollander has proposed the braking of two phase induction servomotors with direct current to one or both phases. (10) When one phase

direct current application was made, the reference phase was left normally excited. He also demonstrated the effect of braking by applying an a.c. potential, of the same phase as the reference phase, to the control phase. He showed that for any given velocity the braking so obtained was greater than that obtained by braking with a comparable d.c. current. The results of his experiments are shown in Figure 15. Besides the braking methods mentioned above, Figure 15 also shows a partial curve obtained by short circuiting the control phase. These experiments were motivated by a desire to obtain a braking torque very near standstill.

Another possibility for braking the two phase induction motor is that of shorting the control phase with a suitable capacitance. The effect is similar to a direct short but has the advantage that the capacitance can be left in the control circuit at all times with little effect on the performance of the motor and still be immediately available for braking.

In this paper it was proposed that the following braking methods be investigated to obtain the desired dead zone viscous damping of the motor-load combination:

1. Direct current application to control phase at relay drop-out.
2. Direct short circuit of control phase at relay drop-out.
3. Capacitive short circuit of the control phase at relay drop-out.
4. Inherent viscous damping with the control phase remaining open at relay drop-out.

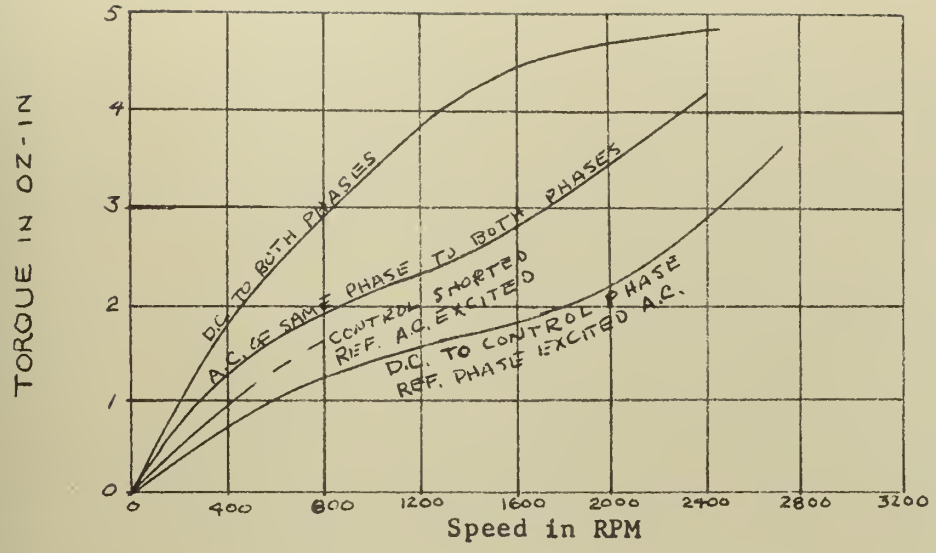

FIGURE 15 - BRAKING TORQUE-SPEED CURVES FOR A TWO PHASE INDUCTION SERVOMOTOR

CHAPTER III

PROPOSED RELAY SERVO

1. Phase Plane Analysis

a. Quasi-Optimum System

The proposed system may be called a quasi-optimum system because it departs only slightly from the optimum or best system for the operating conditions. In the optimum system the load is accelerated under maximum torque to the point where deceleration under maximum torque is commenced. Then the load is driven to a position of zero error, reaching this point simultaneously with a zero error-rate. Another optimizing requirement is that there is no overshoot. In actual practice the attainment of the optimum system would require the use of some type of nonlinear switching device or network to accomplish the torque reversal at the proper instant. Several methods have been proposed and are noted by Thaler (4) but in each case the design is either extremely difficult or expensive.

The proposed system meets the requirements of the optimum system in that there is one accelerating period, one decelerating period, and no overshoot. The departure from the optimum comes in that the deceleration is not accomplished at optimum torque. Hence the time of response will be greater than optimum.

This quasi-optimum system will use a two phase induction servomotor to accelerate the load and velocity proportional viscous damping for braking or decelerating the load. The braking will be accomplished by the application of a d.c. potential across the control phase winding when the relay opens at the end of the accelerating period. Figure 16 shows

trajectories in the dead zone of a relay servo on a phase plane plot where one has only the inherent viscous friction acting and the other has additional viscous damping as proposed.

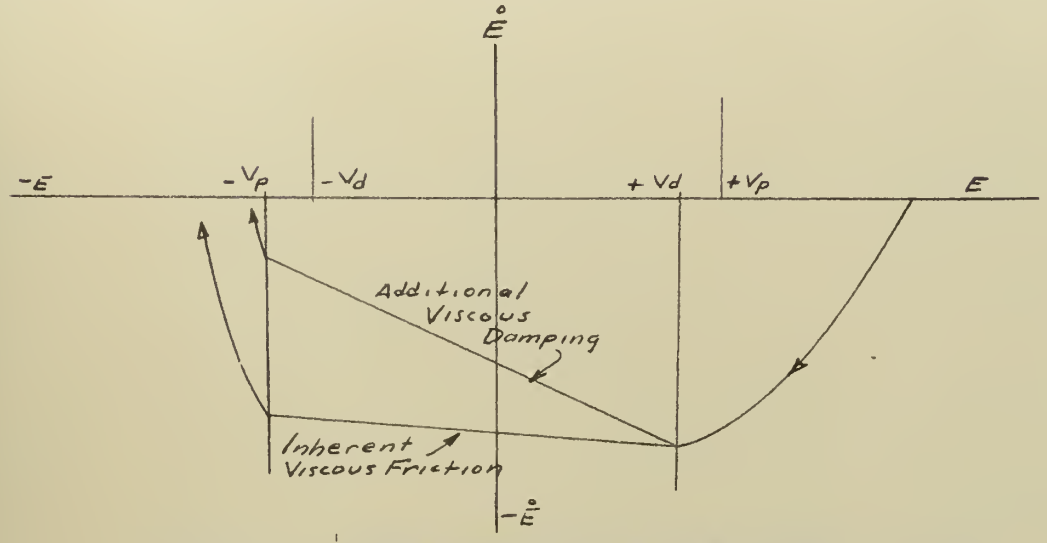

FIGURE 16 - PHASE PLANE PLOT OF RELAY SERVO WITH AND WITHOUT ADDITIONAL VISCOUS DAMPING

In the proposed system the inherent viscous friction will be limited to a very small value. Tachometer feedback will be used to rotate the switching loci counterclockwise to cause relay drop-out anticipation. In this way the trajectory on the phase plane may be shown as in Figure 17.

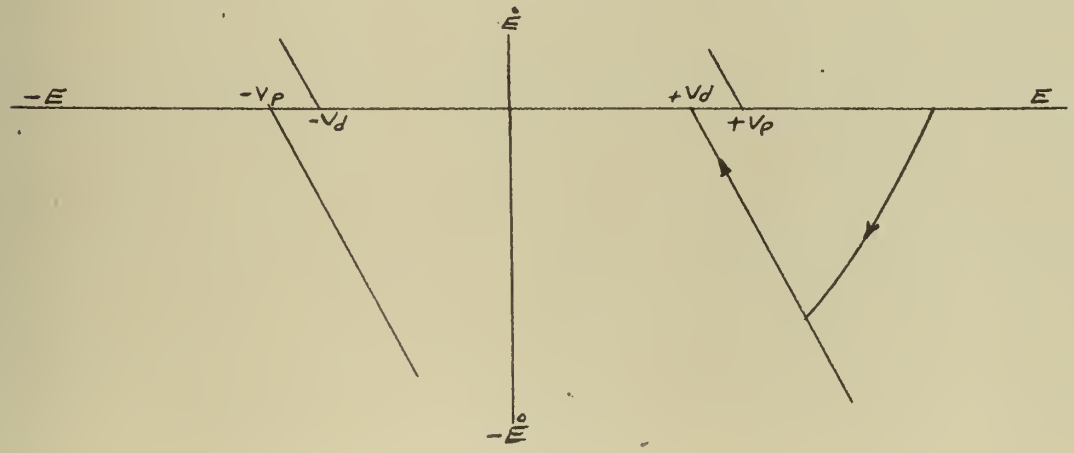

FIGURE 17 - PHASE PLANE REPRESENTATION OF THE PROPOSED RELAY SERVO USING DYNAMIC BRAKING AND TACH FEEDBACK

To analyze the system the following assumptions must be made:

1. There is no time lag in the drop-out of the relay.

2. Introduction of maximum braking force occurs simultaneously with relay drop-out.

Practically, these assumptions will not hold true, and the actual relay servo trajectory must lie within the dead zone and not on the boundary as shown in Figure 17. However, the validity of the two assumptions is subject to design modification; therefore, the analysis will be no worse for having made them.

Figure 18 is a block diagram of the proposed system with a sufficient complexity of relay components to affect both a.c. control and d.c. braking.

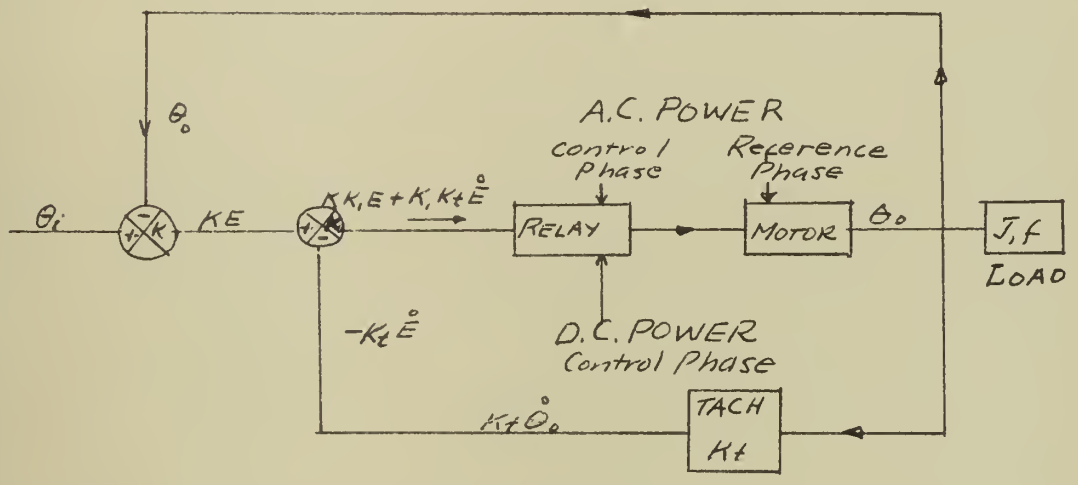

FIGURE 18 - BLOCK DIAGRAM OF THE PROPOSED SYSTEM

This is very similar to the relay servo analyzed in Chapter II, but here we do not wish to ignore coulomb friction and dynamic braking in the dead zone must be accounted for. Also two amplifications are caused to occur as shown in Figure 18. They are denoted by the factors K and K_1.

The equations governing the trajectories in the phase plane for the motor-load unit are,

$$J\ddot{\theta}_o + f\dot{\theta}_o + C = +T \qquad \text{Zone I} \qquad (45)$$

$$J\ddot{\theta}_o + f\dot{\theta}_o + C = -T_{braking} \qquad \text{Zone II} \qquad (46)$$

$$J\ddot{\theta}_o + f\dot{\theta}_o + C = -T \qquad \text{Zone III} \qquad (47)$$

with the understanding that C always opposes the velocity. As with the step input analysis of Chapter II, $\dot{\theta}_o = -\dot{E}$ and $\ddot{\theta}_o = -\ddot{E}$. Thus (45), (46), and (47) may be written

$$J\ddot{E} + f\dot{E} - C = -T \qquad \text{Zone I} \qquad (48)$$

$$J\ddot{E} + f\dot{E} - C = T_B \qquad \text{Zone II} \qquad (49)$$

$$J\ddot{E} + f\dot{E} - C = +T \qquad \text{Zone III} \qquad (50)$$

For the two phase induction servomotor the torque is proportional to the speed and to the voltage applied to the variable phase. (4) Thus,

$$T = \frac{\partial T}{\partial n} n + \frac{\partial T}{\partial e_i} e_i \qquad (51)$$

where

$$\frac{\partial T}{\partial n} = -K_n \qquad (52)$$

and

$$\frac{\partial T}{\partial e_i} = K_e \qquad (53)$$

The assumption that the torque constants K_n and K_e are constant is not always a valid one. (6) However, in this particular application it is.

The physical system will use a servomotor in which the variation of torque with speed will depart from a linear relation by a negligible amount. And in the relay servo, since only rated voltage will be supplied to the variable or control phase, the variation of K_e from an actual constant value is of no consequence.

Thus the Zone I equation may be written as,

$$J\ddot{E} + f\dot{E} - C = -(K_n \dot{E} + K_e e_i) \tag{54}$$

where $K_e e_i$ is a constant value, V_c. Manipulating for phase plane plotting (54) becomes,

$$J\ddot{E} + \dot{E}(f + K_n) - C = -V_c; \quad \text{then} \tag{55}$$

$$\ddot{E}/\dot{E} = \frac{d\dot{E}}{dE} = -\left(\frac{f + K_n}{J}\right) - \left(\frac{V_c + C}{J\dot{E}}\right) \qquad \text{Zone I} \tag{56}$$

Equation (50) for Zone III can be similarly formed into

$$\ddot{E}/\dot{E} = \frac{d\dot{E}}{dE} = -\left(\frac{f - K_n}{J}\right) + \left(\frac{V_c + C}{J\dot{E}}\right) \qquad \text{Zone III} \tag{57}$$

Since in both Zones I and III the motor-load unit is undergoing an acceleration the effect of coulomb friction is negligible. With equations (56) and (57), a knowledge of the motor-load constants allows a plotting of horizontal isoclines for selected slope values for $d\dot{E}/dE$ in Zones I and III quite readily.

In Zone II it was assumed that the braking force acted immediately on relay drop-out. Therefore, the application of a d.c. potential to

the control phase is assumed to build up immediately a stationary field of strength B in the motor air gap. Then the torque opposing the rotation will be,

$$T_b = Bli_r \tag{58}$$

where i_r is the average current induced in a rotor conductor of length l. Since the voltage and, hence, current in the rotor is proportional to the rate at which the conductors cut the lines of flux, (58) may be written,

$$T_b = K_b \dot{\theta}_o \tag{59}$$

or since $\dot{\theta}_o = -\dot{E}$

$$T_b = -K_b \dot{E} \tag{60}$$

Therefore, (49) can be rewritten as,

$$J\ddot{E} + f\dot{E} - C = -K_b\dot{E} \qquad \text{and} \tag{61}$$

for phase plane plotting this may be formed into,

$$\ddot{E}/\dot{E} = \frac{d\dot{E}}{dE} = -\left(\frac{f + K_b}{J}\right) + \frac{C}{J\dot{E}} \quad \text{Zone II} \tag{62}$$

Except for the term $C/J\dot{E}$, the slope, in the dead zone, of the trajectory would be constant and equal to $-(f + K_b/J)$. Thus, the effect of coulomb friction in the dead zone becomes apparent, remembering that coulomb friction always acts in the direction to oppose the velocity. As the error-rate approaches zero, the coulomb friction effect increases

the slope of the trajectory toward the vertical, adding to the braking effect. Thus the system will dead beat with an error slightly larger than if the coulomb friction were ignored. It should be noted that even though $\dot{E}$ approaches zero, the fraction C/J is normally very small. The time that coulomb friction is effective may indeed be quite short, if the amount of viscous damping due to the dynamic braking is large. In other words, if the ratio K_b/J is very much larger than C/J, the effect of coulomb friction on the dead zone trajectory may be negligible.

It is now necessary to determine the various system constants necessary to make the dead zone trajectory and the switching loci parallel. Thus noting that the switching criterion for drop-out when $\dot{E}$ is negative is,

$$KK_1E + K_1 K_t\dot{E} = V_D \tag{63}$$

the slope of the drop-out switching loci at the end of the accelerating phase would be,

$$\frac{d\dot{E}}{dE} = - \frac{K K_1}{K_1 K_t} = - \frac{K}{K_t} \tag{64}$$

By equating applicable parts of equations (62) and (64) and neglecting $CJ/\dot{E}$, we have

$$\frac{(f + K_b)}{J} = \frac{K}{K_t} \tag{65}$$

It was noted above that the proposed system would be designed so that the factor f/J would be negligible. Therefore, the matching of the slope of the trajectory to the relay switching loci is merely a matter of varying the amplification of the error signal and/or the amount of tachometer feedback for a given d.c. braking current. A more detailed

method of the computations required is carried out in Appendix A and Appendix B.

If a ramp input, $\theta_i = wt$, is used instead of a step input, then an alteration in equation (62), the dead zone isocline equation, is to be expected. Equation (46) for Zone II becomes

$$J\ddot{E} + f(\dot{E} - w) - C - T_B = 0 \qquad (66)$$

where $T_b = K_b \dot{\theta}_o = K_b (w - \dot{E})$. Then (66) becomes,

$$J\ddot{E} = -(f + K_b) E + (f + K_b) w + C \qquad (67)$$

Rearranging and dividing by $d\dot{E}/dt$,

$$\ddot{E}/\dot{E} = \frac{d\dot{E}}{dE} = -\left(\frac{f + K_b)(\dot{E} - w)}{J\dot{E}}\right) + \frac{C}{J\dot{E}} \quad \text{Zone II} \qquad (68)$$

Equation (68) is analogous to (62) for the step input. Even if the effect of coulomb friction in (68) is negligible, the fact that $\dot{E}$ is varying with time will make the slope of the trajectory a variable also. The calculations required for the system constants for a ramp input are also shown in Appendix A and Appendix B.

b. The Practical System

In the preceding section the analysis was carried out under a set of idealizing assumptions. These were: that there is no relay time lag at drop-out, negligible inherent viscous friction, immediate application of the d.c. potential at drop-out, and negligible rise time in the build up of the stationary field in the motor. All of these conditions,

if they are not negligible, have an effect on the dead zone trajectory. In any practical system these must be dealt with to assure optimization of the system with the components available. As was noted in Chapter II, drop-out delay is due to the inertia of the moving relay parts in opening to an air gap sufficient to break the arc. In the proposed system wherein a 400 cycle, 115 volt supply is used, the delay at any time will be a combination of the effect of arcing and relay inertia. If the relay starts opening when the control potential is near zero, the total delay will not be as long as if the potential were at its maximum value. Added to this delay will be the delay in the closing of the d.c. contacts. It is possible, however, to have the d.c. arc strike with or slightly before the breaking of the a.c. arc. This could eliminate or at least minimize this delay of d.c. contact closure.

The build up time of the stationary field is not negligible. An initial curvature on the phase plane will be noted immediately after the d.c. contact is made.

With a negligible amount of viscous friction in the motor-load combination one might expect that on the phase plane plot, between the time of true drop-out and the striking of the d.c. arc, that the trajectory would be horizontal. However, the two phase induction servomotor has design criteria that add viscous friction in this particular interval. These are that the motor will not run or start single phase. This feature of the two phase induction servomotor is essential. Thus, although the effect of viscous friction is negligible when the control phase is normally excited, the effect in the dead zone may be noticeable. Figure 19 is a phase plane plot in which all of the above mentioned effects are brought out. If the delays noted in Figure 19 are consistent, then in

the calculations for dead zone width or desirable dead beat error position, the effect of such delays may conveniently be given consideration.

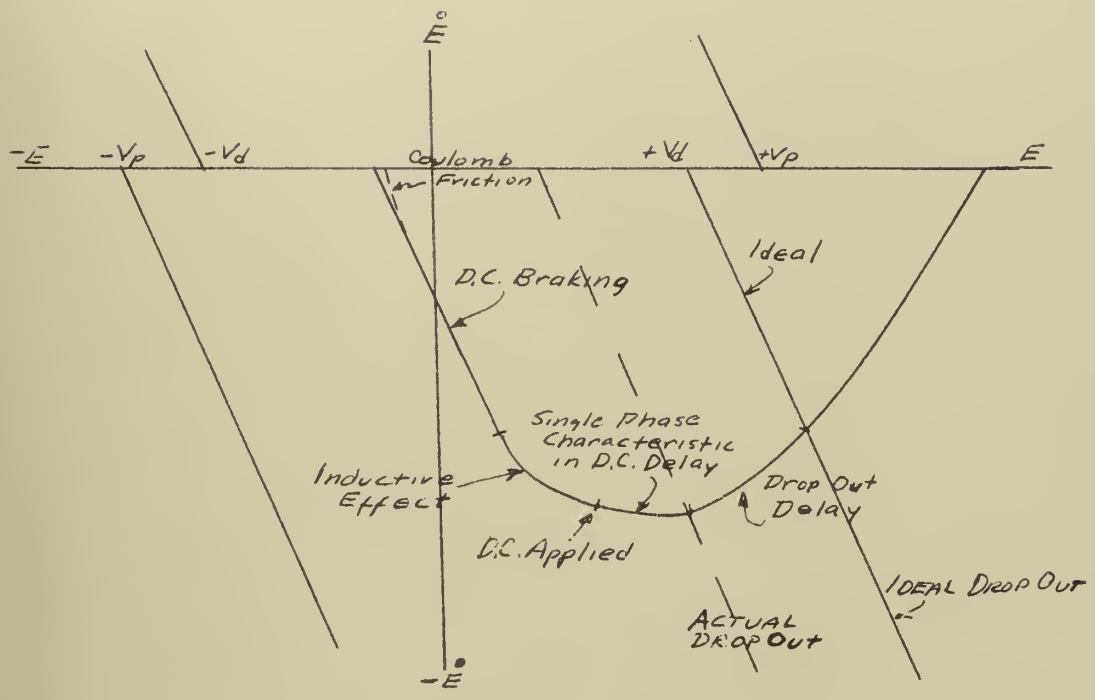

FIGURE 19 - PHASE PLANE PLOT OF AN ACTUAL DEAD ZONE TRAJECTORY AS COMPARED TO THE IDEAL

CHAPTER IV

EXPERIMENTAL RESULTS

To verify the theory as set forth in the preceding chapters, a series of experiments were conducted. These were designed to lead to the evaluation of discontinuous damping of a relay servo, the torque element of the servo being a two phase induction servomotor.

The experiments were of three categories. First, the torque-speed characteristics of three two phase induction servomotors were determined using direct current braking, resistance and capacitance short circuit braking, and open circuit braking. Then the retardation, or position versus velocity, characteristics for one of the three motors were determined under the same braking conditions. Finally the relay servo was built up using the latter motor. The servo was subjected to various step and ramp inputs and the relay operated with various dead zone parameters to determine the effect for the several braking methods upon the rate of response, stability, and the static accuracy of the system.

1. Torque-Speed Tests

   a. Direct Current; Open Circuit; Short Circuit Braking Tests

The three motors chosen for the torque-speed tests were a Kearfott 400 cycle, a Diehl 400 cycle, and a Diehl 60 cycle motor. All three as noted above are two phase induction servomotors. There was no apparent reason to select one two phase induction servomotor in preference to any other. The choice as made was based on the availability of the motors and the manufacturer's data.

A dynamometer was used to obtain the torque-speed characteristic curves. This device utilized a d.c. motor, coupled to the motor being

tested through a hydraulic transmission. The rotor of the induction motor was the driven part and torque developed was observed as an attempted rotation of the stator. The stator was rigidly connected to a cross arm and both were free to rotate. The cross arm was marked so that calibrated weights could be used to counterbalance the torque being transmitted to the stator at various rotational speeds of the rotor. The rotor velocity was measured directly by a hand tachometer or stroboscope.

To examine completely the torque speed characteristics of the three motors when a d.c. current is passed through one or both of the phases, the following tests were made.

CONTROL PHASE	REFERENCE PHASE
1. Direct Current from three sources (battery, full rectified 400 or 60 cycle, half rectified 400 or 60 cycle)	Energized with 115 volts, 400 or 60 cycle.
2. Open Circuit	Energized as in 1.
3. Short Circuit	Energized as in 1.
4. Direct Current - one value from the three sources	Not energized - open
5. Direct Current - one value from the three sources	Not energized - shorted
6. Direct Current - one value	Direct Current - one value

(1) Kearfott 400 Cycle Motor Tests

This motor was the first tested and Figures 20, 21, and 22 describe the results of these tests. Figure 20 shows the variation in braking torque with velocity when various magnitudes of direct current are passed through the control winding with the fixed phase

normally excited. This figure incorporates the torque-speed curves derived when the control was open and when the control was shorted. The motoring torque curve on the left of Figure 20 is from the manufacturer's data on the particular motor.

Figure 21 shows the torque-speed curves developed when a specific direct current magnitude was passed through the control winding and the fixed phase was subjected to various excitation. A direct current of 200 ma. was imposed on the control phase since this was an intermediate value for the magnitudes used in Figure 20. The 200 ma. curve from Figure 20 is plotted on Figure 21 for comparison.

Figure 22 shows a comparison between the use of a battery d.c. source and full wave rectification of the 400 cycle supply. The tests were also made using half wave rectification. However, motoring occurred with all three motors. No attempt was made to stop this motoring by the use of filters.

Various points should be noted in the three figures for this motor. The torque-speed curve when acting with both phases normally energized is nearly linear. The braking curves developed with application of a d.c. supply to the control phase is as linear as the experimental method could detect. The torque due to the inherent viscous friction of the motor with the control phase open is always opposite to the rotation. This is of some importance, since this shows that under normal operating conditions this motor will not single phase from any speed. The torque developed when the control phase only is shorted is also always positive as expected and is linear with respect to velocity. The braking torque developed by shorting the control phase is approximately the same as attained by braking with 75 ma. of direct current. A 25 ma. braking

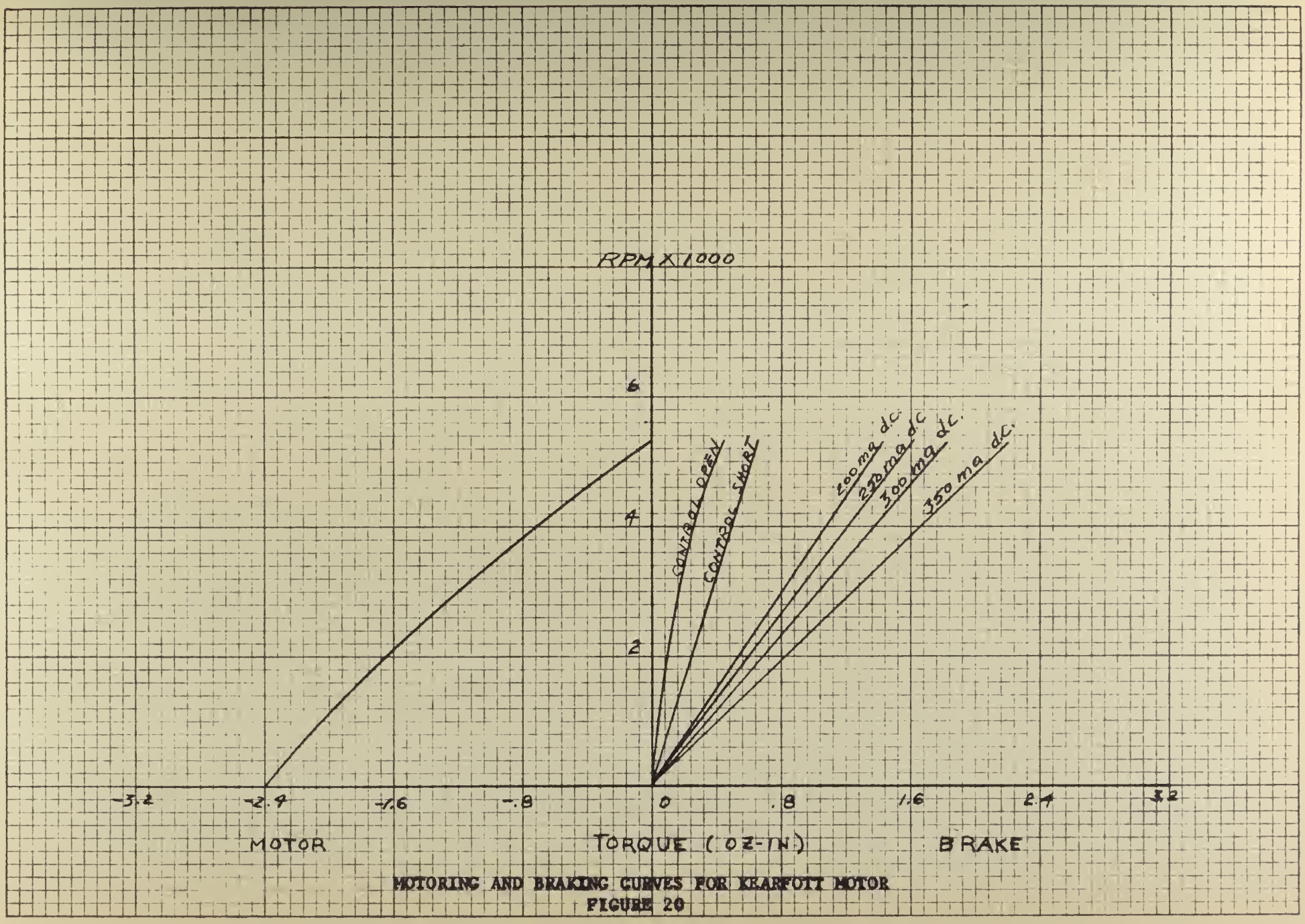

MOTORING AND BRAKING CURVES FOR KRAFFOTT MOTOR
FIGURE 20

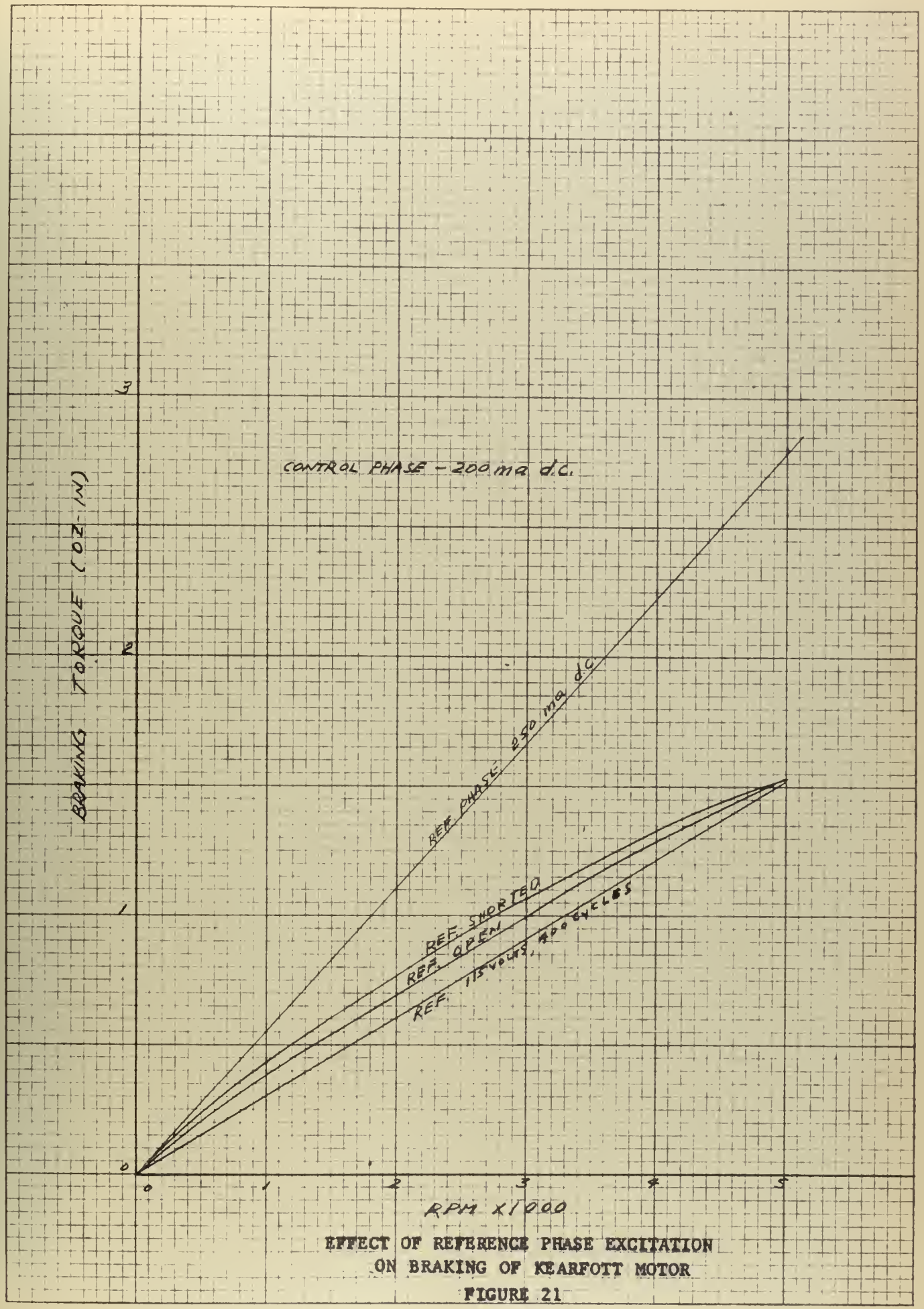

EFFECT OF REFERENCE PHASE EXCITATION
ON BRAKING OF KEARFOTT MOTOR
FIGURE 21

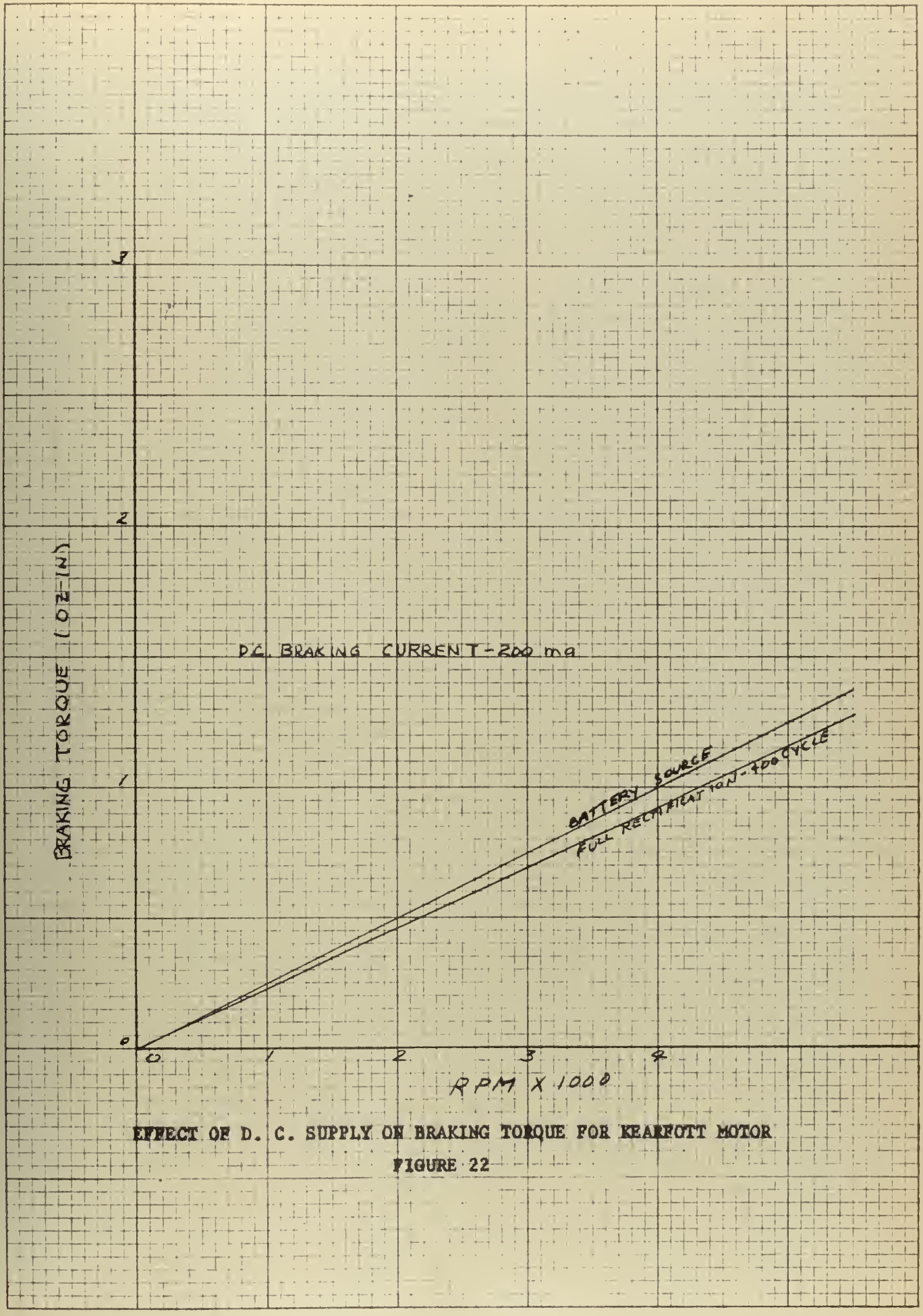

EFFECT OF D. C. SUPPLY ON BRAKING TORQUE FOR KEARFOTT MOTOR

FIGURE 22

current approximates the braking, if the control phase is simply opened. The braking torque for 350 ma. attains a magnitude at rated velocity about equal to the starting torque for the motor. Higher values of braking torque could have been obtained. The effect on braking of the reference phase being open, shorted, or normally energized is negligible when direct current braking is used.

(2) Diehl 400 Cycle Motor Tests

The investigation of this motor was limited to about one-half of its maximum speed due to the output maximum velocity of the dynamometer of about 6000 RPM. However, the values obtained are a good indication of the information desired from the tests and the speed limitation is not important. The stroboscope was used to measure the maximum no load single phase velocity. In this instance the rotor was disconnected from the hydraulic transmission and allowed to run free.

Figures 23, 24, and 25 for the Diehl 400 cycle motor represent the same type of data as given in Figures 20, 21, and 22 for the Kearfott 400 cycle motor. Some pertinent features displayed by these figures should also be noted. The motoring torque-speed curve is much less linear than for the previous motor. The braking torque-speed curves are also not linear. With the use of a high value braking current, the curve obtained is almost an inverted mirror image of the motoring torque curve. The control open circuit curve shows definite single phasing. The braking curve for the condition of the control shorted is linear.

An interesting part of the investigation was noted when the control phase for this motor was shorted through various resistances. At a shorting resistance of 250 ohms or greater the motor would single phase. Below 200 ohms the motor developed braking torque. When a 115 volt d.c. supply was imposed on the control phase with sufficient resistance in-

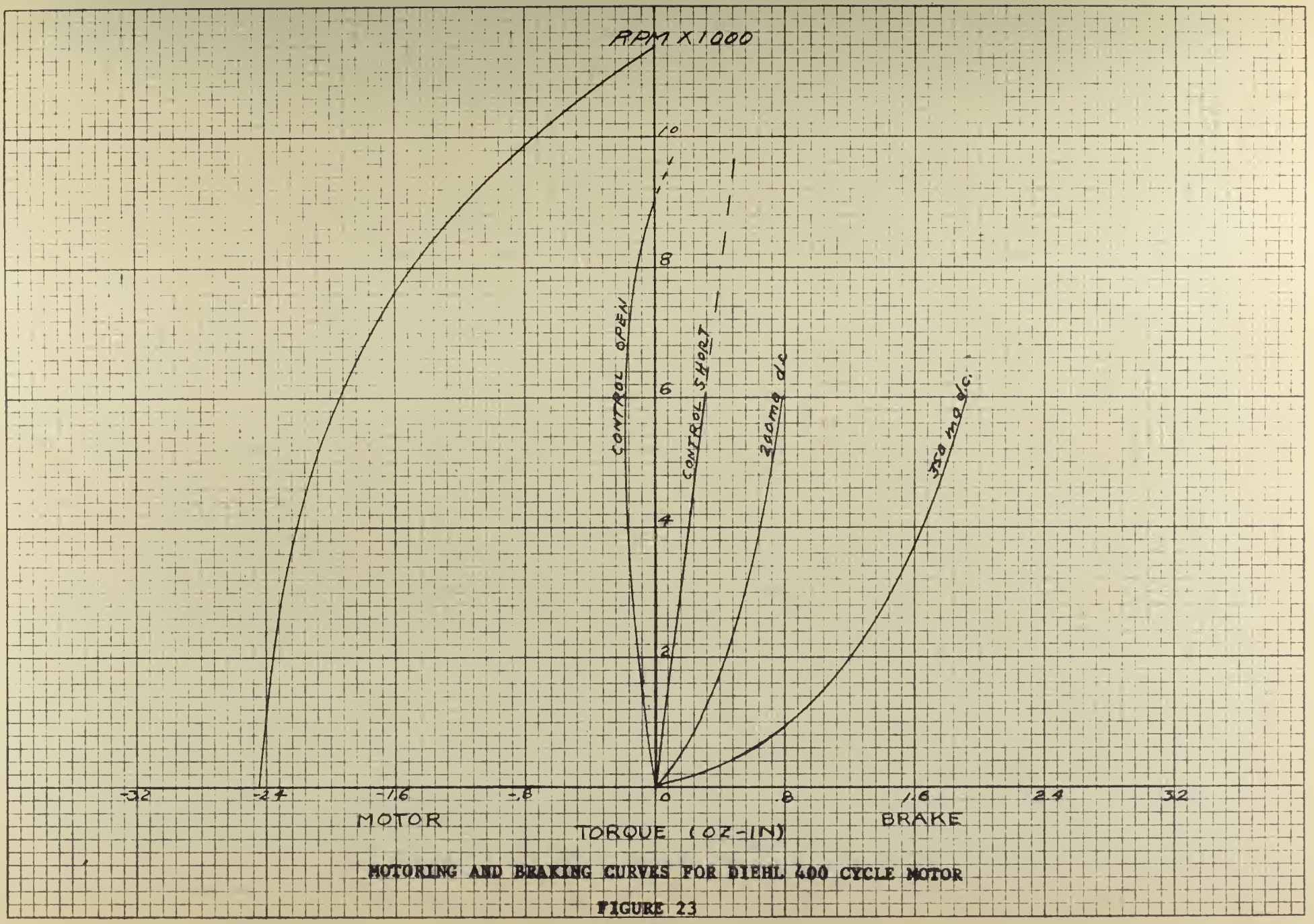

MOTORING AND BRAKING CURVES FOR DIEHL 400 CYCLE MOTOR

FIGURE 23

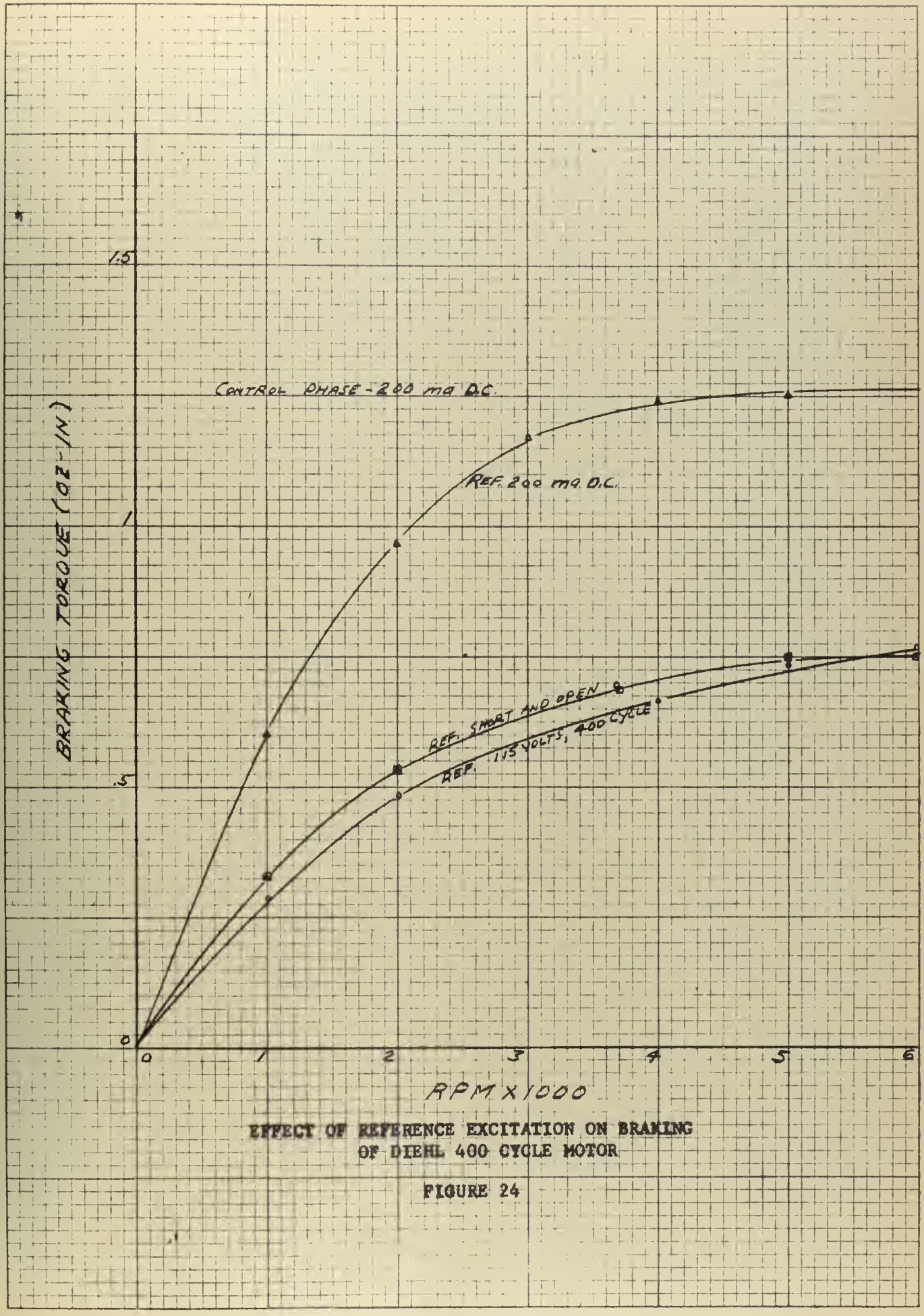

EFFECT OF REFERENCE EXCITATION ON BRAKING
OF DIEHL 400 CYCLE MOTOR

FIGURE 24

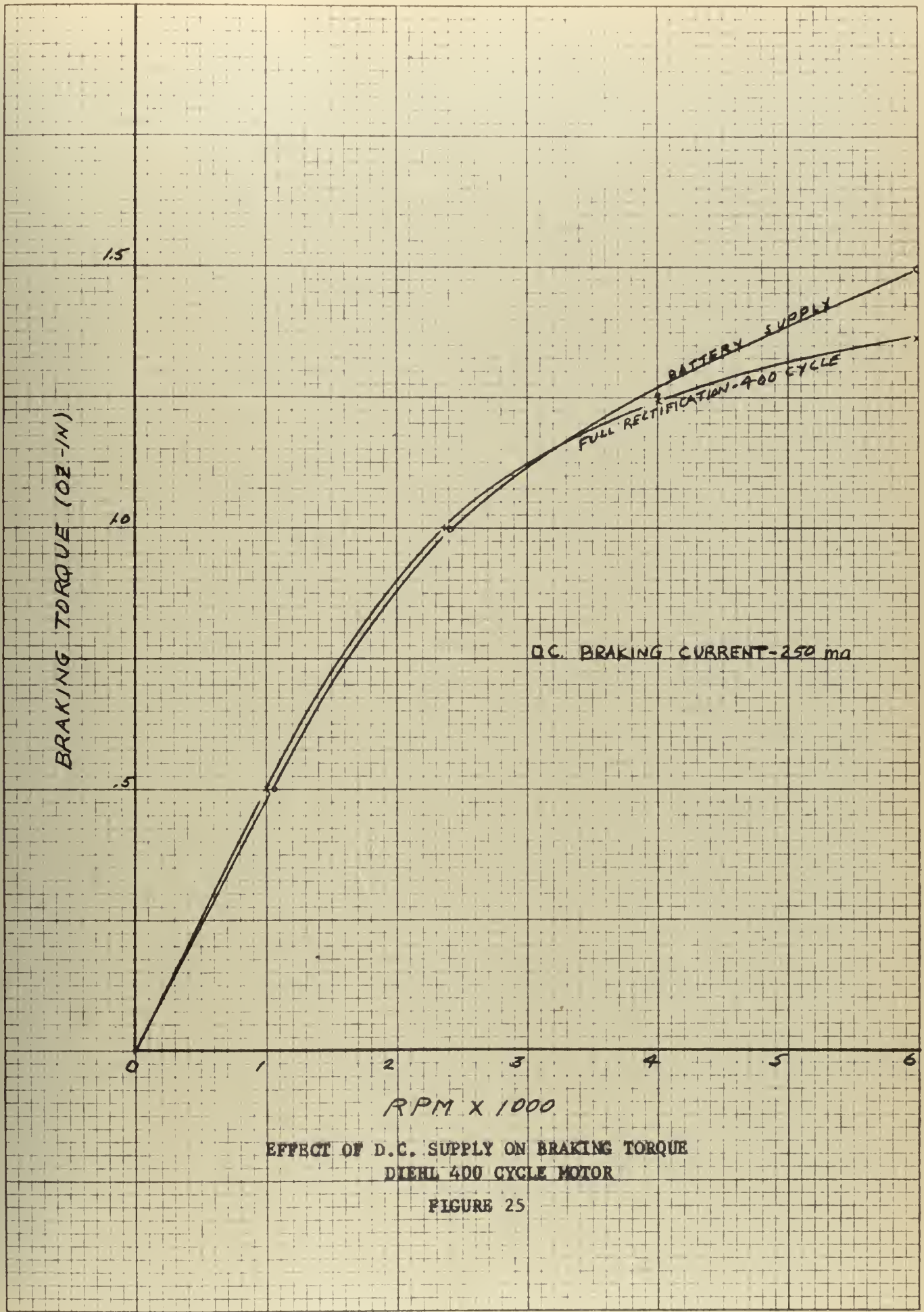

EFFECT OF D.C. SUPPLY ON BRAKING TORQUE
DIEHL 400 CYCLE MOTOR

FIGURE 25

serted as a current limiter, it was found that the motor would single phase and carry a maximum braking current of 100 ma. Since this is essentially the method used in direct current braking, it is obvious that part of the d.c. braking current is being dissipated in overcoming the single phasing torque. Since the single phasing tendency is not a linear relation with speed, the torque speed curves for direct current braking should also not be linear. This has already been pointed out as the case in Figure 23.

The effect on braking by varying the control short circuited resistance led to the use of capacitance short circuit braking. The advantages have been discussed in a previous chapter and the experimental results of such control circuit manipulation will be shown later.

(3) Diehl 60 Cycle Motor

The Diehl 60 cycle motor investigated has a no load speed of approximately 3350 RPM and a maximum starting torque of 5.5 ounce-inches. Figure 26 shows that with only 200 ma. of direct current a higher braking torque can be obtained. Figures 27 and 28 are comparable to Figures 21 and 22 for the Kearfott motor. These latter figures also show the lack of effect of reference excitation on d.c. braking and the small variation when full rectified 60 cycle voltage was used as the braking potential.

It should be noted in Figure 26 that while the braking torque-speed curve is not linear for 200 ma., it is nearly so for velocities under 1500 RPM. For a direct current of 350 ma. the linearity reaches to 2500 RPM. This could be put to advantage wherein the motor speed was restricted by a viscous damping proportional to the speed. So loading the motor to keep its speed within the linear braking range would allow

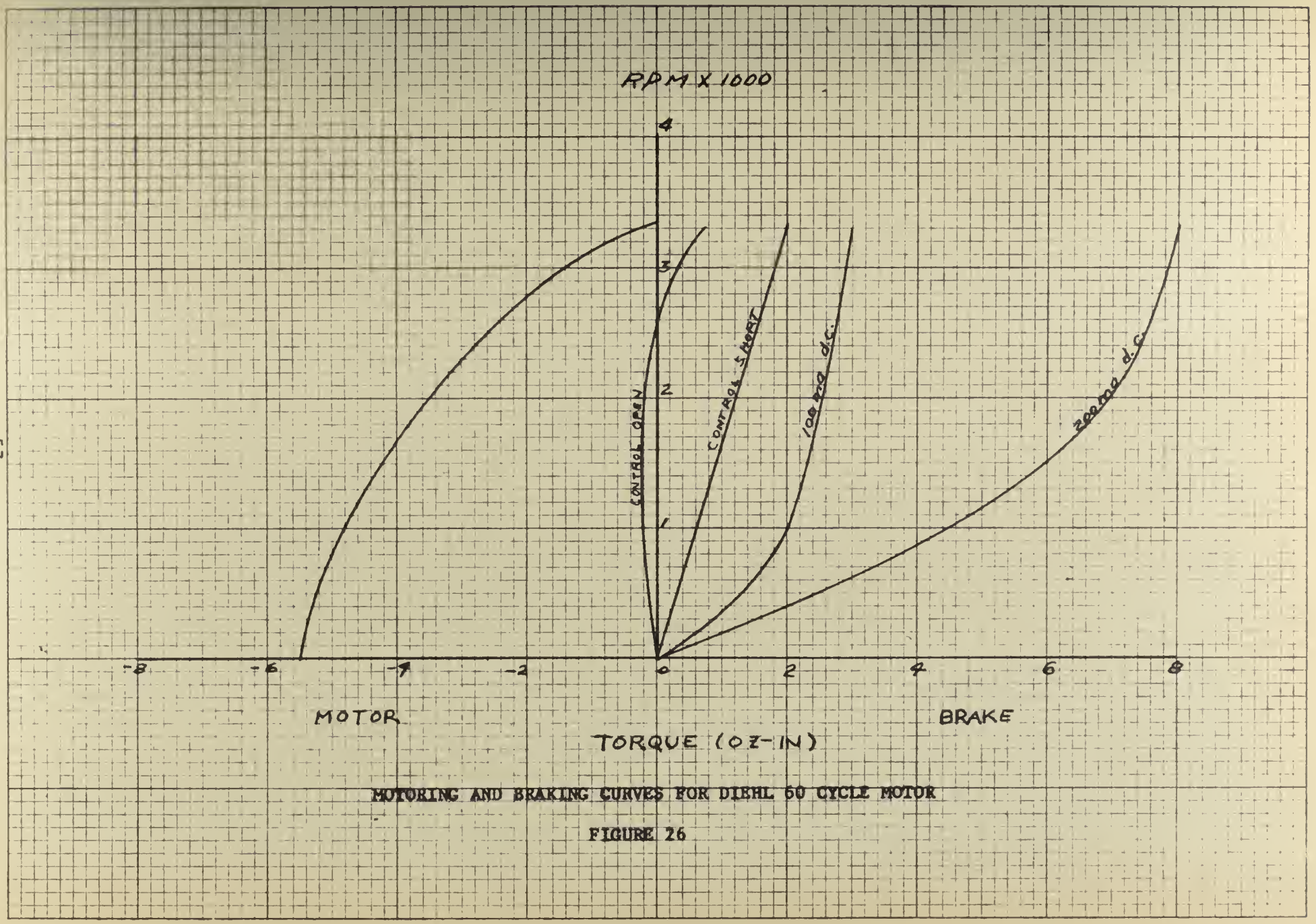

MOTORING AND BRAKING CURVES FOR DIEHL 60 CYCLE MOTOR

FIGURE 26

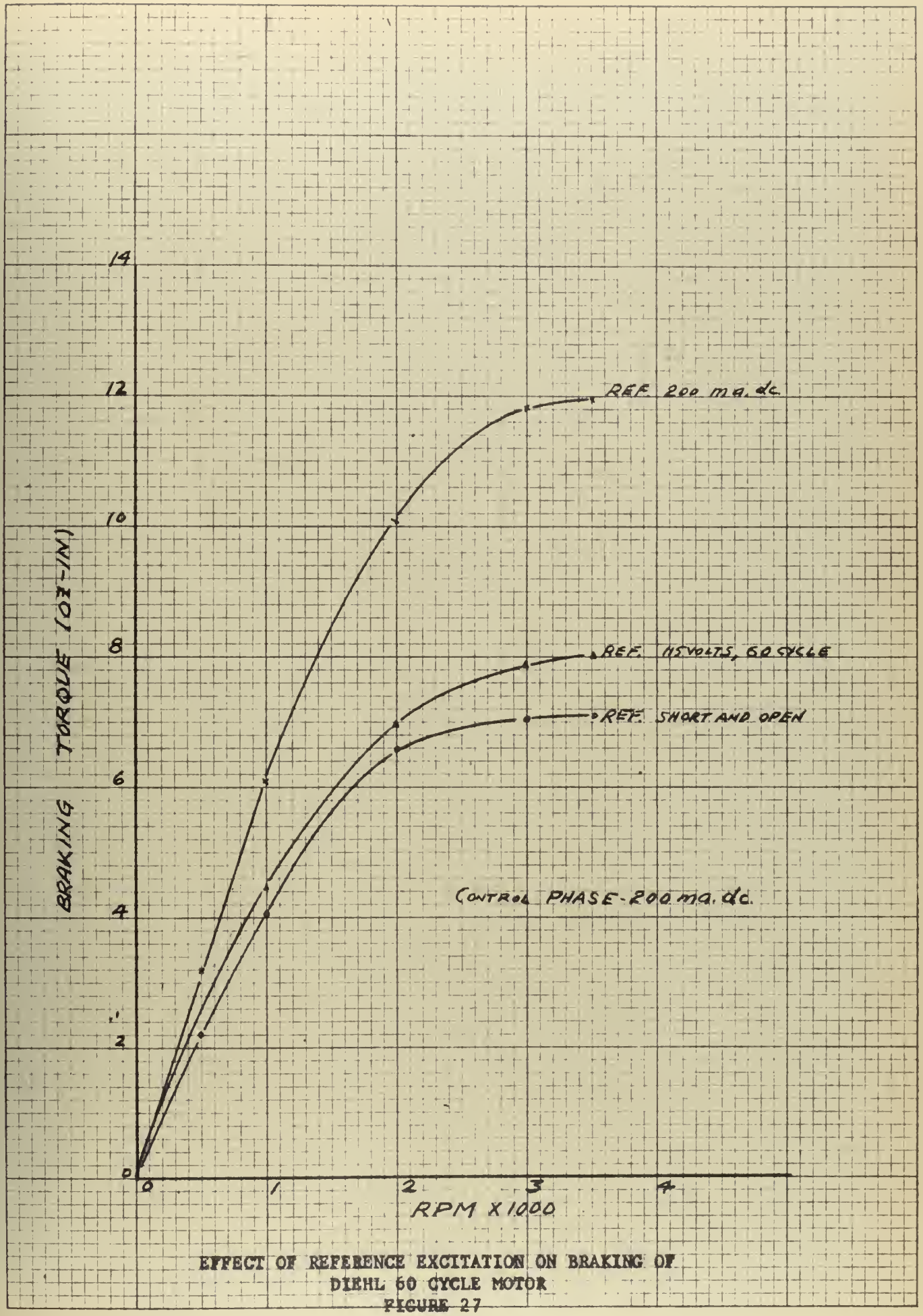

EFFECT OF REFERENCE EXCITATION ON BRAKING OF
DIEHL 60 CYCLE MOTOR
FIGURE 27

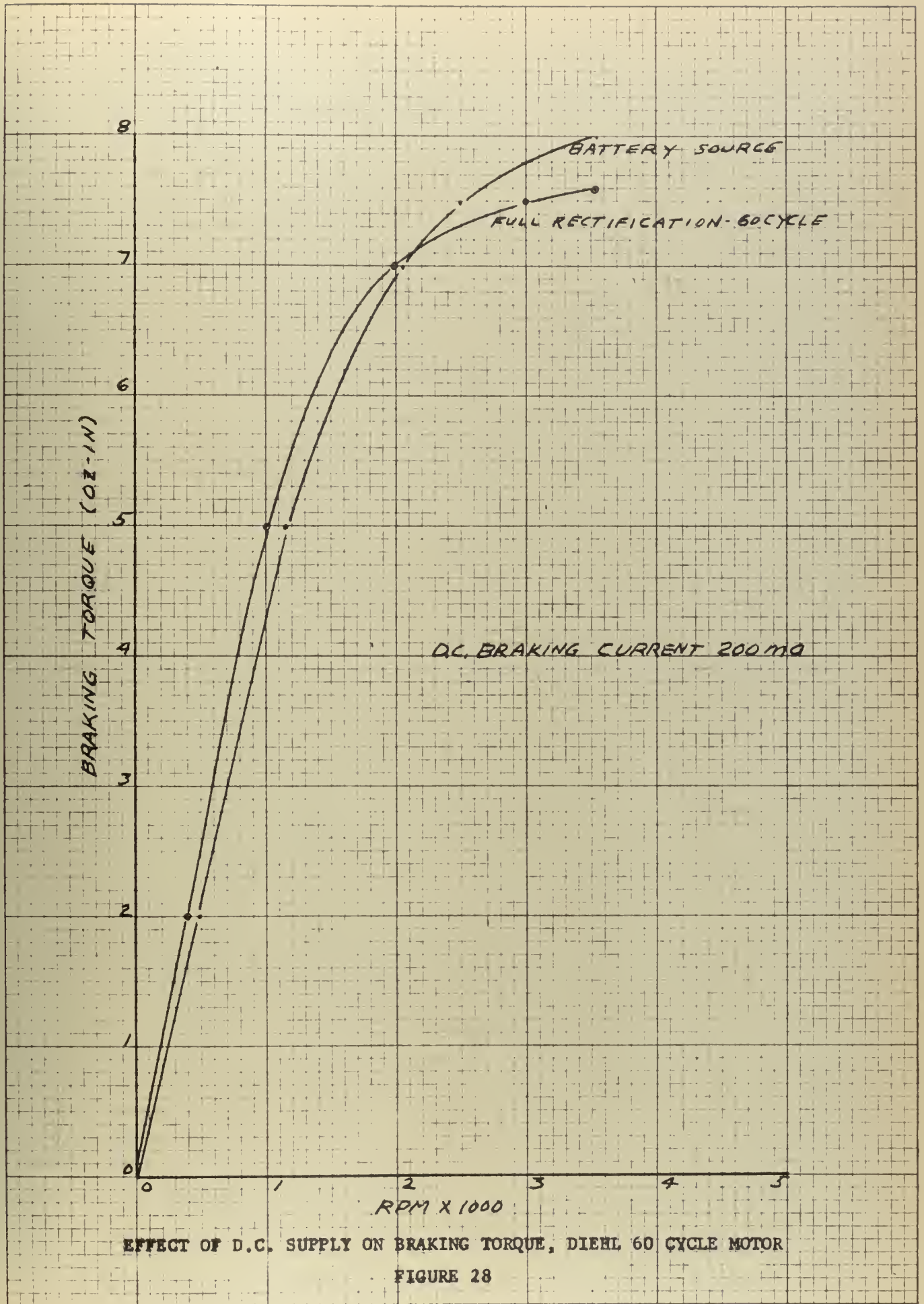

EFFECT OF D.C. SUPPLY ON BRAKING TORQUE, DIEHL 60 CYCLE MOTOR

FIGURE 28

partial utilization of the advantages of the proposed system.

b. Braking with Capacitance Short on Control Field

The torque-speed curves for the three motors already discussed were then determined under the condition of a shorting capacitor being inserted across the control terminals of the motor. The fixed phase was energized with the appropriate 400 or 60 cycle supply and the rotor was driven by the dynamometer at a fixed velocity in the mid-speed range of the particular motor. The value of capacitance was varied from zero (open circuit condition) to a value above that necessary to provide voltage and current resonance of the control winding.

With each motor so connected it was found as shown in Figures 29, 30, and 31 that the braking torque developed dropped to a minimum and then increased to a value where it remained relatively constant regardless of the magnitude of capacitance used. The minimum braking occurred at a value greater than that necessary for current resonance. With both the Diehl motors, single phasing torque increased at voltage resonance. The Kearfott 400 cycle motor could also be made to single phase at low velocities where the peak negative torque was sufficient to overcome the open circuit braking torque. However, the optimum capacitance determination for the Kearfott 400 cycle motor was made at a velocity of 4000 RPM where, regardless of capacitance, single phasing will not occur.

In any situation where such a scheme is used for braking, the smallest capacitor compatible with obtaining the near maximum braking torque would be used. This optimum capacitance as noted in Figures 29, 30, and 31 was then used to develop the torque velocity curves for the particular motor.

The results determined as shown in Figures 32, 33, and 34 have superimposed upon them the short circuit braking curves for comparison. It

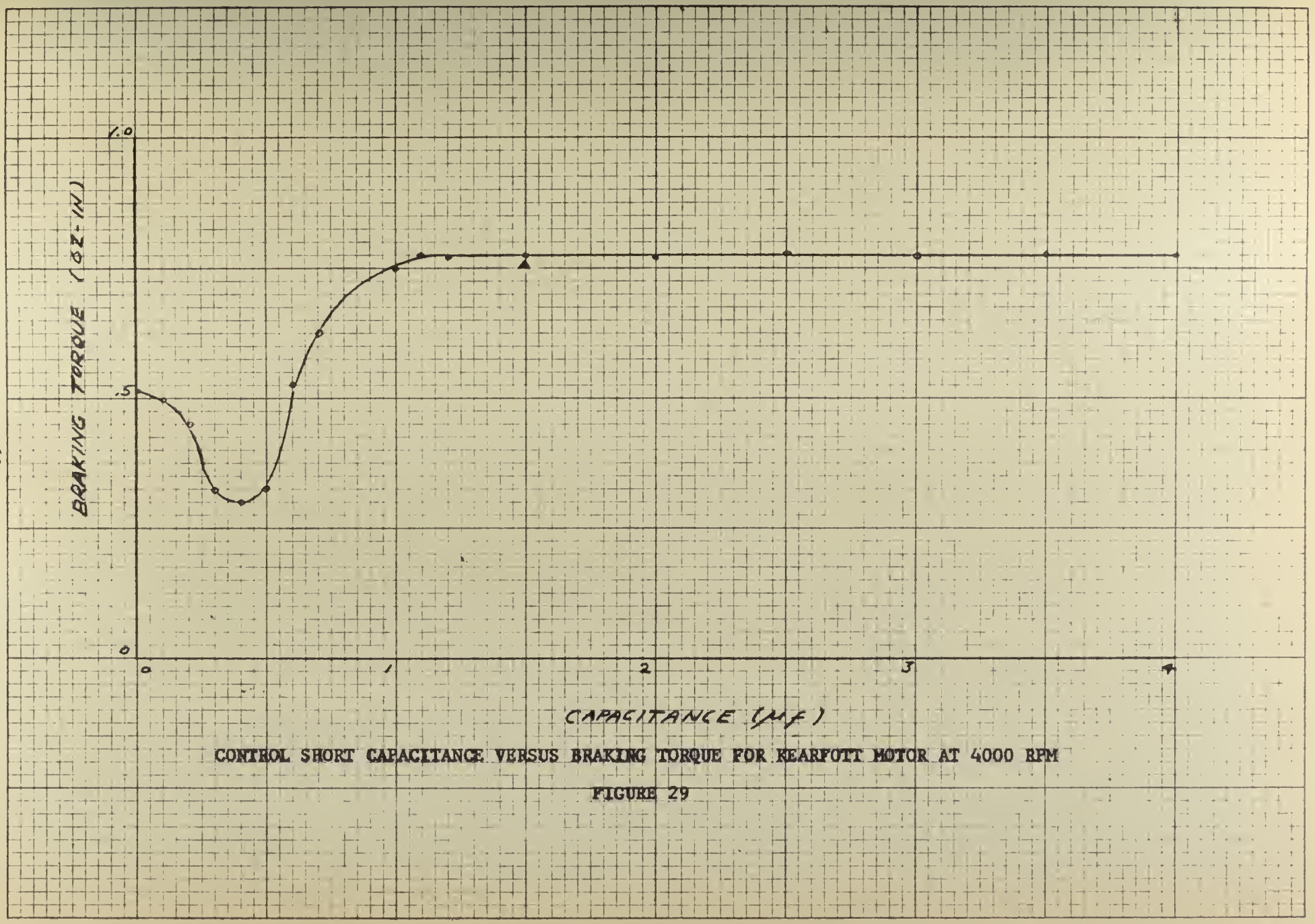

CONTROL SHORT CAPACITANCE VERSUS BRAKING TORQUE FOR KEARFOTT MOTOR AT 4000 RPM

FIGURE 29

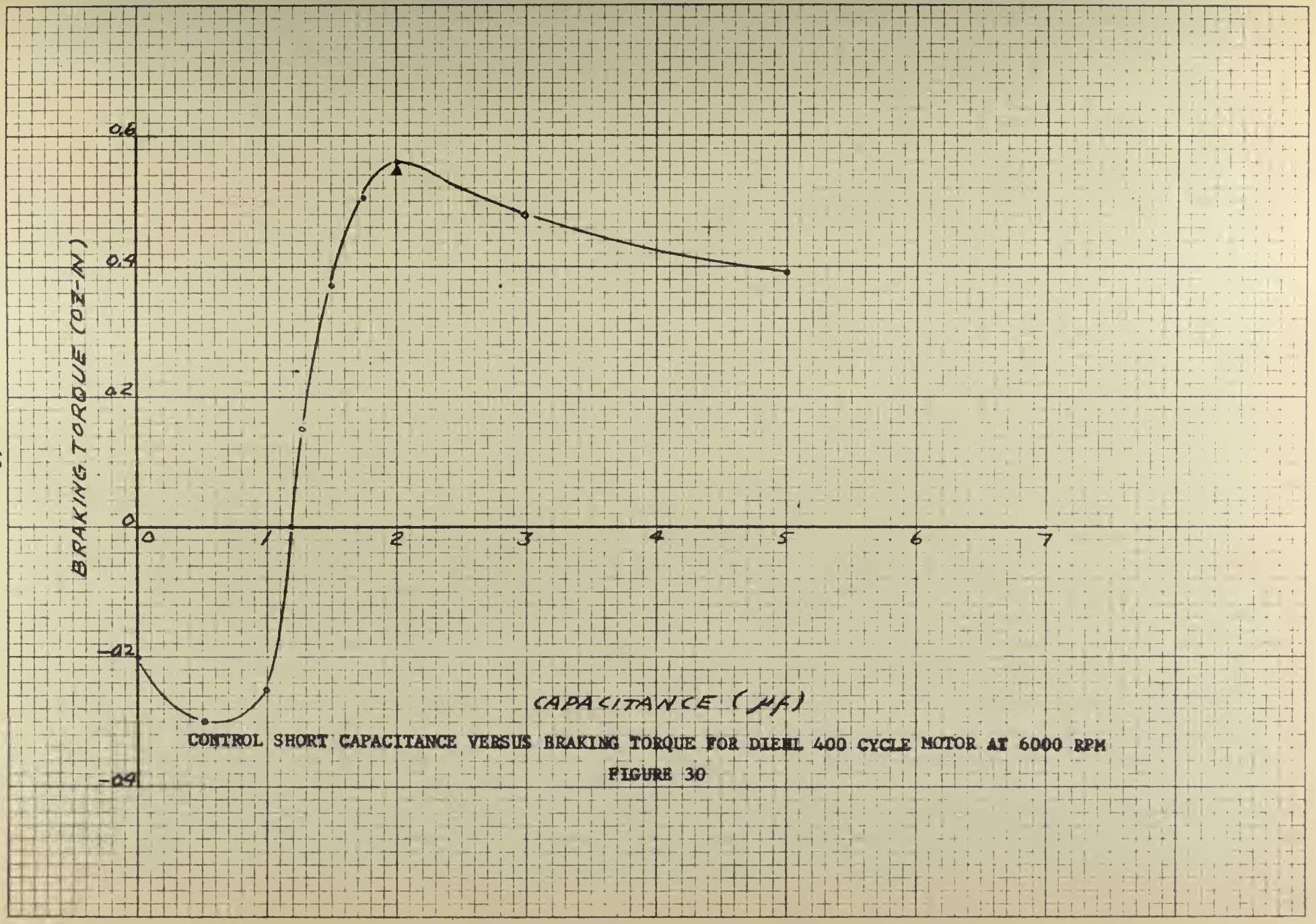

CONTROL SHORT CAPACITANCE VERSUS BRAKING TORQUE FOR DIEHL 400 CYCLE MOTOR AT 6000 RPM

FIGURE 30

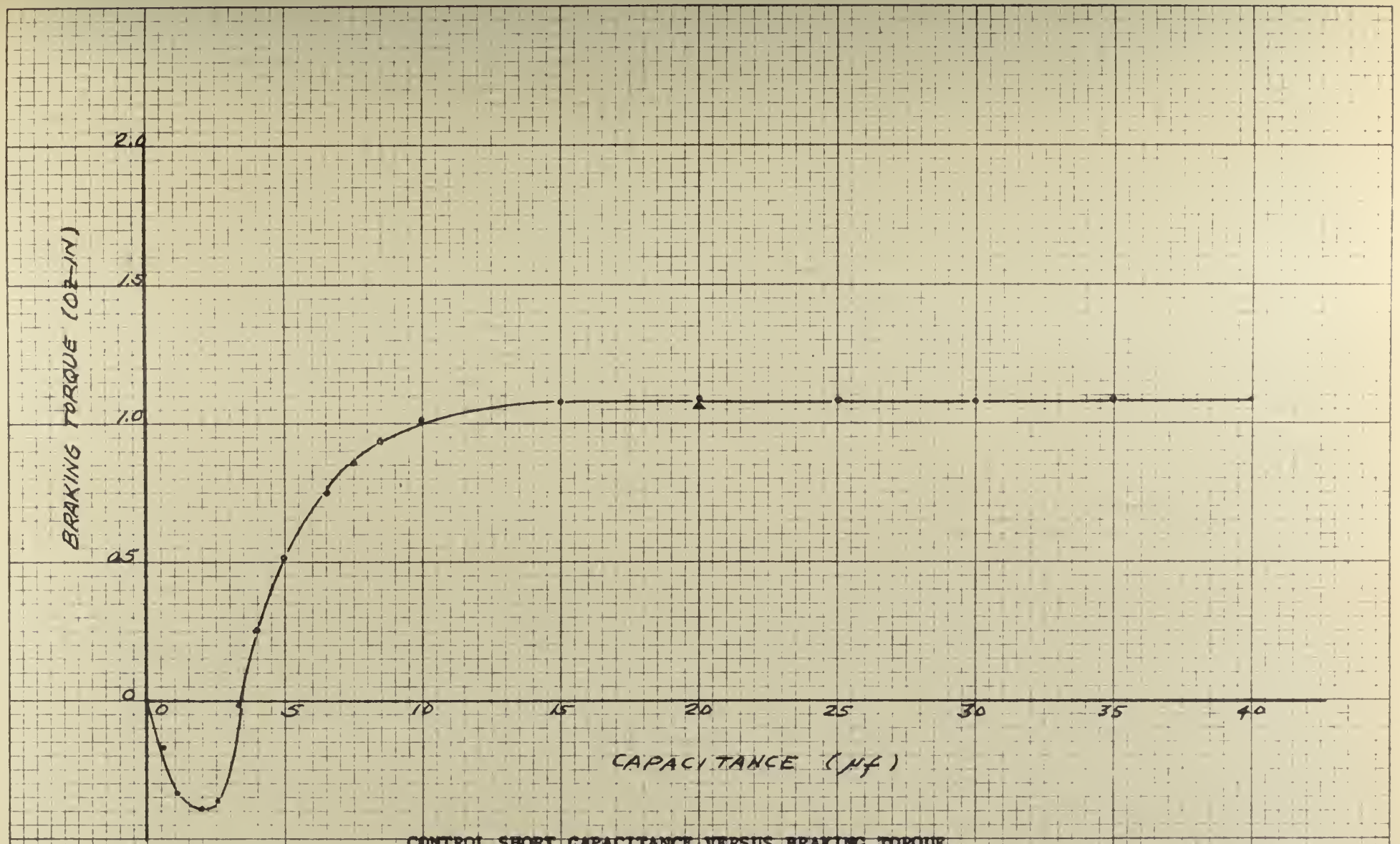

CONTROL SHORT CAPACITANCE VERSUS BRAKING TORQUE
FOR DIEHL 60 CYCLE MOTOR AT 2000 RPM

FIGURE 31

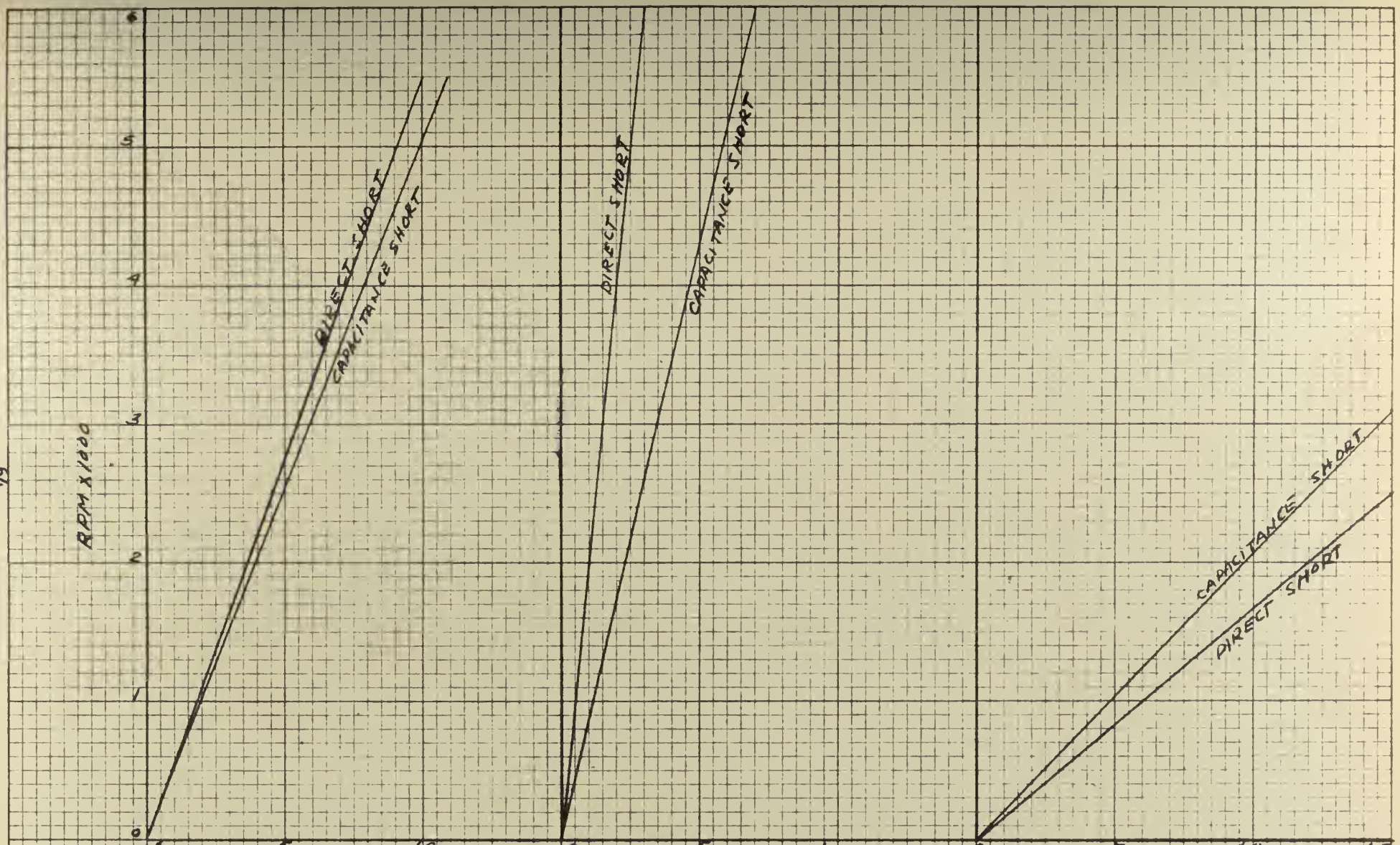

FIGURE 32
KEARFOTT MOTOR

FIGURE 33
DIEHL 400 MOTOR

FIGURE 34
DIEHL 60 MOTOR

DIRECT AND CAPACITANCE SHORT BRAKING CURVES

should be noted that this type of braking also gives particularly linear torque-speed curves. In the 400 cycle motor tests the capacitance short method gives slightly better braking results.

2. Retardation Tests

Due to the linearity of the torque-speed braking curves for all of the imposed conditions, it was decided to use a Kearfott 400 cycle motor for the actual relay servo.

From the results of the previous experiments, it could be concluded that the retardation--velocity versus position--curves for the motor will be linear. However, this is without any consideration being given to the effects of coulomb friction. The motor will possess some coulomb friction and this effect, which will manifest itself in the dead zone, can be determined.

For this determination the Kearfott motor, the gear train, tachometer, and error detector were assembled as they were to be used in the complete servo. Such an assembly includes all of the friction bearing members of the servo. The relay was closed by hand until saturation velocity of the mechanism was attained. The relay was then released and the assembly allowed to coast or was braked to standstill. The voltage output of the tachometer, as an indication of velocity, and the output of the error detector, as an indication of position, were fed as inputs to a two channel Brush Recorder. The recorder tapes were replotted in Figures 35 and 36 to obtain the velocity-position curves. These curves will then be the same as the servo system dead zone trajectory curves on the phase plane except for the effect of circuit inductance and the various time delays.

Figure 35 shows the retardation curves for the particular assembly with the control phase shorted, open, and with various amounts of direct

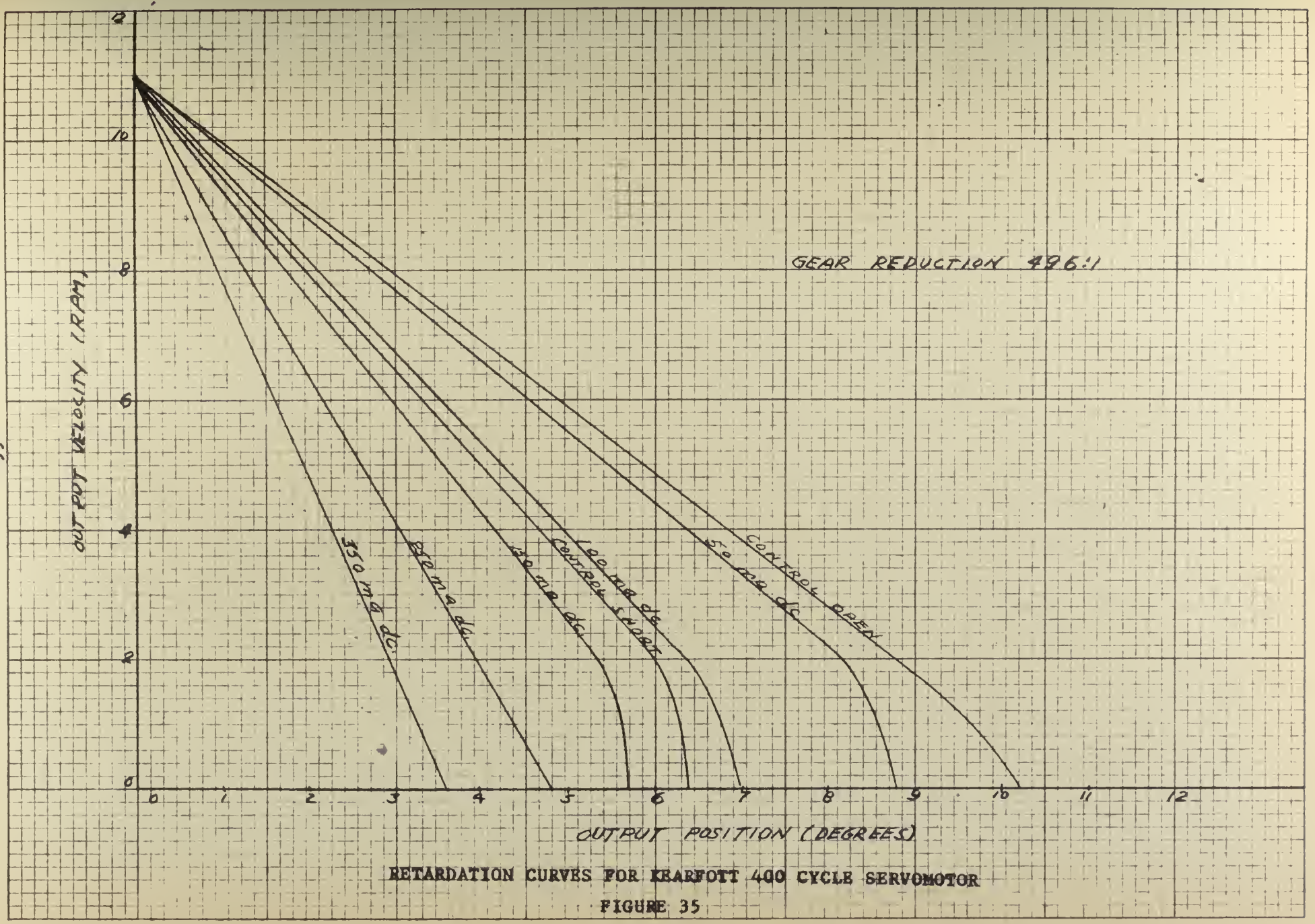

RETARDATION CURVES FOR KRAFFOTT 400 CYCLE SERVOMOTOR

FIGURE 35

current applied for braking. It can be seen that the effect of coulomb friction is greatest at lower values of direct current and negligible for magnitudes of direct current above 250 ma.

Figure 36 records the effect of coulomb friction when a capacitor short is applied to the control phase. It can be seen that the effect for capacitance shorting is less than for a direct short. In these particular tests a capacitance of 1.05 micro-farads is near optimum. The reason for this variation from that shown for the capacitance braking runs is that a different motor, although the same model, was used.

The gear train reduced the velocity of the motor to the error detector potentiometer by 496 to 1. The saturation velocity of the motor was 454 RPM. The angular travel of the potentiometer under 350 ma. of braking current was found to be 2.2 degrees. This would then represent 3.05 revolutions, from saturation velocity to standstill, for the motor.

3. The 400 Cycle Servo System

Figure 37 is a schematic diagram of the relay servo as used to test the proposed theory. Amplifiers from a Boeing Computer were used to afford both amplification and addition of the various signals. A two channel Brush Recorder was used with pickups at the points shown for recording of error and error rate simultaneously.

This servo as shown was used for step inputs up to values near amplifier saturation. The reference voltage was chosen as 36 volts merely for convenience in making calculations. Higher step inputs could have been obtained with lower reference voltages. However, since the system did velocity saturate with the step inputs obtainable, no experimental worth was lost in using the convenient voltage.

Fifty-nine runs were made to examine the dead zone trajectory of the system operating under the various methods of dynamic braking already

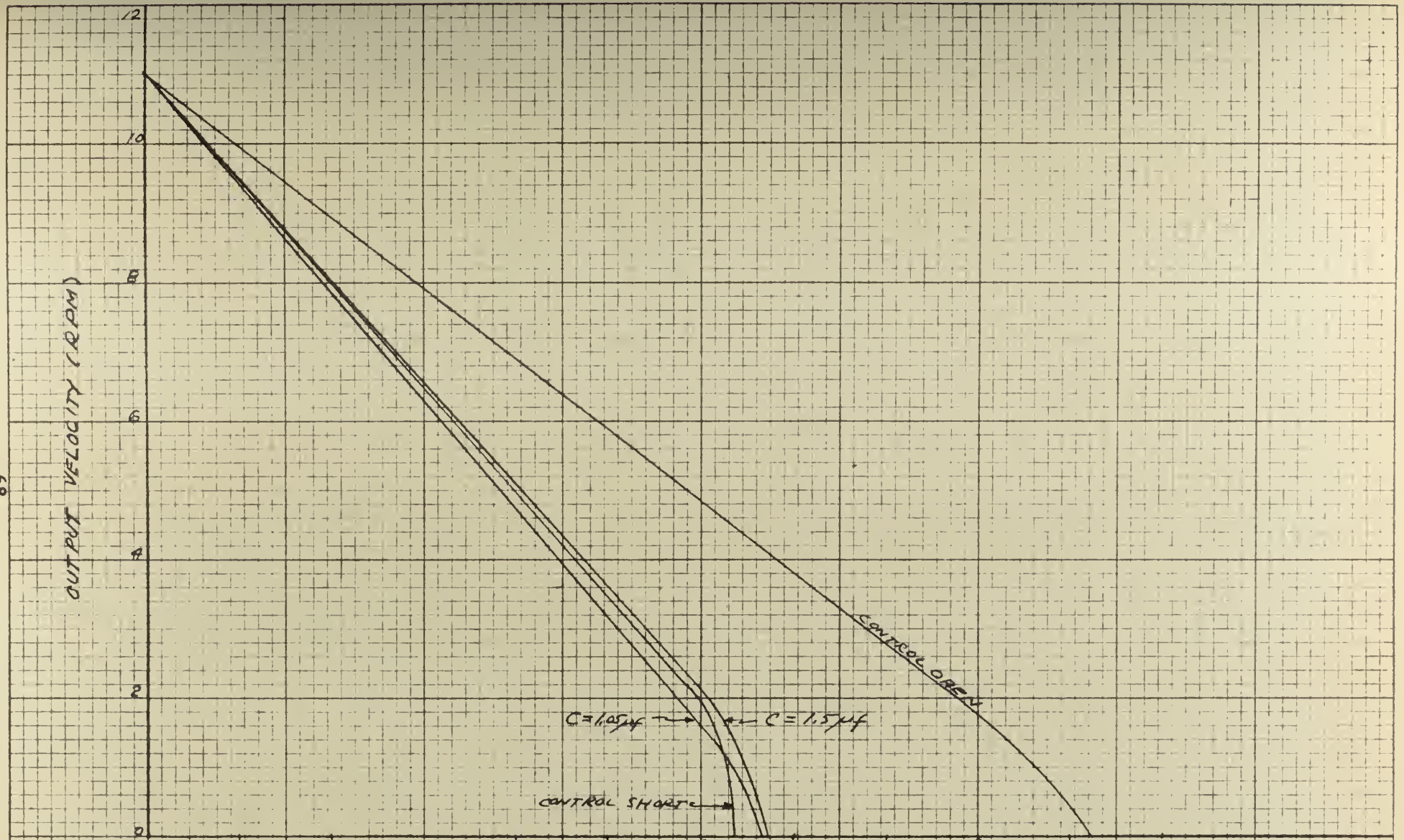

RETARDATION CURVES FOR KEARFOTT 400 CYCLE MOTOR

FIGURE 36

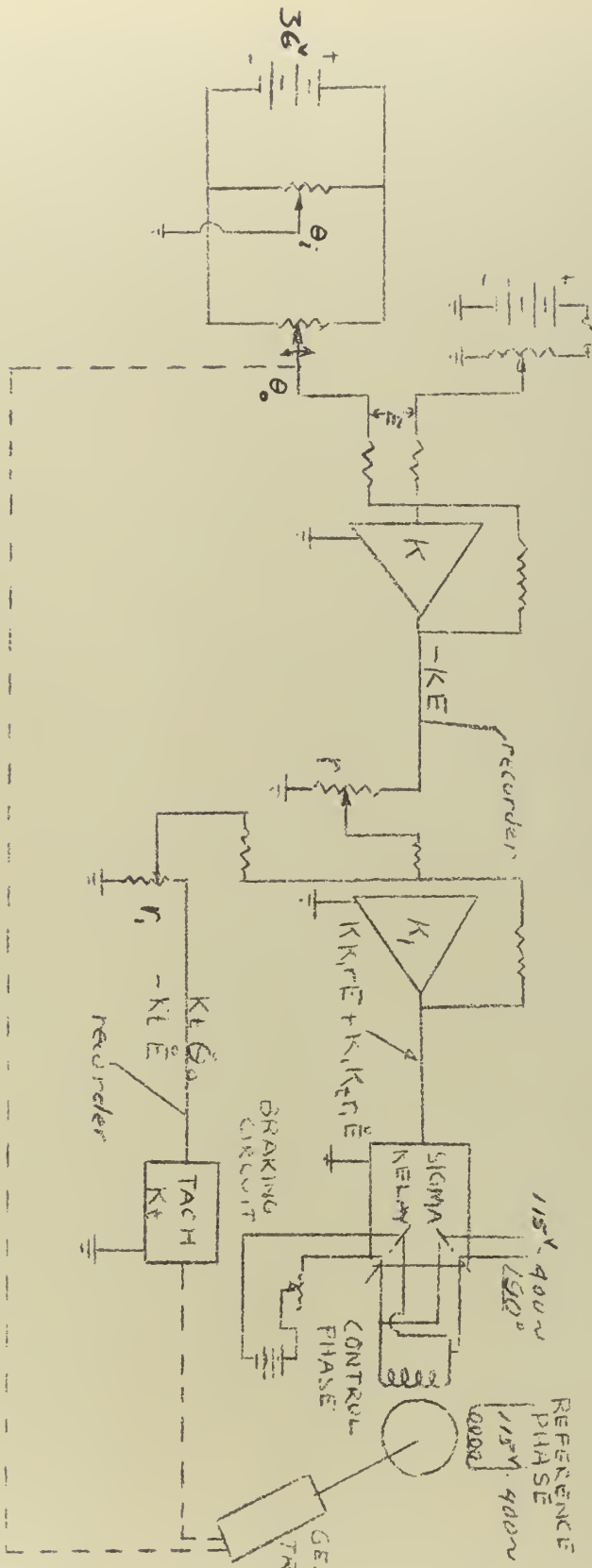

SCHEMATIC DIAGRAM OF TEST RELAY SERVO

FIGURE 37

enumerated. In some cases tach feedback was varied or omitted to check relay drop-out time lag. In others it was varied along with the dead zone width to obtain parallelism between the drop-out switching locus and the trajectory of the system. The system gain was varied to obtain the minimum dead zone that would allow the system to dead beat without oscillation. Retardation runs were repeated for the system operating automatically to investigate the effect of the various braking methods on relay drop-out. This would allow a comparison of the control short circuit methods of braking. Forty-seven runs were thus used to develop or firm up methods of calculation and to establish operating procedures. The remaining twelve runs were precalculated and the system gain constants preset and runs made without any adjustments to afford better results. It was felt that in this way the advantage of the predictability of the dynamic braking methods could be exploited. If any variation occurred that would show detrimental effects, then this method would point them out.

Since the runs preceding the system retardation runs were for developing operating procedures only, no further discussion of them will be made. Figure 38 shows the results of runs (38) to (47) which were the repeated retardation runs. Except for the indication of relay drop-out delay, these runs are essentially the same as those shown previously in Figure 36. The one point that is highlighted in these runs is the variation in drop-out delay and the magnitude of the delay itself. With any appreciable braking current, the travel during the delay exceeds the braking travel. The relay time lag averaged .056 seconds which represented a 3.7 degree error travel at saturation velocity. Also the variation in drop-out (which is counted from the opening of the relay control contacts to the introduction of braking) amounted to one degree of error

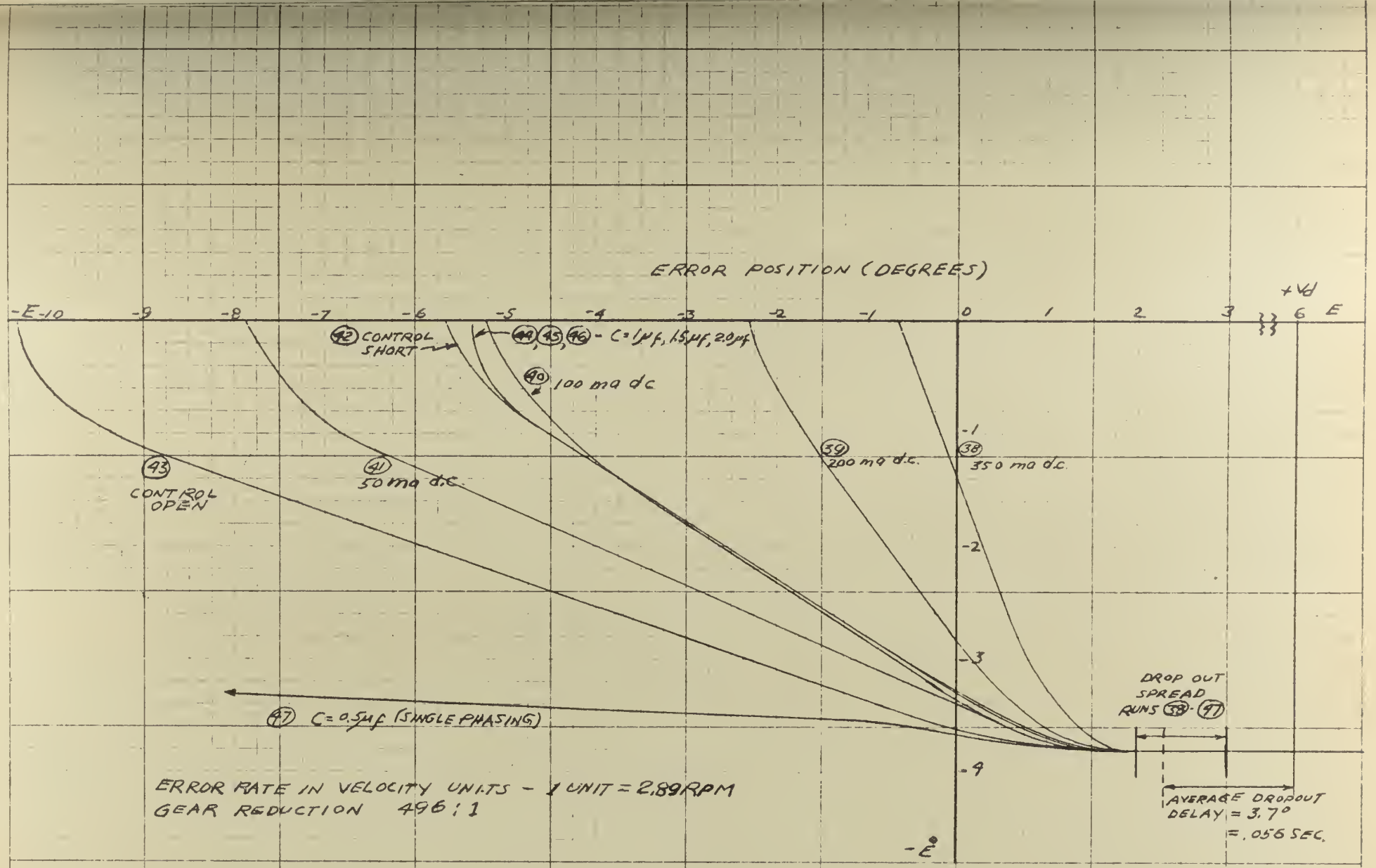

FIGURE 38 - RETARDATION RUNS FOR KEARFOTT 400 CYCLE RELAY SERVO

travel. Thus, at best, it could be predicted that the dead zone travel due to relay drop-out time lag would be 3.5 degrees plus or minus 0.5 degrees. On all future runs it was assumed that the dead zone delay time travel was 3.5 degrees at saturation velocity. This does not account for the effect of delay time upon those runs which were to be made where the step input was insufficient to allow the motor-load unit to velocity saturate. At this point it was assumed that any run, which was made so that relay drop-out occurred at less than saturation velocity, would dead beat with less error travel. This assumption was based on the fact that error travel at a lower than saturation velocity would be less for the same time delay than that at saturation velocity. It will be shown that this assumption was not valid.

a. Direct Current Braking

For the retardation runs a maximum direct current for braking of 350 ma. was used. This gave a maximum braking torque about equal to the starting torque for the motor. Thus runs (48) through (51) were made with 350 ma. The retardation curve of Figure 38 was used to predict dead zone travel and the gain constants were calculated for the various amplifiers and potentiometers. The theory of these calculations is shown in Appendix A and a sample in Appendix B. Basically this involves matching the drop-out switching locus slope with the braking line slope (this is governed by tach feedback) and minimizing the dead zone (governed by the gain).

The results of these four runs from a step input of 20 degrees down to a step input of 5 degrees is shown in Figure 39. The most obvious deviation from predicted results is the wide spread in the dead beat error position. This varies from - 1.1 degrees to - 2.7 degrees or is a 1.6 degree spread. Part of this variation can be explained by drop-out delay time lag spread as noted for the retardation runs. This would account

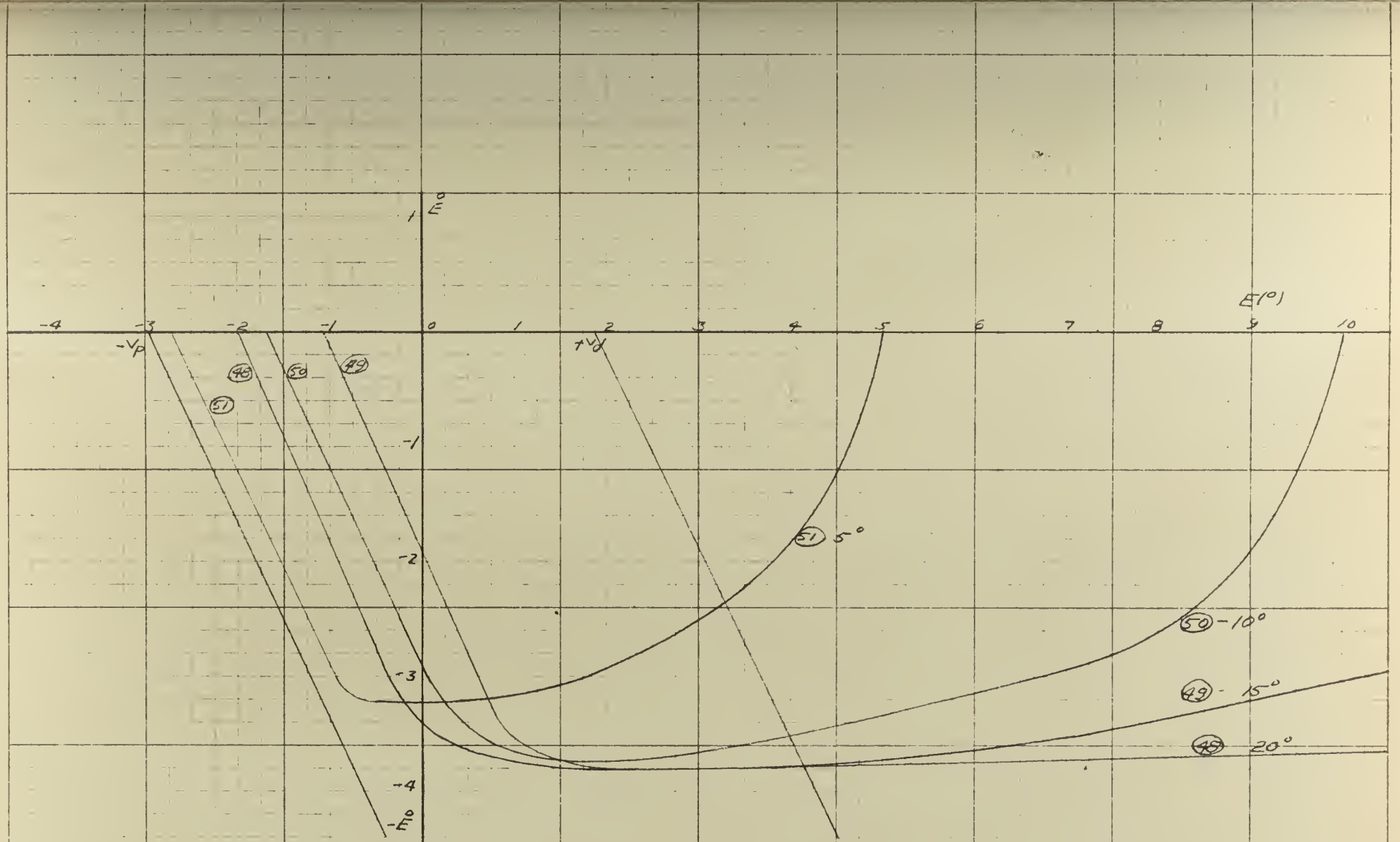

SERVO RUNS WITH 350 ma D. C. BRAKING IN DEAD ZONE

FIGURE 39

for a one degree spread. It should be noticed that the 20, 15, and 10 degree runs do fall within the predicted variation. Also it should be noted that the 5 degree step run, which did not produce velocity saturation, did not dead beat with the least error as assumed earlier but with the most. Thus it can be assumed that the 5 degree step run is the one that provides the discrepancy in the dead beat error spread. Also it is worthy to note that the previous assumption about less than velocity saturating steps is not valid. The reason for this may be found in an analogy to the reasoning followed by McDonald (3) for essentially the same observation. The extended dead beat position occurred for low order steps in a study wherein dynamic braking of a D.C. shunt motor is accomplished by use of a shunting resistor. He allowed that at velocity saturation the current in the motor armature was less than for velocities lower than saturation. This armature current must then be reversed in braking. Thus at low velocities the delay in build up of the braking force was longer. At low speeds the torque is greater and the rotor currents are larger than at high speed. The dissipation of these currents and the build up of the stationary field induced currents logically requires a longer period of time for the lower speeds. Hence the apparent inductive effect, which produces the curvature of the trajectory in the phase plane plot before the onset of linear braking, acts for a longer period of time. Thus the dead zone error travel is increased for step inputs that do not cause velocity saturation.

It should be noted that the slope of the trajectories under full braking are nearly identical with each other and with the predicted switching loci.

b. Control Short Circuit Braking

Figures 40 and 41 show the test results of runs (52) through (59). Runs (52) through (55) were made with a capacitor across the control winding of 1.5 micro-farads. Runs (56) through (59) were made with a small resistor shorted across the control field winding. The small resistor was used instead of a dead short to prevent excess current flow in the 400 cycle supply circuit in case the shorting contacts closed prior to the opening of the control contacts.

The capacitance short runs follow the results expected when the drop-out delay and the low order step effect are taken into account. The runs made at 20, 15, and 10 degrees all dead beat just inside the reverse pull-in point. The 5 degree step did overshoot and pull-in reversed. As noted a half oscillation occurred with final dead beat at zero error. This point of final static position was not predicted.

The resistance short runs of Figure 41 show the poorest results with considerable deviation of trajectory slope from the precalculated slope. Also there is some divergence of trajectories among the individual runs. The 20 and 10 degree step runs were practically identical showing considerable curvature as with coulomb friction acting. However, the 15 degree step run was more nearly parallel to the switching loci and shows less coulomb friction effect. Again the 5 degree step produced an overshoot and dead beat with zero error. The reason for the lack of similarity among these runs is not definitely understood at the present time. It is believed that the shorting contacts did not close on runs (56), (58), and (59) since the trajectories of these runs parallel an open circuit trajectory. In general, however, it can be said that a comparison of the two Figures--40 and 41--indicates that there is little

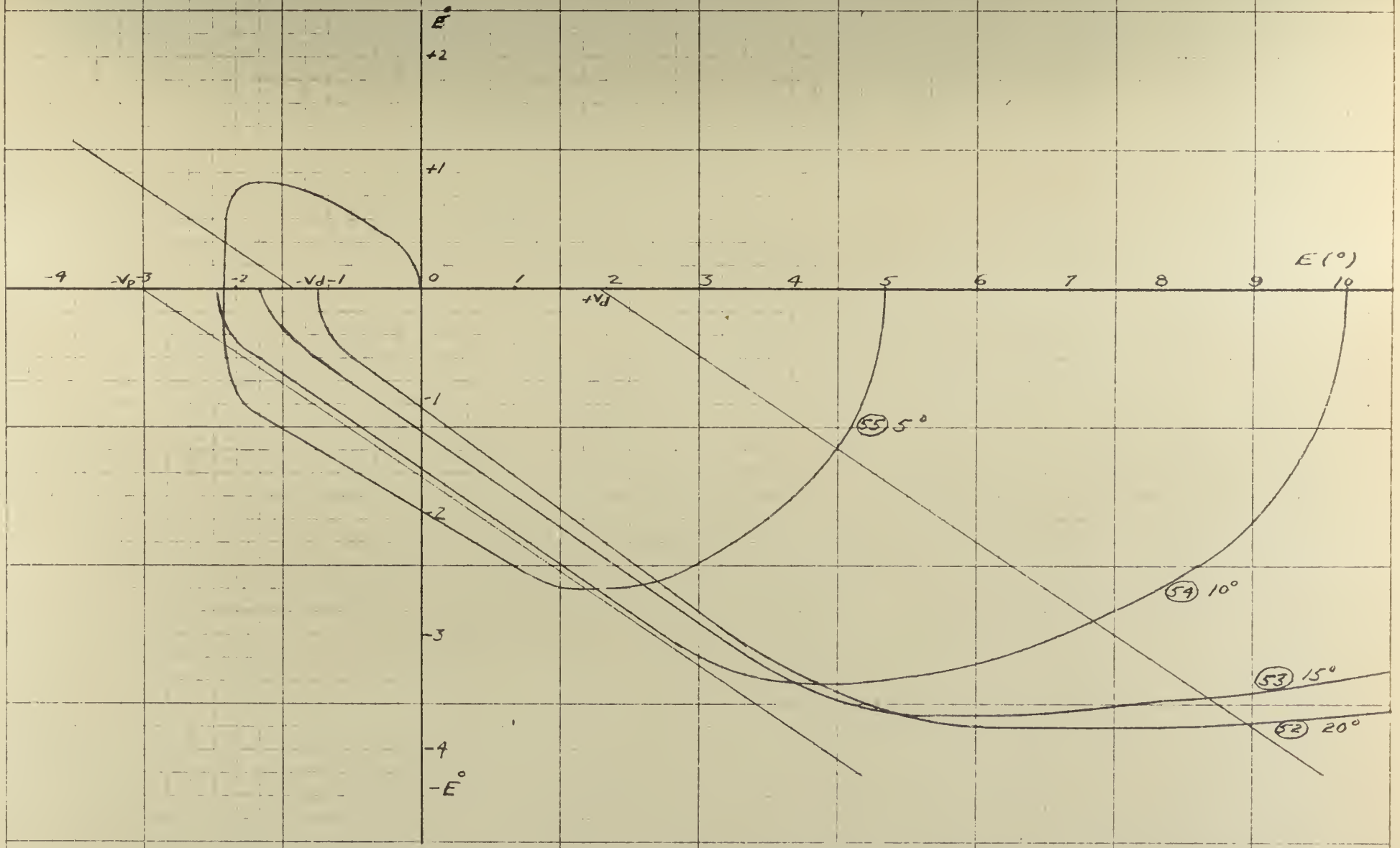

SERVO RUNS WITH 1.5 MICRO-FARAD CONTROL SHORT IN DEAD ZONE

FIGURE 40

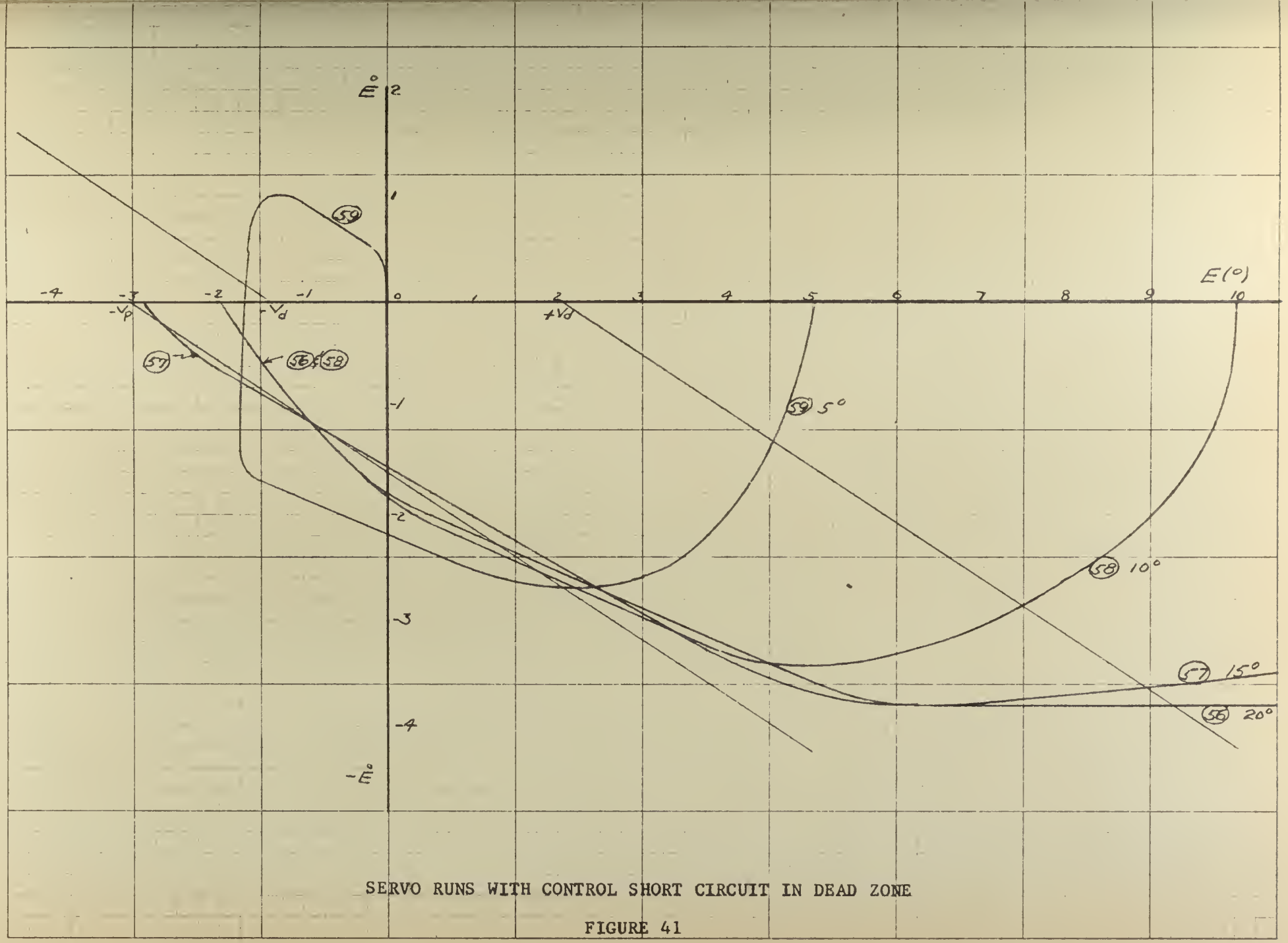

SERVO RUNS WITH CONTROL SHORT CIRCUIT IN DEAD ZONE

FIGURE 41

to choose from between the two types of braking. In a system that used a faster acting relay than was available here, the advantage of having the braking implement already in the circuit in the form of the capacitor should show a distinct timewise advantage.

c. Ramp Input: $\theta_i = wt$

To examine the effect of dynamic braking and tach feedback on the limit cycle obtained when a ramp input is used instead of a step, three additional runs were made. These three runs are shown in Figures 42 and 43. In Figure 42 run (62) shows the limit cycle attained with a minimum dead zone for which the system does not overshoot. No tach feedback was employed. No braking was used. The ramp input velocity was 1.58 degrees per second. The maximum $\dot{\theta}_o$ was 4.58 degrees per second.

Run (61) shows the change in the limit cycle with a braking current of 350 ma. introduced at the relay drop-out. Run (60) in Figure 43 shows the change in the limit cycle when tach feedback and d.c. braking are both employed.

Table I below shows the variation in frequency of oscillation, error deviation, error rate deviation, and minimum dead zone for the three operating conditions. The percentages shown are in comparison to the values obtained from run (62).

For the ramp input only two changes were necessary in the physical setup from that shown in Figure 18. The ramp input, obtained from a Hewlitt-Packard oscillator, replaced the step input, and it was necessary to feed into the second amplifier a signal proportional to w. The second change was necessary because with a ramp input the error rate is a function of both w and $\dot{\theta}_o$. The calculations required for the

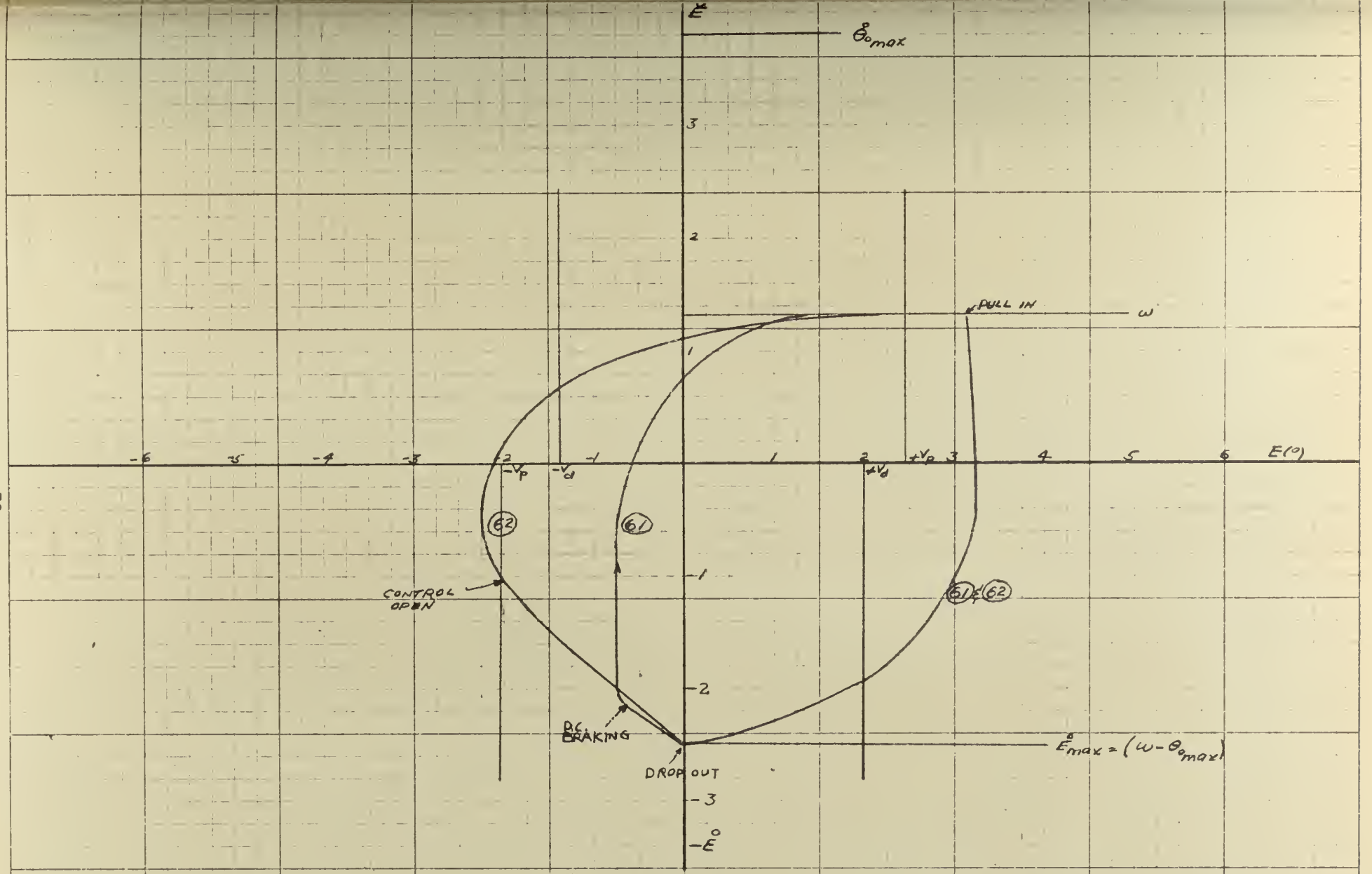

SERVO RUNS UNDER RAMP INPUT, WITH AND WITHOUT D.C. BRAKING

FIGURE 42

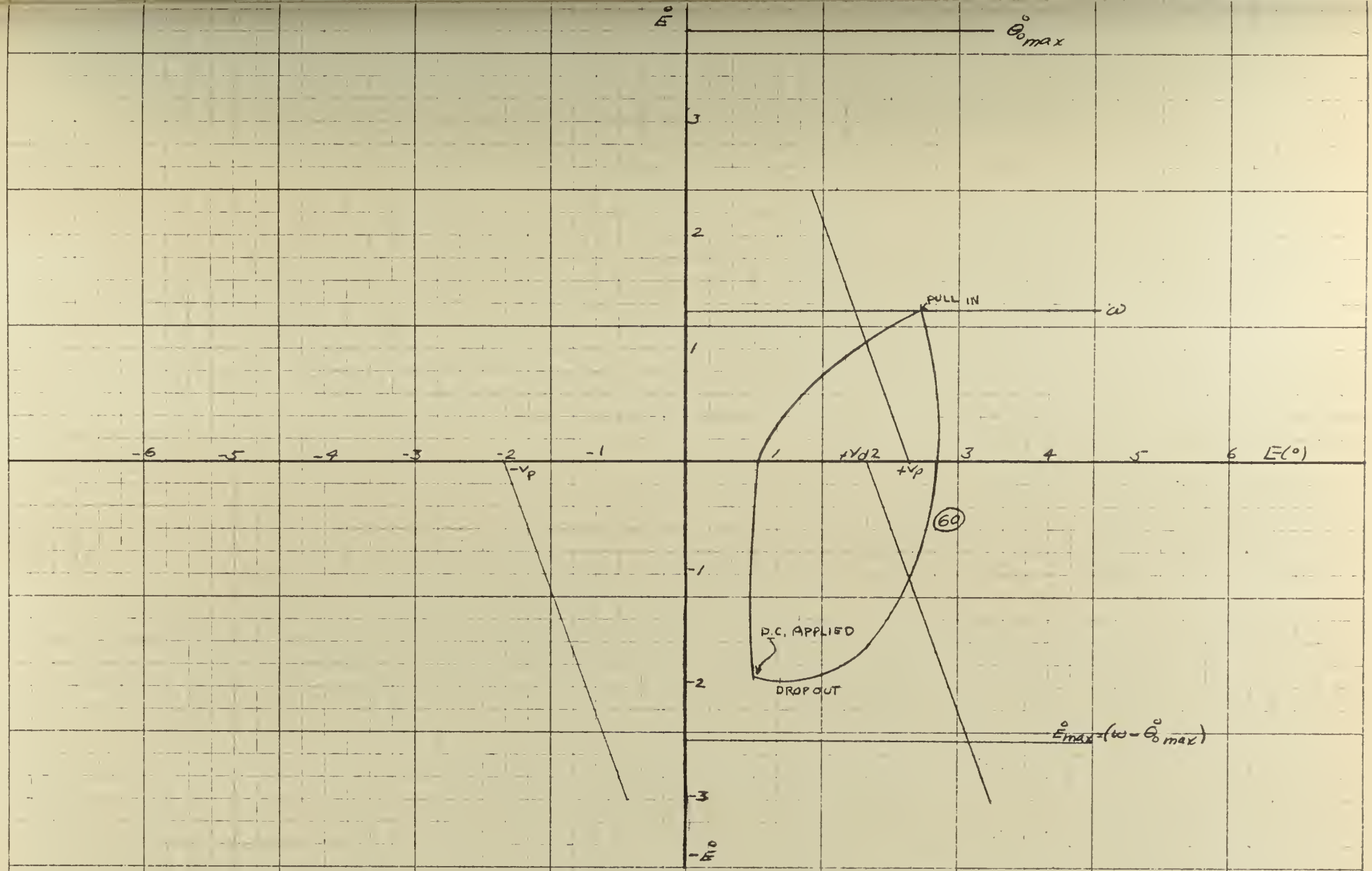

SERVO RUN FOR RAMP INPUT WITH TACH FEEDBACK AND D.C. BRAKING

FIGURE 43

system constants are also shown in Appendix A and Appendix B.

TABLE I

RUN	FREQUENCY Cycle/Sec	MINIMUM DEAD ZONE	ERROR DEVIATION	ERROR RATE DEVIATION
62	1.28	4.07	5.74	3.75
61	2.36 (+84.5%)	3.45 (-15.25%)	4.01 (-30.2%)	3.75 (0.0%)
60	3.73 (+191.5%)	3.22 (-26.4%)	2.10 (-63.3%)	3.25 (-13.1%)

4. Conclusions

The conclusions fall into two categories. The examination of the three two phase induction servomotors under various braking conditions was done to obtain a servo which produced a particular type curve on the phase plane plot. That is, it was desired that the slope of the braking curve of the motor load unit in the dead zone of the relay be constant. The second phase of the investigation was the development of the servo and examination of its response characteristics to verify the theory introduced in Chapter III.

From the induction motor braking tests it was concluded that:

a. Direct current may be used for dynamic braking of the two phase induction servomotor. Braking torques equal to and greater than motor starting torque are obtainable with no difficulty.

b. When the maximum braking torque developed is approximately the same as the starting torque for the motor, as normally energized, the shape of the braking torque speed curve is an inverted mirror image of the motoring torque speed curve. Thus the linearity of the motoring torque speed curve as supplied by the manufacturer can be used as an indication of the usefulness of a motor for the type of relay servo proposed.

c. If the maximum braking torque developed by direct current braking is of the same order of magnitude as the starting torque, the effect of coulomb friction on the retardation of the motor-load combination is negligible.

d. Short circuit braking, either capacitive or direct, produces nearly linear braking torque-speed curves regardless of the shape of the motoring torque speed curves. The magnitude of the braking torque in the two cases is nearly equal.

e. The linearity of the torque speed curve, which is an indication of the relative magnitude of rotor resistance, may be used to predict the single phasing tendencies of the motor. If the motoring curve is nearly linear, the motor will not single phase when the rotor is made to turn at any speed.

From the response curves of the servo on the phase plane, with employment of dynamic braking in the dead zone of the relay, it was concluded that:

a. The relay servo may be made to dead beat at a predicted static error position.

b. The minimum dead zone, as controlled by the gain of the system, is limited by the relay drop-out delay and the inductive effect of the braking circuit.

c. The use of dynamic braking and tachometer feedback decrease the error deviation, the error-rate deviation, and increase the frequency of the limit cycle response of the relay servo to a ramp input.

5. Recommendations for Future Study

It is recommended that further study be made of the relay servo using dynamic braking of the two phase induction servomotor in the relay

dead zone. This study is thought advisable because of the possibility of enhancing the use of the relay servo as a practical system.

More attention should be given to the overshoot caused by small step inputs. As explained in the discussion of the experimental results, step inputs which do not cause velocity saturation may cause the system to overshoot. This is due to the increased drop-out time delay as introduced by the motor inductive effects. It may be assumed that even smaller steps--in the limit, the smallest that will allow relay pull-in--may tend to create a magnitude of inductive delay sufficient to produce a limit cycle.

Referring back to Figures 40 and 41 for short circuit braking the overshoot at a five degree step may be noted. However, it would have been possible to cause relay pull-in with a 2.6 degree step and the results may have been as shown in Figure 44 below.

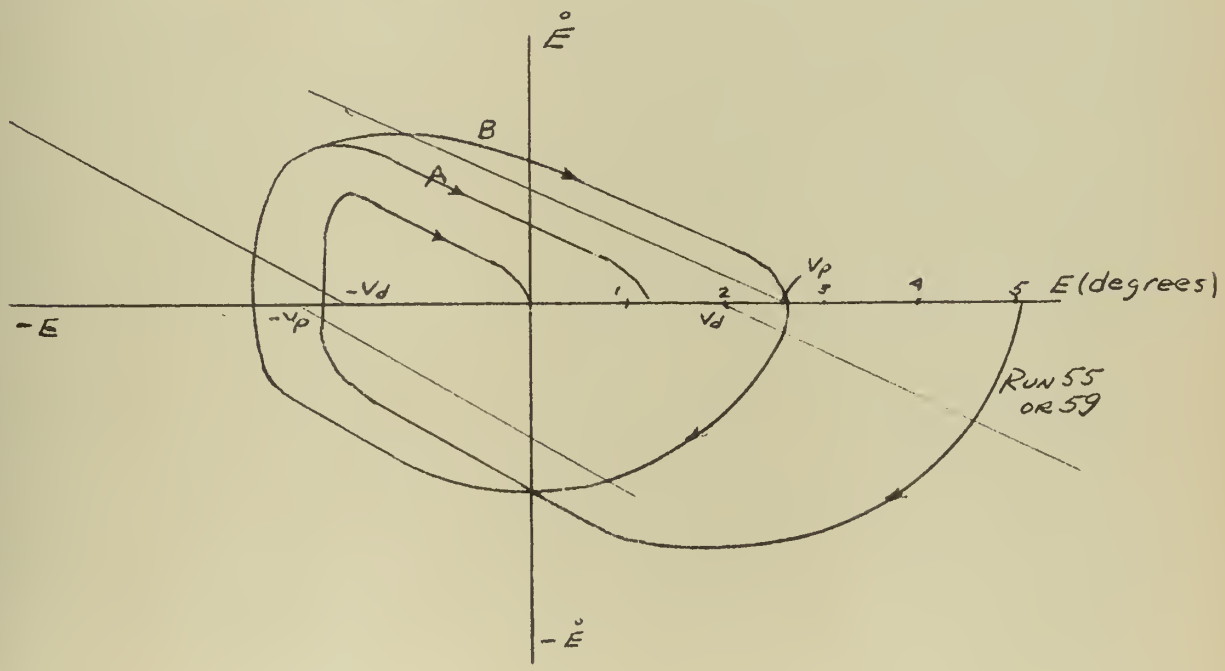

FIGURE 44 - POSSIBLE RESPONSE TO VERY SMALL STEP INPUTS

If, as shown in Figure 44, the overshoot is more drastic for the smallest actuating step, the response may be one of three forms. The system may dead beat with only one overshoot as in A, as did the five degree step run, or it may dead beat after one or more oscillations. If, however, the first overshoot produces a pull-in in the initial direction so that the error axis is crossed at the same point that the step originated from as in B, then the limit cycle will be formed. A characteristic of the relay used in the experimental setup that places this point in doubt is the excessive drop-out and pull-in time delays due to the movement of the parts of the relay. This can be seen in the extensive travel of the five degree run parallel to the pull-in switching locus. Pull-in occurred near zero velocity. Thus the results obtained are not considered adequate to fully predict the action of the relay servo under small step inputs. It is believed that practical utilization of an otherwise sound servo system will be hindered without further investigation.

Several possibilities are available for refining the investigation methods. The simplest is to use a relay with considerably less inherent time delay in the making and braking of the a.c. circuit. Also the relay used should be designed with braking contacts that close immediately on the opening of a.c. contacts. With the relay used it was necessary to modify the relay in an attempt to accomplish this, and in so doing the inertia of the moving parts was increased, adding to the delay time. Frequently during the test runs the data presented some difficulty in reduction due to the fact that error change during delay was about equal to the error change under the braking load. And at best the wideness of the dead zone left much to be desired.

Refer back to Figure 39 for the 350 ma. braking current. Discounting relay time lags, the inductive effect alone would require only a dead zone of one degree instead of the 4.85 degree dead zone necessitated in this setup. This reduction would be a considerable improvement and should be obtainable, or at least approached, by the simple expediency of using a quicker acting relay. It is well to recall, however, that in any electro-mechanical relay there is going to be some inherent time lag. Thus any practical system which uses one will display some of the faults pointed up experimentally here. However, to provide a more rigorous verification of the theory of the proposed system it would be better to use an electronic relay. Practically this would be a more expensive, space consuming system and the disadvantages might well outweigh the gain of eliminating the time delays of the relay.

For experimental purposes, a complete unit would not have to be assembled to eliminate the relay inertia effects. It would only be necessary to establish an electronic relay which pulls in and drops out in one direction. Likewise, the control voltage and braking current would only have to be controlled for rotor rotation in one direction since this half system cannot overshoot. The reason for using such a half system is that, with predictable dead beat error position in the dead zone, the error at zero error-rate for the negative electronic pull-in point can be assumed exactly equal to the positive pull-in error position. Thus by merely plotting the phase plane curve which will show the dead beat position of the servo, one could see whether overshoot would have occurred or not.

Such a half system would not allow for an investigation of the inductive effect at small steps because pull-in could not occur in a neg-

ative sense. For this investigation a complete relay simulator would be required along with the electronic circuitry needed to control the control phase voltage for motor rotation in both directions and to add direct current to the control phase only during dead zone travel.

BIBLIOGRAPHY

1. G. J. Thaler, W. L. Harris, and C. McDonald, Quasi-Optimization of Relay Servos by Use of Discontinuous Damping.

2. W. L. Harris, Discontinuous Damping of Relay Servomechanisms, U. S. Naval Postgraduate School, Master's Thesis, 1956.

3. C. McDonald, Quasi-Optimization of D.C. Shunt Motor Relay Servos, U. S. Naval Postgraduate School, Master's Thesis, 1957.

4. G. J. Thaler, Unpublished notes in non-linear servomechanisms, Presented in Advanced Servomechanisms Course, U. S. Naval Postgraduate School.

5. C. V. O. Terwilliger, Lecture notes presented in advanced course in Electrical Machinery Design, U. S. Naval Postgraduate School, 1956-1957.

6. R. J. W. Koopman, Operating Characteristics of 2-Phase Servomotors, AIEE Transactions, 68, Part I, 1949.

7. S. S. Chang, Discussion on paper presented by R. J. W. Koopman in reference 6 above.

8. H. C. Specht, Induction Motor Braking, AIEE Transactions, 31, 1912.

9. T. P. Kirkpatrick, Dynamic Braking Characteristics of Induction Motors, Electric Journal, p. 131, March 1923.

10. G. L. Hollander, Electric Braking of Servomotors, Electrical Manufacturing, 48, pp. 268-272, Dec. 1951.

APPENDIX A

DETERMINATION OF RELAY SERVO CONSTANTS

1. Step Input

Figure 45 is a schematic of the proposed relay servo showing the constants that require determination.

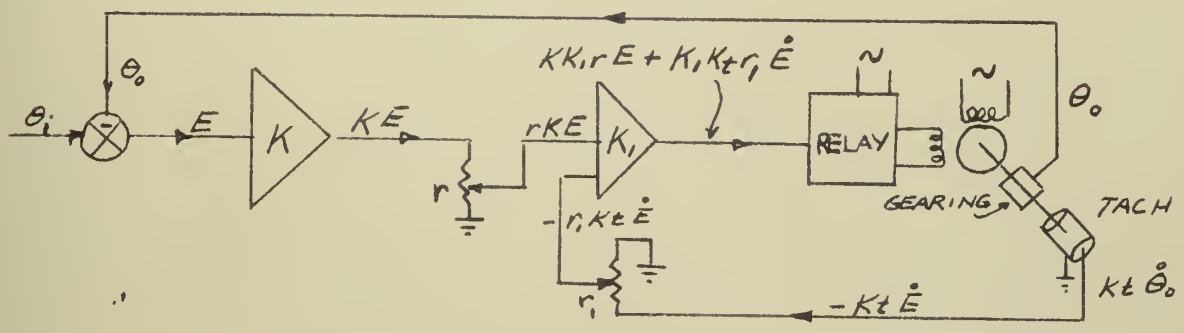

FIGURE 45 - PROPOSED RELAY SERVO

If the relay drops out at a voltage represented by V_d then at drop out,

$$KK_1rE + K_1Kt \cdot r_1\dot{E} = V_d \qquad (69)$$

For the servo shown in Figure 45 the following sign convention is assumed:

a. K_1, K, and Kt are negative quantities, so that at the output of the first amplifier KE is a negative potential if error is positive. And $-Kt\dot{E}$ is a positive potential if $\dot{E}$ is a positive potential. K and K_1 are negative due to the characteristics of the amplifiers and Kt is made negative by the appropriate selection of the tach output ground lead.

b. K, K_1, and Kt are normally not variable, once a value has been selected, while r and r_1 may be varied from 0 to 1, being helical potentiometers.

It is desired to set up the servo so that: (1) the drop-out switching locus will be parallel to a predicted dead zone trajectory of the motor-load combination, and (2) the servo will dead beat at a specified error position assuming drop-out is ideal. This discounts any time delay and inductive effects.

For a relay servo which undergoes discontinuous viscous braking in the dead zone, the dead zone differential equation is, ignoring coulomb friction,

$$J\ddot{E} + f\dot{E} + K_b\dot{E} = 0 \qquad (70)$$

Then the phase plane trajectory has the slope given by

$$\ddot{E}/\dot{E} = d\dot{E}/dE = -\left[\frac{f + K_b}{J}\right] \qquad (71)$$

For a given motor, gear train, tach and load combination the only variable is K_b, which is constant for a given braking current. The right hand side of Equation (71) is determined by the retardation tests and is designated m_r, the slope in the phase plane that the switching locus is required to match.

Figure 46 is a sample retardation curve obtained when 350 ma. direct current was used for braking.

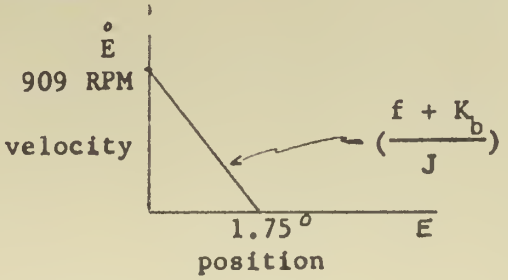

FIGURE 46 - A SAMPLE RETARDATION CURVE

Since it is desired that the phase plane plot of the switching locus parallel this trajectory, then it is required that the slope of line AB in Figure 47 fulfill this requirement.

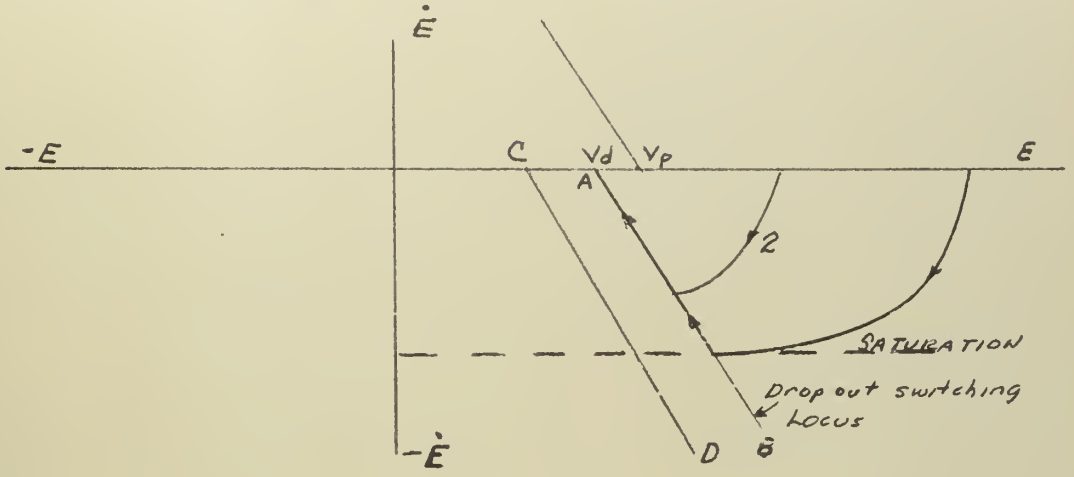

FIGURE 47 - COINCIDENCE OF PHASE PLANE TRAJECTORY AND SWITCHING LOCUS

When a positive error is introduced into the servo the motor-load unit will be accelerated to saturation velocity, if the rate of error reduction is low enough. However, if the step is not large enough, or if the response is rapid then drop-out may occur before saturation velocity can be reached. Then the trajectory would be shown by curve 2 in Figure 47. Whether or not saturation velocity is reached has no bearing on the calculations of the switching locus slope or the dead zone parameters as long as the tachometer output is linear with velocity.

From Equation (69) the intercept form of the switching locus equation becomes,

$$\dot{E} = -\frac{E\,Kr}{Kt(r_1)} + \frac{V_d}{K_1 Kt(r_1)} \qquad (72)$$

and the switching locus slope is given by,

$$m_{s1} = - \frac{Kr}{Kt(r_1)} \tag{73}$$

Inspection of (73) shows that when the tach feedback is zero ($Ktr_1 = 0$), then m_{s1} is infinite and the switching locus is vertical. To rotate the switching locus counterclockwise as shown in Figure 47, it is merely necessary to increase Ktr_1. Since Kt is a constant, r_1 must be increased to obtain the desired feedback and rotation of the switching locus.

If the slope of the retardation curve expected to be duplicated is given by m_r, then to obtain this slope,

$$m_r = m_{AB} = - \frac{Kr}{Ktr_1} \tag{74}$$

So far in this discussion K and r have been held constant.

To obtain the rest position, A, in Figure 47, Equation (69) is manipulated so that

$$\frac{E_A Kr}{Ktr_1} = \frac{V_d}{K_1 Ktr} \tag{75}$$

or further,

$$E_A = \frac{V_d}{K K_1 r} \tag{76}$$

[1]In a practical system E_A cannot be the intersection of the switching locus and the E axis due to relay drop-out delay and inductive effects. If these terms are represented in error position units as e_d and e_i then $E_A' = E_A + e_d$ and e_i, where E_A is the position change of the motor-load combination under braking and E_A' is the actual rest position. Then E_A' is substituted for E_A in (76).

Thus the requirements expressed above are completed by use of Equations (74) and (76). An example of the calculations is given in Appendix B.

If it is desired to alter the dead zone width so that E_A is reduced to E_C, it is seen by (76) that r must be increased. The new value of r is designated r_i. Since r also appears in (74) the slope of the switching locus also changes and becomes

$$m_i = -\frac{Kr_i}{Ktr_1} \tag{77}$$

which is more nearly vertical than before. To rotate the switching locus back to its original desired slope of $-Kr/Ktr_1$ it is necessary to vary r_1 to a value r_{1i}, such that

$$-\frac{Kr_i}{Ktr_{1i}} = -\frac{Kr}{Ktr_1} \tag{78}$$

Solving (78) for r_{1i}

$$r_{1i} = \frac{r_1 r_i}{r} \tag{79}$$

and

$$m_{CD} = -\frac{Kr_i}{Ktr_1 r_i/r} \tag{80}$$

or cancelling factors on the right side,

$$m_{CD} = -\frac{Kr}{K\ t\ r_1} = m_{AB} \tag{81}$$

as desired. Equation (81) seems to indicate that in the actual servo that a change in dead zone width does not change the slope of the switching locus. This is not so. Once a change of the dead zone width is made by varying r to r_i, r_1 must be changed by a factor r_i/r as shown in (80). Equation (81) shows that having done this, the slope of the switching locus before and after dead zone width variation is the same. It should be noted that since r_1 does not occur in (76) the slope of the switching locus can be varied without changing the dead zone width.

Since the magnitude of the error voltage into the second amplifier is dependent not only on K and r but also on the magnitude of the reference voltage in the error detector, the variation in dead zone width may be accomplished by leaving r constant and varying the reference voltage. However, if 360 degree potentiometers are used in the error detector, a voltage of 36 volts or some multiple or submultiple of this value, used as the reference and left constant, with r variable, enhances the ease with which calculations may be made and with which data form a Brush Recorder tape may be reduced for plotting.

2. Ramp Input: $\theta_i = wt$

The schematic for a ramp input is the same as in Figure 45 except for an additional input to the K_1 amplifier. This is shown in Figure 48 as $r_1 K_t w$.

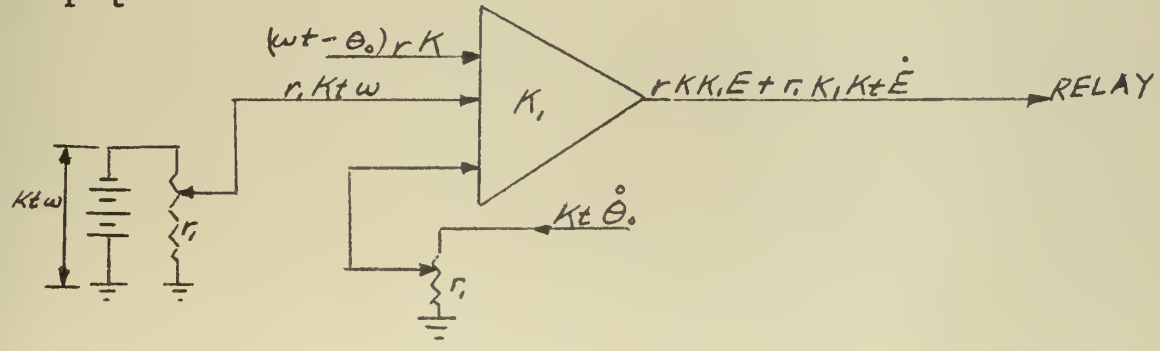

FIGURE 48 - SECOND AMPLIFIER WITH RAMP INPUT

The equation for the switching locus at relay drop-out is

$$rKK_1E + r_1K_1Kt\dot{E} = V_d \tag{83}$$

which is the same as (69) for the step input. However, here it must be recognized that $\dot{E}$ is represented by $w - \dot{\theta}_o$ and for calculation of K, K_1, r, and r_1 both w and $\dot{\theta}_o$ must be known. With this information substituted for $\dot{E}$ in the pertinent equations, the calculations of the constants are the same as for the step input. An example is given in Appendix B.

APPENDIX B

CALCULATIONS FOR RELAY SERVO CONSTANTS

1. Step Input

a. Results desired: dead beat error position of zero degrees when 350 ma. direct current is used for braking.

b. Known constants:

(1) Tach output at saturation velocity	20	volts
(2) Tach saturation velocity	909	RPM
(3) Tach constant, Kt,	20/909	$\frac{\text{volts}}{\text{RPM}}$
(4) Reference voltage	36	volts
(5) Error detector sensitivity	.1	volt/degree
(6) Retardation slope for 350 ma.	-909/1.75	$\frac{\text{RPM}}{\text{degree}}$
(7) Error change during linear braking, E_A	1.75	degrees
(8) Error change during inductive delay, e_i	0.50	degrees
(9) Error change during relay delay, e_d	1.00	degrees
(10) Drop-out potential, V_d	3.4	volts

c. Predicted phase plane plot

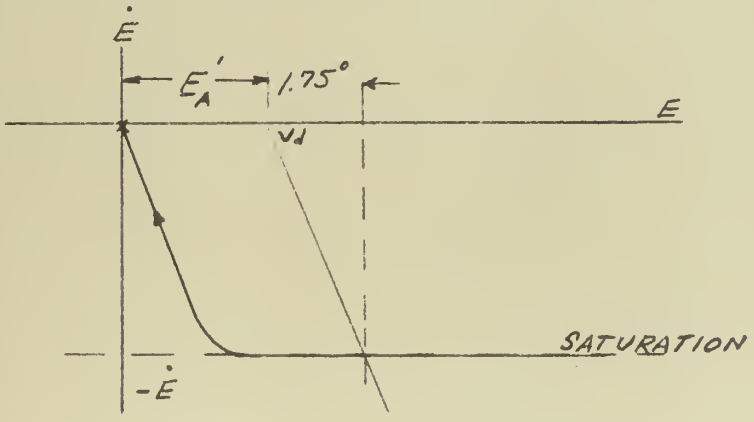

FIGURE 49 - PREDICTED PHASE PLANE PLOT

d. Calculations

Using Equation (74),

$$m_r = m_{AB} = - Kr/Ktr_1 \qquad (74)$$

$$-909/1.75\ (.1) = - Kr/20/909r_1, \text{ or}$$

$$-Kr/r_1 = 20/1.75\ (.1) \qquad (84)$$

Using Equation (76)

$$E_A' = V_d/KK_1r \qquad (76)$$

where $E_A' = E_A + e_d + e_i = 3.25$ degrees

K_1 Kr $3.4/3.25\ (.1) = 10.46$

To keep $0 < r < 1$

choose $\underline{K \text{ and } K_1 = 10}$, then

$\underline{r = .105}$

Then substituting for K and r in (84),

$$r_1 = 1.75\ (.1)/20\ (1.05)$$

$$\underline{r_1 = .092}$$

2. Ramp Input: $\theta_i = wt$

a. Results desires:

(1) Relay switching locus for drop-out and error axis intersection at + 2 degrees.

(2) Slope of switching locus, $-\dot{E}_{max}/1.75$ degrees

b. Known constants

(1) Ramp input velocity, w,	1.9 volts/sec
(2) Maximum output velocity, $\dot{\theta}_{o\ max}$,	5.5 volts/sec
(3) Relay drop-out potential, V_d,	5.6 volts
(4) Error detector sensitivity	.083 $\frac{\text{volts}}{\text{degree}}$
(5) Tach constant, Kt,	3.46 $\frac{\text{volts}}{\text{volt/sec}}$
(6) Tach output, max, $Kt\,\dot{\theta}_{o_{max}}$,	19.0 volts
(7) Error at $-\dot{E}_{max}$ at relay drop-out	3.75 degrees

c. Calculations

Using Equation (83)

$$rKK_1E + r_1K_1Kt\,(w - \dot{\theta}_o)\,V_d \qquad (83)$$

for $\dot{E} = 0$, $(w - \dot{\theta}_o) = 0$, at $E = 2$ degrees

and

$$rKK_1 = 5.6/2(.083), \text{ or}$$

$$rKK_1 = 33.6 \qquad (85)$$

Then at $\dot{E}_{max}$,

$$(w - \dot{\theta}_{i\ max})Kt = (19\text{-}1.9 \times 3.46) \text{ or,}$$

$$(w - \dot{\theta}_{o_{max}})Kt = 12.43 \text{ volts}$$

Then from (83)

$$r_1 K_1 = \frac{5.6 - (33.6)(3.75)(.083)}{12.43} \text{ or}$$

$$r_1 K_1 = .386 \tag{86}$$

Then for $0 < r < 1$ and $0 < r_1 < 1$

choose $K = K_1 = 10$, then by (85) and (86)

$$r = .336$$

$$r_1 = .0386$$

APPENDIX C

EQUIPMENT

Motors:	Diehl, FPE 25-26, 115/115 volts, 400 cycle, 4 pole, 2 phase, Serial B-62376
	Diehl, FPE 25-11, 115/75 volts, 60 cycle, 2 pole, 2 phase, Serial C-18709
	Kearfott Type R 111-2-B, 115/115 volts, 400 cycle, 2 phase, Serial K-3039
Tachometer:	F.D.-38, Electric Indicator Company
Relay:	Four pole, double throw; Sigma Instrument Company, Type 6FX4C-5000 GD-SIL
Amplifiers:	Direct current amplifiers from Boeing Electronic Analog Computer, Model 7000
Recorder:	Amplifier, Brush Company, Model B1-932 Oscillograph, Brush Company, Model BL-202
Potentiometers:	Linear continuous turn; Helipot Company, Series G, 10,000 ohms.
Oscillator:	Low frequency function generator, Hewlett-Packard Company, Model 202A.

JA 17 58
JL 1 64
AG 11 64
JL 28 64
19 APR 68
26 MAY 69
BINDERY
Univ. Microfilm
16886
18222

Thesis
E264 Egan
35705
Quasi-optimazation of two phase induction motor relay servos.